DISSERTATION

A THEORETICAL AND EXPERIMENTAL STUDY OF ADAPTIVE WOOD COMPOSITES

Submitted by

Watanachai Smittakorn

Department of Civil Engineering

In partial fulfillment of the requirements

for the Degree of Doctor of Philosophy

Colorado State University

Fort Collins, Colorado

Spring 2001

COLORADO STATE UNIVERSITY

March 15, 2001

WE HEREBY RECOMMEND THAT THE DISSERTATION PREPARED UNDER OUR SUPERVISION BY WATANACHAI SMITTAKORN ENTITLED A THEORETICAL AND EXPERIMENTAL STUDY OF ADAPTIVE WOOD COMPOSITES BE ACCEPTED AS FULFILLING IN PARTIAL REQUIREMENTS FOR THE DEGREE OF DOCTOR OF PHILOSOPHY.

Committee on Graduate Work

_____
Committee Member

_____
Committee Member

_____
Committee Member

_____
Adviser

_____
Department Head

ABSTRACT OF DISSERTATION

A THEORETICAL AND EXPERIMENTAL STUDY OF ADAPTIVE WOOD COMPOSITES

A piezoelectric material is introduced to use with a wood element and produce an adaptive wood composite in a form of multilayered laminated plate. Steady-state and transient behaviors of the laminate are investigated under the coupled effects of mechanical, electrical, thermal and moisture fields. To analyze such a structure, a mathematical model in three dimensions, namely a discrete-layer model, is developed, treating the displacements, electric potential, temperature, and moisture concentration as primary unknowns. One-dimensional Lagrange linear interpolation functions are employed for the variation in the through-thickness direction. The variation in the two-dimensional in-plane domains is approximated by two approaches: analytical and finite element functions.

Numerical examples verify the accuracy of the discrete-layer model by comparing with available exact solutions as well as demonstrate the behavior of adaptive wood composites subject to various types of excitations. The capability to actuate the composites and counter-balance unfavorable deformation by applying an electric field to the piezoelectric layer is then discussed. Also, representative experiments are conducted on adaptive wood composites in order to examine the degree of actuation induced by the piezoelectric phenomena and confirm the validity of the discrete-layer model.

Watanachai Smittakorn
Civil Engineering Department
Colorado State University
Fort Collins, CO 80523
Spring 2001

ACKNOWLEDGEMENTS

I would like to express my gratitude and appreciation to my adviser, professor Paul Heyliger, for his support, encouragement, guidance, and useful comments throughout the process of developing and completing this work. I also want to thank professors Erik Thompson, Marvin Criswell, and Paul DuChateau for being part of my graduate committee and for their valuable teachings throughout my graduate courses. I also extend my gratitude to Dr. Bryan Hartnagel and Joe Wilmetti for their enormous help on the experimental work.

This work was supported by Award 9702548 from the NRI Competitive Grants Program of the United States Department of Agriculture. This support is gratefully acknowledged.

The love, support, and encouragement from my whole family is also deeply appreciated, especially from my wife Sunisa and my daughter Muchima.

DEDICATION

To my mother.

CONTENTS

LIST OF TABLES

LIST OF FIGURES

LIST OF SYMBOLS

c_v	specific heat coefficient per unit mass at constant volume
C_{ijkl}	elastic stiffness coefficients
d_t	specific heat-moisture coefficient
D_i	components of the electric displacement
D_n	normal component of the electric displacement
e_{ikl}	piezoelectric coefficients
E_i	components of the electric field
H	moisture concentration
H_0	stress-free reference moisture concentration
n_i	components of the unit outward normal vector to the bounding surface
p_i	heat flux components
p_n	normal heat flux
q_i	moisture flux components
q_n	normal moisture flux
r_i	pyroelectric coefficients
S_{ij}	components of the infinitesimal strain tensor
t_i	surface traction components
T	absolute temperature
T_0	stress-free reference temperature
u_i	components of the displacement

α_{kl} coefficients of thermal expansion

β_{kl} coefficients of moisture expansion

γ change of moisture concentration ($\gamma = H - H_0$)

ϵ_{il} dielectric constants (or permittivities)

ζ^M_{ijkl} strain-moisture diffusivity coefficients

ζ^E_{ijl} electric-moisture diffusivity coefficients

ζ^T_{ij} heat-moisture diffusivity coefficients

ζ^H_{ij} moisture diffusivity coefficients

η entropy density

θ small temperature change ($\theta = T - T_0$)

κ^M_{ijkl} strain-thermal conductivity coefficients

κ^E_{ijl} electric-thermal conductivity coefficients

κ^T_{ij} thermal conductivity coefficients

κ^H_{ij} moisture-thermal conductivity coefficients

λ_{ij} stress-temperature coefficients ($\lambda_{ij} = C_{ijkl}\alpha_{kl}$)

μ_{ij} stress-moisture coefficients ($\mu_{ij} = C_{ijkl}\beta_{kl}$)

ρ mass density

σ_{ij} components of the stress tensor

ϕ electrostatic potential (or voltage)

χ_i electric-moisture coefficients

CHAPTER 1

INTRODUCTION

1.1 Background

Since being discovered in the late nineteenth century, piezoelectricity has fascinated those who have encountered it. The direct piezoelectric effect (the generation of an electric field in response to applied stress) provides sensing capability, whereas the converse piezoelectric effect (an induced strain in response to applied electric field) provides actuation capability. Piezoelectric materials have been used to develop electromechanical devices such as ultrasonic generators, sensors, and actuators. In structural applications, piezoelectric materials, when attached on or embedded into structural systems as a composite, provide the capability of self-monitoring and self-controlling. The terms *smart*, *intelligent* or *adaptive* are often used to denote such structures. Studies of adaptive composites have been explored in structures involving many types of material: steel, aluminum, graphite-epoxy, glass-epoxy, and so on. In this study, the effects of piezoelectric layers on wood composite structures are investigated.

Wood is a highly nonhomogeneous, anisotropic, and porous material. It is one of the materials in which temperature and moisture can have strong influence especially concerning shape change. These effects are often not small, and significant errors in analysis of these structures can occur if they are ignored. When adaptive wood composite structures, composed of wood and piezoelectric materials, are exposed to

changes in environmental conditions, their structural behavior is under the effects of the mechanical, electrical, thermal, and moisture fields. A solid under the coupled effects of these four fields is denoted as a *hygrothermopiezoelectric* medium.

In this study, adaptive wood composite structures are investigated through the use of piezoelectric elements integrated with wood layers in the form of laminated plates. Adaptive elements have the advantage of changing their physical characteristics (primarily dimensions) under a change in environment. Piezoelectric materials allow composites to achieve the capability of self-monitoring and actuation. Therefore, with the piezoelectric elements, the structural response caused by external excitations (e.g., temperature, moisture, and load) can be sensed, countered, or supplemented.

1.2 Objectives

The overall purpose of this study is to develop a mathematical model for a hygrothermopiezoelectric laminated plate, apply this model to representative adaptive wood composites to determine the basic behavior and what levels of actuation strain can be imposed, and to construct several prototypical adaptive composites to assess their limitations and the differences between theory and experiment. These objectives are next discussed in more detail.

1. *Develop a mathematical model for a hygrothermopiezoelectric laminated plate.*

   Adaptive wood composites can be influenced by mechanical, electrical, thermal, and moisture fields, conditions for a material describable as a hygrothermopiezoelectric medium. The coupled effects of these four fields for laminated media have never been studied before; therefore, it is necessary to create a new mathematical model for such a structure. A discrete-layer plate theory and computational model in three dimensions will be developed for analyzing

the steady-state and transient behavior of hygrothermopiezoelectric laminated plates. This model will be capable of solving the equations of motion and Maxwell's equation for electrostatics along with the equations of heat conduction and moisture diffusion simultaneously in the composite. The interrelations (or coupled effects) of the mechanical, electrical, thermal, and moisture fields within the linear range of the material properties will also be taken into account. By employing the discrete-layer theory, this model can represent an accurate variation through the thickness of the laminate for all the primary unknowns taken as displacement, electric potential, temperature, and moisture concentration. This model will also specifically account for the dissimilar material properties between the different layers. Excitation to the composites can be specified as imposed traction, displacement, normal electric displacement, electric potential, normal heat flux, temperature, normal moisture flux, or moisture concentration on the bounding surfaces. Then, the accuracy of the discrete-layer model will be verified by comparing with available exact solutions.

2. *Analyze representative examples of adaptive wood composites to describe the basic behavior.*

   The developed discrete-layer model will be applied to analyze representative problems of adaptive wood composite plates. Steady-state and transient responses of the laminates will be investigated subject to the influences of applied load, applied electric field, applied temperature, and applied moisture concentration. In the steady-state analyses, the levels of deformation in the adaptive wood composites caused by the external excitations (applied load, temperature, and moisture) will be calculated. Also, the degree of actuation to the laminates produced by appling the electric field to the piezoelectric layer will be evaluated.

Such information is critical in the application of these solids, as it gives an idea of ranges of operating behavior for these materials.

In the transient analyses, the time required for the effects of applied temperature and moisture to dissipate or propagate in the adaptive wood composites along with the variations of these fields in the composites at various times will be examined.

3. *Construct physical samples of adaptive wood composites and measure levels of adaptive actuation.*

   Representative samples of adaptive wood composites will be constructed and studied experimentally to determine the degree of actuation that can be obtained by including the piezoelectric elements in the wood systems. The composite laminates which are composed of layers of wood and piezoelectric materials will be tested for the responses (e.g., strains and/or displacements) subject to the applied electric fields on the piezoelectric layer. Then, from these experimental data, the agreement between the theory and experiment can be determined and also the limits in their construction can be assessed.

1.3 Structure of Dissertation

Past researches and studies concerning the behavior of solids under some coupled effects among the mechanical, electrical, temperature, and moisture fields are outlined in Chapter 2, Literature Review, along with wood composite and multilayered laminated plate structures. Mathematical formulation for the weak form of the governing equations and a general analytical model for a homogeneous anisotropic solid subject to elastic, electric, thermal, and moisture fields simultaneously are developed in Chapter 3, Theory. Next, the proposed theoretical plate model (discrete-layer model)

for analyzing multilayered hygrothermopiezoelectric laminated plates are presented along with several numerical examples are demonstrated in Chapter 4. Chapter 5 presents the experimental studies of the adaptive wood composite plates. These results are also compared with those predicted by the discrete-layer model. Finally, the conclusions and some recommendation for future studies are discussed in Chapter 6.

CHAPTER 2

LITERATURE REVIEW

The study of adaptive wood composites involves the knowledges of the following four fields on a deformable body: elastic, electric, temperature, and moisture fields. Although the coupled effects of all of these fields together have not previously been studied simultaneously, there exists some reports on the interrelations among these fields. Piezoelectricity is a study of the interaction between elastic and electric fields. When the effect of temperature is included, the theory is called thermopiezoelectricity. The theory of hygrothermoelasticity describes the behavior of solids under the influences of temperature and moisture fields.

The adaptive wood composite structures considered in this study are in the form of multilayered laminated plates. Several techniques have been developed for analyzing such laminated structures. The following sections will review the historical background of the research and studies involving the theories of piezoelectricity, thermopiezoelectricity, and hygrothermoelasticity along with the wood composite structures and the analysis methods for multilayered composite plates, repectively.

2.1 Piezoelectricity and Thermopiezoelectricity

The history of piezoelectricity started with the paper published in 1880 by Pierre and Jacques Curie [17]. The paper reported their experimental measurement of the electrical charges on the surface of the dielectric crystals when subjected to mechan-

ical stress. This phenomenon was named *piezoelectricity*. In 1881, Lippmann predicted the converse piezoelectric effect (i.e., the stress in response to applied electric field) as deduced mathematically from fundamental thermodynamic principles. The mathematical foundations and governing equations for piezoelectricity as obtained by applying the knowledge of solid mechanics and electricity appeared in the work by Voight [89] which later became accepted as a standard reference. The other classical works of Cady [8] and Mason [43] about piezoelectricity illustrated the physical properties of crystals and practical applications. One of the most comprehensive study of piezoelectric plates was the work by Tiersten [81]. The governing equations for a linear piezoelectric media were developed and applied to various wave and vibration problems.

The study of piezoelectricity has been extended to incorporate the effect of temperature in thermopiezoelectricity. The governing equations for a linear thermopiezoelectric medium in three dimensions, considering the coupled effects of elastic, electric, and thermal fields, were given by Mindlin [45] and appeared also in the work by Nowacki [49]. Also, the equations for high frequency vibrations of crystal plates in two dimensions has been derived [46]. Altay and Dokmeci [1] later expressed these governing equations in a variational form as the Euler-Lagrange equations for the discontinuous thermopiezoelectric fields.

Recently, a number of research works have been carried out in order to study the thermopiezoelectric effects on the behavior of composite plate and shell structures. Tauchert [79] examined the static behavior of a laminated piezothermoelastic plate subject to the thermal and electric fields using the classical lamination theory. Tang and Xu [78] extended the work by Tauchert to analyze the dynamic problems. The use of the first-order shear deformation theory to solve the problems of thermopiezo-

electric composite plates was discussed by Jonnalagadda et al. [35], and by Kapuria et al. [36]. An analytical solution in three dimensions for the static behavior of multilayered thermopiezoelectric composite plates was presented by Xu et al. [92]. Furthermore, the problems of thermopiezoelectric cylindrical shells have been studied by Chen and Shen [10], and by Kapuria et al. [37, 38]. The application of thermopiezoelectricity to structural control problems has been a subject of considerable interest [53, 77, 84, 86, 87]. The nonlinear behavior of laminated piezothermoelastic plates due to both material and geometrical nonlinearity has also been discussed [85, 88].

2.2 Hygrothermoelasticity

Hygrothermoelasticity is a study of the effects of temperature and moisture to the elasticity of a solid. Temperature and moisture can induce significant strains which are of concern to many structural applications. These environmental effects on the structural behavior have received remarkable amount of attention, especially for modern composite materials. The effects of the environmentally-induced strains on the bending, buckling, and vibrations of layered composite plates have been presented by Whitney and Ashton [90], and later also by Sai Ram and Sinha [61, 62, 63, 64]. Bouadi and Sun studied these hygrothermal effects on stress field [5] and on the structural stiffness and structural damping of laminated composites [6]. A vibration problem of a laminated plate under unsteady temperature and unsteady moisture environment was presented by Eslami and Maerz [21]. Besides the studies in laminated plate structures, Doxsee [19] and Doxsee and Springer [20] have developed a theory for describing the hygrothermal behavior of laminated composite shells. However, the effects of temperature and moisture on the structures were considered independently, without any coupled effects.

In some porous composite materials, the coupling effects of temperature and mois-

ture fields are significant and cannot be neglected [9]. Shen and Springer [68] studied the diffusion of moisture in composite materials. Shirrell [69] and Springer [76] investigated the combined effects of temperature and moisture fields in some composite materials experimentally. A theory of diffusion including the interaction between temperature and moisture was described by Hartranft et al. [25]. The theory was applied to the problem of heat and moisture diffusion into a thick plate from its surfaces in the paper by Hartranft and Sih [24]. Sih et al. [72] investigated the transient stresses in composites under the coupled effects of heat and moisture.

A very complete mathematical theory of hygrothermoelasticity was shown in the work by Sih et al. [71]. The coupled and uncoupled effects of temperature, moisture, and elasticity were shown. Also, the finite element technique was applied to solve problems of hygrothermoelasticity. Later, a numerical procedure obtained from combining the finite element method, Laplace, and inverse Laplace transform techniques was employed to analyze problems of coupled heat and moisture by Chen and Hwang [11] and Chen et al. [12].

2.3 Wood Composite Structures

Wood materials are widely used in structural applications in the form of composite structural elements. The studies of wood composite structures have been discussed by many authors, including in the text books by Bodig and Jayne [4], Breyer [7], and the references cited therein. The properties and the utilization of wood have also been demonstrated by Haygreen and Bowyer [26], Tsoumis [83], and Desch and Dinwoodie [18]. However, only purely elastic effects have been the major focus in most studies involving wood. Hygroscopic deformation has been separately considered [40, 91], and other studies regarding wood-cement composites [48], general wood composites [67], and dynamic panel measurements [60, 66] have all been based on elements of

laminated wood mechanics. The problems of wood drying have received a considerable amount of attention from many researchers. The effects of moisture and temperature in wood have been investigated in the studies by Choong et al. [13], Cloutier and Fortin [15], Cloutier et al. [16], Gui et al. [23], Irudayaraj et al. [33], McMillen [44], Morgan et al. [47], Plumb et al. [52], Siau [70], Simpson [73], Skaar [74], Thomas et al. [80], and Tremblay et al. [82].

It is possible for piezoelectric materials, which have the capability of both sensing and actuation, to be integrated into wood composites. This results in what can be termed an adaptive wood composite structure. Wood has also been reported to exhibit some piezoelectric effects [22, 39]. When adaptive wood composites are exposed to changes in environment, temperature and moisture can have significant effects on the structural behavior and need to be taken into account along with the mechanical and electrical effects. In this research, the effects from these four fields to the composites are considered simultaneously. The discussion in more details are shown in the following chapters.

2.4 Analyses of Laminated Plates

Many theories have been developed for analyzing multilayered laminated composite plates. Equivalent-single-layer (ESL) theories in two-dimensions, such as classical lamination theory (CLT) first- and higher-order shear deformation theories, simplify the analysis by making kinematic assumptions through the thickness of the laminate [32, 34, 59]. In the CLT, it is assumed that the laminated plates are thin, and the effects of through-thickness shear strain and the transverse normal strain are ignored. Hence, some errors are inevitable in the CLT solutions. The use of first- and higher-order shear deformation theories can help to obtain better solutions. However, the results from these ESL theories yield very good approximations only when applying to

relatively thin plate problems. More accurate results, when needed, can be obtained by employing 3-D theories. Recently, many 3-D theories, both exact and approximate, have been developed to solve the laminated plate problems.

An exact solution in three-dimensions for a simply-supported rectangular laminated elastic plate was derived by Pagano [50]. Years later, the exact solutions were found for the laminated plates under the effects of piezoelectricity by Ray et al. [54], Heyliger [27, 28], and Heyliger and Saravanos [30], and thermopiezoelectricity by Xu et al. [92]. Besides these exact solutions, approximate solutions in three-dimensions have also been developed using a layerwise theory by discretizing the through-thickness dimension into several sublayers. Pauley and Dong [51] first introduced this concept and applied it to analyze the free vibration of infinite laminated piezoelectric plates. A similar approach also appeared in the papers by Reddy [56, 57] for elastic laminates. The limitations of those theories which model the laminated plate as an equivalent-single-layer plate (ESL theories) were overcome since the layerwise theory takes into account the variation in the through-thickness behavior of the laminates when material properties among the layers are different. Later, discrete-layer models using the layerwise theory were developed for analyzing laminated piezoelectric plates by Heyliger et al. [29] and Saravanos et al. [65]. Furthermore, Lee and Saravanos [41, 42] extended the use of discrete-layer technique for solving the problems of laminated piezoelectric composites to incorporate the effects of temperature. The coupling of mechanical, electrical, and thermal effects was considered for layered composite beams and plates. However, none of these studies has considered the combined effects of elasticity, moisture, temperature, and electric field.

Adaptive wood composites, composed of wood and piezoelectric layers, are such structural elements that all the mechanical, electrical, temperature, and moisture

fields can have strong influences on their structural behavior. It is an objective of this research to study these effects on the composite structures using a new computational model. A discrete-layer technique is employed to obtain an approximate solution to the laminated plate problems.

CHAPTER 3

THEORY

3.1 Problem Statement

This research addresses the behavior of adaptive wood composites. Structures of interest are in the form of multilayered laminated plates as shown in Figure 3.1. Laminated plates composed of layers of wood, graphite-epoxy, and/or piezoelectric materials (e.g., PZT and PVDF) are discussed. The layers of the laminated plates are assumed perfectly bonded together with an adhesive of very thin and negligible thickness. In such structures, elastic, electric, thermal, and moisture fields can have strong influence on the structural behavior. The effects of these fields when all are applied simultaneously, both steady-state and transient, on the composites are considered. Since the coupled effects of elastic, electric, temperature, and moisture fields have never been studied before, here we combine the theory of thermopiezoelectricity and hygrothermoelasticity together. A theory of hygrothermopiezoelectricity is introduced with the assumptions that all materials have linear properties, that is, the changes of strain, electric field, temperature, and moisture in the solid are considered to be within their individual linear range. Also, the residual effect of permanent deformation is ignored. (That is, in the volume of solid at the reference temperature T_0 and the reference moisture concentration H_0, all the strain components $S_{ij} = 0$ when all the electric field components $E_i = 0$.)

The domains of investigation are treated as x- and y-coordinates in the plane of

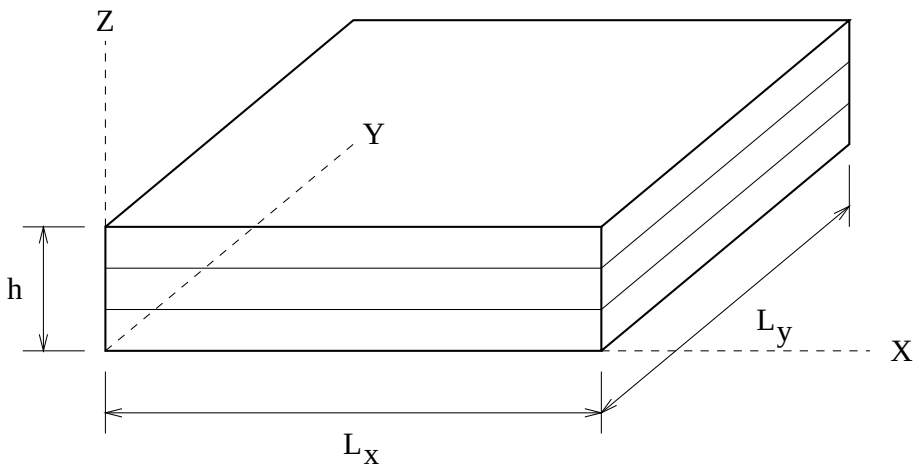

Figure 3.1: Geometry of the laminated composite plate.

the laminates, and z-coordinate in the direction through the thickness. The descriptions used in this document are based on the material coordinates where the spatial variables x, y, and z are measured in the undeformed configuration. Indicial notation is employed in writting equations with spatial variables (i.e., $x_1 = x$, $x_2 = y$, $x_3 = z$, $a_1 = a_x$, $a_2 = a_y$, and $a_3 = a_z$). The comma notation represents the derivatives with respect to the spatial variables (i.e., $a_{,i} = \partial a/\partial x_i$, and $a_{,ij} = \partial^2 a/\partial x_i \partial x_j$). Also, the symbols dot $\dot{}$ and double dots $\ddot{}$ over a variable represent its first and second derivatives with respect to time (i.e., $\dot{a} = \partial a/\partial t$, and $\ddot{a} = \partial^2 a/\partial t^2$).

3.2 Governing Equations

A theory of hygrothermopiezoelectricity in this research is based on work presented by Mindlin [46], Nowacki [49], Reddy [59], and Sih et al. [71]. The governing equations in three-dimensions for a linear anisotropic hygrothermopiezoelectric medium defined pointwise in the solid volume Ω at any time $t \geq 0$ can be shown in two categories: conservation equations and constitutive relations. Then, the boundary and initial conditions necessary for solving the problems are discussed. All variables introduced in this section are defined in the List of Symbols.

3.2.1 Conservation Equations

The equations of motion in the absence of body forces are

$$\sigma_{ij,j} = \rho \ddot{u}_i \tag{3.1}$$

The Maxwell's equation for electrostatics (conservation of charge) in the absence of free charge is

$$D_{i,i} = 0 \tag{3.2}$$

The heat conduction equation in the absence of heat source/sink is

$$p_{i,i} = -T_0 \dot{\eta} \tag{3.3}$$

The moisture diffusion equation (conservation of mass of moisture) in the absence of moisture source/sink is

$$q_{i,i} = -\dot{\gamma} \tag{3.4}$$

Equations (3.1) to (3.4) are in general forms and will be used for transient problems. For steady-state problems, these equations turn out to be the following equilibrium equations:

$$\begin{aligned} \sigma_{ij,j} &= 0 \\ D_{i,i} &= 0 \\ p_{i,i} &= 0 \\ q_{i,i} &= 0 \end{aligned}$$

where $i, j = 1, 2, 3$.

3.2.2 Constitutive Relations

The stress tensor, electric displacement vector, and entropy density constitutive relations are assumed to be linear and have the following relations:

$$\sigma_{ij} = C_{ijkl}S_{kl} - e_{lij}E_l - \lambda_{ij}\theta - \mu_{ij}\gamma \tag{3.5}$$

$$D_i = e_{ikl}S_{kl} + \epsilon_{il}E_l + r_i\theta + \chi_i\gamma \tag{3.6}$$

$$\eta = \lambda_{kl}S_{kl} + r_lE_l + \frac{\rho c_v}{T_0}\theta - d_t\gamma \tag{3.7}$$

The strain-displacement relations for infinitesimal deformation are given by

$$S_{ij} = \frac{1}{2}(u_{i,j} + u_{j,i}) \tag{3.8}$$

The relationship between the electric field vector and electrostatic potential is defined as

$$E_i = -\phi_{,i} \tag{3.9}$$

The heat flux and moisture flux vectors are assumed to be dependent on the gradients of strain tensor, electric field, temperature, and moisture as

$$p_i = \kappa^M_{ijkl}S_{kl,j} - \kappa^E_{ijl}E_{l,j} - \kappa^T_{ij}\theta_{,j} - \kappa^H_{ij}\gamma_{,j} \tag{3.10}$$

$$q_i = \zeta^M_{ijkl}S_{kl,j} - \zeta^E_{ijl}E_{l,j} - \zeta^T_{ij}\theta_{,j} - \zeta^H_{ij}\gamma_{,j} \tag{3.11}$$

where $i, j, k, l = 1, 2, 3$.

Here the electric-moisture coefficients (χ_i) in equation (3.6) are assumed for the moisture field in a similar manner as the temperature field. The equations (3.10) and (3.11) for the heat flux and moisture flux vectors are deduced from Sih et al. [71] p. 147 and the constitutive equation (3.5). Also, to help visualize all the coupling parameters among the mechanical, electrical, temperature, and moisture fields, see the diagram in Figure 3.2.

FROM / TO	MECH.	ELEC.	TEMP.	MOIST.
MECH.	ρ, C_{ijkl}	e_{lij}	λ_{ij}	μ_{ij}
ELEC.	e_{ikl}	ϵ_{il}	r_i	χ_i
TEMP.	$(T_0\lambda_{kl})$, κ^M_{ijkl}	$(T_0 r_l)$, κ^E_{ijl}	(ρc_v), κ^T_{ij}	$(T_0 d_t)$, κ^H_{ij}
MOIST.	ζ^M_{ijkl}	ζ^E_{ijl}	ζ^T_{ij}	ζ^H_{ij}

Figure 3.2: Diagram showing the interrelation parameters among the mechanical, electrical, temperature, and moisture fields.

3.2.3 Boundary and Initial Conditions

The governing equations, as shown in the previous section, are stated pointwise in the solid volume Ω and are of initial-boundary-value problem type. Appropriate boundary and initial conditions must be specified so that there exists a unique solution to the system. The boundary conditions for the mechanical, electrical, thermal, and moisture fields are specified on the bounding surface Γ of the solid body at time $t > 0$ in the following forms:

$$u_i = \hat{u}_i(x, y, z, t) \quad \text{on} \quad \Gamma_1^{u_i} \tag{3.12}$$

$$\sigma_{ij} n_j = \hat{t}_i(x, y, z, t) \quad \text{on} \quad \Gamma_2^{u_i} \tag{3.13}$$

$$\phi = \hat{\phi}(x, y, z, t) \quad \text{on} \quad \Gamma_1^{\phi} \tag{3.14}$$

$$D_i n_i = \hat{D}_n(x, y, z, t) \quad \text{on} \quad \Gamma_2^{\phi} \tag{3.15}$$

$$\theta = \hat{\theta}(x, y, z, t) \quad \text{on} \quad \Gamma_1^{\theta} \tag{3.16}$$

$$p_i n_i = \hat{p}_n(x, y, z, t) \quad \text{on} \quad \Gamma_2^{\theta} \tag{3.17}$$

$$\gamma = \hat{\gamma}(x, y, z, t) \quad \text{on} \quad \Gamma_1^{\gamma} \tag{3.18}$$

$$q_i n_i = \hat{q}_n(x, y, z, t) \quad \text{on} \quad \Gamma_2^{\gamma} \tag{3.19}$$

where the overhat symbol ˆ above a variable denotes a specified value or function. Γ_1^a and Γ_2^a are parts of the boundary for variable a, and they constitute the entire solid boundary Γ (i.e., $\Gamma_1^a + \Gamma_2^a = \Gamma$). The boundary conditions specified on Γ_1 are the essential boundary conditions, which are the Dirichlet conditions. Those specified on Γ_2 are the natural boundary conditions, which are the Neumann conditions. No mixed boundary conditions are considered in this study.

Steady-state problems are special cases in which only the specified boundary conditions are needed. In general or for the case of transient analysis, initial conditions are also needed to be specified pointwise in the entire solid body in order for a unique solution to exist. The initial conditions for the mechanical, electrical, thermal, and moisture fields are specified in the solid volume Ω at time $t = 0$ as follows:

$$u_i = u_i^0(x, y, z) \tag{3.20}$$

$$\dot{u}_i = \dot{u}_i^0(x, y, z) \tag{3.21}$$

$$\phi = \phi^0(x, y, z) \tag{3.22}$$

$$\theta = \theta^0(x, y, z) \tag{3.23}$$

$$\gamma = \gamma^0(x, y, z) \tag{3.24}$$

3.3 Material Symmetry

Here we note that the stress and strain tensors are always symmetric [75]. Along with the symmetry of material properties, the following properties of symmetry also hold:

$$\sigma_{ij} = \sigma_{ji}$$

$$S_{kl} = S_{lk}$$

$$C_{ijkl} = C_{ijlk} = C_{jikl} = C_{klij}$$

$$e_{ikl} = e_{ilk}$$

$$\epsilon_{il} = \epsilon_{li}$$

$$\lambda_{ij} = \lambda_{ji}$$

$$\mu_{ij} = \mu_{ji}$$

Using the above properties of symmetry, the unknowns for stress and strain components can be reduced from nine to six unknowns. Then, we can redefine the stress and strain vectors using the contracted notation as follows:

$$\sigma_p = \left\{ \begin{array}{c} \sigma_1 \\ \sigma_2 \\ \sigma_3 \\ \sigma_4 \\ \sigma_5 \\ \sigma_6 \end{array} \right\} = \left\{ \begin{array}{c} \sigma_{11} \\ \sigma_{22} \\ \sigma_{33} \\ \sigma_{23} \\ \sigma_{13} \\ \sigma_{12} \end{array} \right\}$$

$$S_q = \left\{ \begin{array}{c} S_1 \\ S_2 \\ S_3 \\ S_4 \\ S_5 \\ S_6 \end{array} \right\} = \left\{ \begin{array}{c} S_{11} \\ S_{22} \\ S_{33} \\ 2S_{23} \\ 2S_{13} \\ 2S_{12} \end{array} \right\}$$

Similarly, the indices of the coefficients can be transformed using the following rules:

$$11 \rightarrow 1\ ,\ 22 \rightarrow 2\ ,\ 33 \rightarrow 3\ ,\ 23 \rightarrow 4\ ,\ 13 \rightarrow 5\ ,\ 12 \rightarrow 6$$

Then, the constitutive relations may be rewritten as:

$$\begin{aligned}
\sigma_p &= C_{pq}S_q - e_{lp}E_l - \lambda_p\theta - \mu_p\gamma \\
D_i &= e_{iq}S_q + \epsilon_{il}E_l + r_i\theta + \chi_i\gamma \\
\eta &= \lambda_q S_q + r_l E_l + \frac{\rho c_v}{T_0}\theta - d_t\gamma
\end{aligned}$$

where $p, q = 1, ..., 6$ and $i, l = 1, ..., 3$. In the above equations, we may write the elastic, piezoelectric, dielectric, stress-temperature, stress-moisture, pyroelectric, and electric-moisture coefficients in matrix forms as:

$$C_{pq} = \begin{bmatrix} C_{11} & C_{12} & C_{13} & C_{14} & C_{15} & C_{16} \\ & C_{22} & C_{23} & C_{24} & C_{25} & C_{26} \\ & & C_{33} & C_{34} & C_{35} & C_{36} \\ & & & C_{44} & C_{45} & C_{46} \\ & \text{sym.} & & & C_{55} & C_{56} \\ & & & & & C_{66} \end{bmatrix}$$

$$e_{lp} = \begin{bmatrix} e_{11} & e_{12} & e_{13} & e_{14} & e_{15} & e_{16} \\ e_{21} & e_{22} & e_{23} & e_{24} & e_{25} & e_{26} \\ e_{31} & e_{32} & e_{33} & e_{34} & e_{35} & e_{36} \end{bmatrix}$$

$$\epsilon_{il} = \begin{bmatrix} \epsilon_{11} & \epsilon_{12} & \epsilon_{13} \\ & \epsilon_{22} & \epsilon_{23} \\ \text{sym.} & & \epsilon_{33} \end{bmatrix}$$

$$\lambda_p = \begin{Bmatrix} \lambda_1 \\ \lambda_2 \\ \lambda_3 \\ \lambda_4 \\ \lambda_5 \\ \lambda_6 \end{Bmatrix}$$

$$\mu_p = \begin{Bmatrix} \mu_1 \\ \mu_2 \\ \mu_3 \\ \mu_4 \\ \mu_5 \\ \mu_6 \end{Bmatrix}$$

$$r_i = \begin{Bmatrix} r_1 \\ r_2 \\ r_3 \end{Bmatrix}$$

$$\chi_i = \begin{Bmatrix} \chi_1 \\ \chi_2 \\ \chi_3 \end{Bmatrix}$$

In general, there are 21 independent elastic constants, 18 independent piezoelectric constants, 6 independent dielectric constants, 6 independent stress-temperature constants, 6 independent stress-moisture constants, 3 independent pyroelectric constants, and 3 independent electric-moisture constants. In reality, most materials exhibit symmetric properties in some directions in such a way that the number of material constants can be reduced to a fewer numbers. However, for the generality of the numerical calculation, the computer programs developed for this research will have the capability to take into account all of these material constants.

3.4 Transformation of Tensors

In the laminated plate structures composed of layers of anisotropic materials, the lamina are rarely aligned in the same angle. We usually construct the composites with their lamina in different angles in order to achieve the composite's best performance. For an anisotropic material with symmetric properties in some directions, the material properties are often specified by a local coordinate system corresponding to their directions of symmetry. The material properties in the coordinate system other than their local coordinates (see Figure 3.3) can be computed using the transformation rules for tensors. These rules for the tensors of order one to order four are as follows:

$$
\begin{aligned}
r'_i &= a_{im} r_m && \text{for order one} \\
\epsilon'_{ij} &= a_{im} a_{nj} \epsilon_{mn} && \text{for order two} \\
e'_{ikl} &= a_{im} a_{kp} a_{lq} e_{mpq} && \text{for order three} \\
C'_{ijkl} &= a_{im} a_{jn} a_{kp} a_{lq} C_{mnpq} && \text{for order four}
\end{aligned}
$$

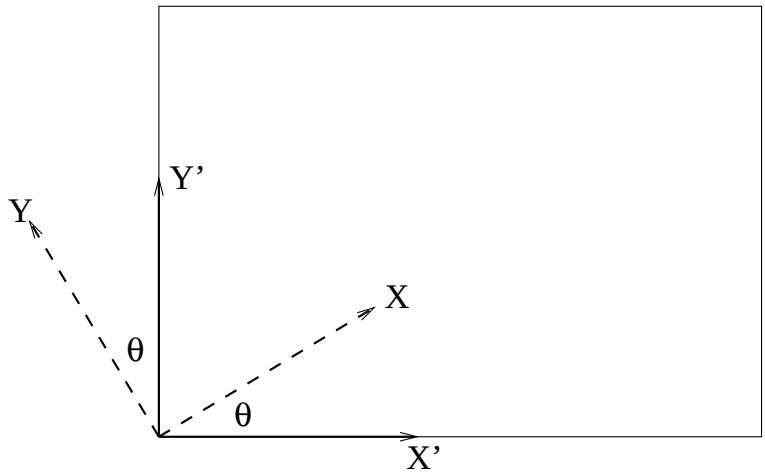

Figure 3.3: Transformation of coordinates

where a_{ij} are the cosines of the angles between x_i' and x_j directions, and for such case can be written in matrix form as

$$a_{ij} = \begin{bmatrix} \cos\theta & -\sin\theta & 0 \\ \sin\theta & \cos\theta & 0 \\ 0 & 0 & 1 \end{bmatrix}$$

3.5 Mathematical Formulation

The problems of adaptive composite plates involve the solving of the governing equations (3.1) to (3.4) subject to the boundary and initial conditions (3.12) to (3.19). Our intent is not to solve for an exact solution in a pointwise sense (or closed form), but instead to seek for an approximate solution (or numerical solution) to these governing equations. In doing so, the governing equations are needed to be first formulated in a weak form. Then, any solution which satisfies the weak form will be an approximate solution to the actual problem. Different types of approximate solutions will be sought here in this study, and they will be shown later in the next section and the next chapter.

3.5.1 Weak Formulation

In order to seek an approximate solution to the system of partial differential equations as shown ealier, a weak formulation of these equations is needed. First we rewrite the constitutive equations (3.5) to (3.11) by substituting the strain-displacement relation and the relation between electrostatic field and electrostatic potential. Along with the properties of material symmetry, the constitutive equations for the stress tensor, the electric displacement vector, and the entropy density become

$$\sigma_{ij} = C_{ijkl}u_{k,l} + e_{lij}\phi_{,l} - \lambda_{ij}\theta - \mu_{ij}\gamma \tag{3.25}$$

$$D_i = e_{ikl}u_{k,l} - \epsilon_{il}\phi_{,l} + r_i\theta + \chi_i\gamma \tag{3.26}$$

$$\eta = \lambda_{kl}u_{k,l} - r_l\phi_{,l} + \frac{\rho c_v}{T_0}\theta - d_t\gamma \tag{3.27}$$

Similarly, the heat flux and the moisture flux may be rewritten as

$$p_i = \kappa^M_{ijkl}u_{k,lj} + \kappa^E_{ijl}\phi_{,lj} - \kappa^T_{ij}\theta_{,j} - \kappa^H_{ij}\gamma_{,j} \tag{3.28}$$

$$q_i = \zeta^M_{ijkl}u_{k,lj} + \zeta^E_{ijl}\phi_{,lj} - \zeta^T_{ij}\theta_{,j} - \zeta^H_{ij}\gamma_{,j} \tag{3.29}$$

Next, the weak form of the governing equations (3.1) to (3.4) for a homogeneous medium can be formulated using the method of weighted residuals as follows:

$$0 = \int_\Omega [\delta u_i(\sigma_{ij,j} - \rho\ddot{u}_i) + \delta\phi D_{i,i} + \delta\theta(p_{i,i} + T_0\dot{\eta}) + \delta\gamma(q_{i,i} + \dot{\gamma})]d\Omega \tag{3.30}$$

where δu_i, $\delta\phi$, $\delta\theta$, and $\delta\gamma$ are arbitrary and independent weight functions. After integrating this equation by parts, we get

$$\begin{aligned}&\int_\Omega(\delta u_i\rho\ddot{u}_i - \delta\theta T_0\dot{\eta} - \delta\gamma\dot{\gamma})d\Omega + \int_\Omega(\delta u_{i,j}\sigma_{ij} + \delta\phi_{,i}D_i + \delta\theta_{,i}p_i + \delta\gamma_{,i}q_i)d\Omega \\ &= \int_\Omega[(\delta u_i\sigma_{ij})_{,j} + (\delta\phi D_i)_{,i} + (\delta\theta p_i)_{,i} + (\delta\gamma q_i)_{,i}]d\Omega\end{aligned} \tag{3.31}$$

Now, after we apply the divergence theorem to the right side of the equation, the equation becomes

$$\int_\Omega(\delta u_i\rho\ddot{u}_i - \delta\theta T_0\dot{\eta} - \delta\gamma\dot{\gamma})d\Omega + \int_\Omega(\delta u_{i,j}\sigma_{ij} + \delta\phi_{,i}D_i + \delta\theta_{,i}p_i + \delta\gamma_{,i}q_i)d\Omega$$

$$= \oint_\Gamma (\delta u_i \sigma_{ij} n_j + \delta\phi D_i n_i + \delta\theta p_i n_i + \delta\gamma q_i n_i) d\Gamma \tag{3.32}$$

The terms on the boundary may be rewritten using Cauchy's formula for the stress tensor ($t_i = \sigma_{ij} n_j$), and by substituting the normal electric displacement ($D_n = D_i n_i$), normal heat flux ($p_n = p_i n_i$), and normal moisture flux ($q_n = q_i n_i$). The equation then becomes

$$\begin{aligned}
&\int_\Omega (\delta u_i \rho \ddot{u}_i - \delta\theta T_0 \dot{\eta} - \delta\gamma\dot{\gamma}) d\Omega + \int_\Omega (\delta u_{i,j}\sigma_{ij} + \delta\phi_{,i} D_i + \delta\theta_{,i} p_i + \delta\gamma_{,i} q_i) d\Omega \\
&= \oint_\Gamma (\delta u_i t_i + \delta\phi D_n + \delta\theta p_n + \delta\gamma q_n) d\Gamma
\end{aligned} \tag{3.33}$$

Now, after substituting the constitutive equations (3.25) to (3.29) for σ_{ij}, D_i, η, p_i and q_i, we reach the final weak form as

$$\begin{aligned}
&\int_\Omega [\delta u_i \rho \ddot{u}_i - \delta\theta T_0 (\lambda_{kl}\dot{u}_{k,l} - r_l \dot{\phi}_{,l} + \frac{\rho c_v}{T_0}\dot{\theta} - d_t \dot{\gamma}) - \delta\gamma\dot{\gamma}] d\Omega \\
&+ \int_\Omega [\delta u_{i,j} (C_{ijkl} u_{k,l} + e_{lij}\phi_{,l} - \lambda_{ij}\theta - \mu_{ij}\gamma) \\
&\quad + \delta\phi_{,i} (e_{ikl} u_{k,l} - \epsilon_{il}\phi_{,l} + r_i\theta + \chi_i\gamma) \\
&\quad + \delta\theta_{,i} (\kappa^M_{ijkl} u_{k,lj} + \kappa^E_{ijl}\phi_{,lj} - \kappa^T_{ij}\theta_{,j} - \kappa^H_{ij}\gamma_{,j}) \\
&\quad + \delta\gamma_{,i} (\zeta^M_{ijkl} u_{k,lj} + \zeta^E_{ijl}\phi_{,lj} - \zeta^T_{ij}\theta_{,j} - \zeta^H_{ij}\gamma_{,j})] d\Omega \\
&= \oint_\Gamma (\delta u_i t_i + \delta\phi D_n + \delta\theta p_n + \delta\gamma q_n) d\Gamma
\end{aligned} \tag{3.34}$$

If we let $u_1 = u$, $u_2 = v$, $u_3 = w$, $t_1 = t_x$, $t_2 = t_y$, and $t_3 = t_z$, then the weak form equation may be rewritten as

$$\begin{aligned}
&\int_\Omega [\delta u \rho \ddot{u} + \delta v \rho \ddot{v} + \delta w \rho \ddot{w}] d\Omega \\
&+ \int_\Omega [\delta\theta T_0 (-\lambda_{1l}\dot{u}_{,l} - \lambda_{2l}\dot{v}_{,l} - \lambda_{3l}\dot{w}_{,l} + r_l\dot{\phi}_{,l} - \frac{\rho c_v}{T_0}\dot{\theta} + d_t\dot{\gamma}) - \delta\gamma\dot{\gamma}] d\Omega \\
&+ \int_\Omega [\delta u_{,j} (C_{1j1l} u_{,l} + C_{1j2l} v_{,l} + C_{1j3l} w_{,l} + e_{l1j}\phi_{,l} - \lambda_{1j}\theta - \mu_{1j}\gamma) \\
&\quad + \delta v_{,j} (C_{2j1l} u_{,l} + C_{2j2l} v_{,l} + C_{2j3l} w_{,l} + e_{l2j}\phi_{,l} - \lambda_{2j}\theta - \mu_{2j}\gamma) \\
&\quad + \delta w_{,j} (C_{3j1l} u_{,l} + C_{3j2l} v_{,l} + C_{3j3l} w_{,l} + e_{l3j}\phi_{,l} - \lambda_{3j}\theta - \mu_{3j}\gamma)
\end{aligned}$$

$$
\begin{aligned}
&+\delta\phi_{,i}(e_{i1l}u_{,l}+e_{i2l}v_{,l}+e_{i3l}w_{,l}-\epsilon_{il}\phi_{,l}+r_i\theta+\chi_i\gamma)\\
&+\delta\theta_{,i}(\kappa^M_{ij1l}u_{,lj}+\kappa^M_{ij2l}v_{,lj}+\kappa^M_{ij3l}w_{,lj}+\kappa^E_{ijl}\phi_{,lj}-\kappa^T_{ij}\theta_{,j}-\kappa^H_{ij}\gamma_{,j})\\
&+\delta\gamma_{,i}(\zeta^M_{ij1l}u_{,lj}+\zeta^M_{ij2l}v_{,lj}+\zeta^M_{ij3l}w_{,lj}+\zeta^E_{ijl}\phi_{,lj}-\zeta^T_{ij}\theta_{,j}-\zeta^H_{ij}\gamma_{,j})]d\Omega\\
&=\oint_\Gamma(\delta ut_x+\delta vt_y+\delta wt_z+\delta\phi D_n+\delta\theta p_n+\delta\gamma q_n)d\Gamma
\end{aligned}
\tag{3.35}
$$

or in matrix form as

$$
\begin{aligned}
&\int_\Omega(\delta u\rho\ddot{u}+\delta v\rho\ddot{v}+\delta w\rho\ddot{w})d\Omega\\
&+\int_\Omega(\delta\theta T_0(-\{\lambda^x\}^T\{\nabla\dot{u}\}-\{\lambda^y\}^T\{\nabla\dot{v}\}-\{\lambda^z\}^T\{\nabla\dot{w}\}+\{r\}^T\{\nabla\dot{\phi}\}-\frac{\rho c_v}{T_0}\dot{\theta}+d_t\dot{\gamma})-\delta\gamma\dot{\gamma})d\Omega\\
&+\int_\Omega(\{\nabla\delta u\}^T([C^{xx}]\{\nabla u\}+[C^{xy}]\{\nabla v\}+[C^{xz}]\{\nabla w\}+[e^x]^T\{\nabla\phi\}-\{\lambda^x\}\theta-\{\mu^x\}\gamma)\\
&\quad+\{\nabla\delta v\}^T([C^{yx}]\{\nabla u\}+[C^{yy}]\{\nabla v\}+[C^{yz}]\{\nabla w\}+[e^y]^T\{\nabla\phi\}-\{\lambda^y\}\theta-\{\mu^y\}\gamma)\\
&\quad+\{\nabla\delta w\}^T([C^{zx}]\{\nabla u\}+[C^{zy}]\{\nabla v\}+[C^{zz}]\{\nabla w\}+[e^z]^T\{\nabla\phi\}-\{\lambda^z\}\theta-\{\mu^z\}\gamma)\\
&\quad+\{\nabla\delta\phi\}^T([e^x]\{\nabla u\}+[e^y]\{\nabla v\}+[e^z]\{\nabla w\}-[\epsilon]\{\nabla\phi\}+\{r\}\theta+\{\chi\}\gamma)\\
&\quad+\{\nabla\delta\theta\}^T([\kappa^{Mx}]\{\nabla\nabla u\}+[\kappa^{My}]\{\nabla\nabla v\}+[\kappa^{Mz}]\{\nabla\nabla w\}+[\kappa^E]\{\nabla\nabla\phi\}-[\kappa^T]\{\nabla\theta\}-[\kappa^H]\{\nabla\gamma\})\\
&\quad+\{\nabla\delta\gamma\}^T([\zeta^{Mx}]\{\nabla\nabla u\}+[\zeta^{My}]\{\nabla\nabla v\}+[\zeta^{Mz}]\{\nabla\nabla w\}+[\zeta^E]\{\nabla\nabla\phi\}-[\zeta^T]\{\nabla\theta\}-[\zeta^H]\{\nabla\gamma\}))d\Omega\\
&=\oint_\Gamma(\delta ut_x+\delta vt_y+\delta wt_z+\delta\phi D_n+\delta\theta p_n+\delta\gamma q_n)d\Gamma
\end{aligned}
\tag{3.36}
$$

where

$$
\{\nabla a\}=\begin{Bmatrix}a_{,x}\\a_{,y}\\a_{,z}\end{Bmatrix}
$$

$$
\{\nabla\nabla a\}=\begin{Bmatrix}a_{,xx}\\a_{,yy}\\a_{,zz}\\2a_{,yz}\\2a_{,xz}\\2a_{,xy}\end{Bmatrix}
$$

and the coefficient matrices or vectors are

$$
C^{xx}_{jl}=C_{1j1l}=\begin{bmatrix}C_{11}&C_{16}&C_{15}\\C_{16}&C_{66}&C_{56}\\C_{15}&C_{56}&C_{55}\end{bmatrix}
$$

$$C_{jl}^{xy} = C_{1j2l} = \begin{bmatrix} C_{16} & C_{12} & C_{14} \\ C_{66} & C_{26} & C_{46} \\ C_{56} & C_{25} & C_{45} \end{bmatrix}$$

$$C_{jl}^{xz} = C_{1j3l} = \begin{bmatrix} C_{15} & C_{14} & C_{13} \\ C_{56} & C_{46} & C_{36} \\ C_{55} & C_{45} & C_{35} \end{bmatrix}$$

$$C_{jl}^{yx} = C_{2j1l} = \begin{bmatrix} C_{16} & C_{66} & C_{56} \\ C_{12} & C_{26} & C_{25} \\ C_{14} & C_{46} & C_{45} \end{bmatrix} = C_{lj}^{xy}$$

$$C_{jl}^{yy} = C_{2j2l} = \begin{bmatrix} C_{66} & C_{26} & C_{46} \\ C_{26} & C_{22} & C_{24} \\ C_{46} & C_{24} & C_{44} \end{bmatrix}$$

$$C_{jl}^{yz} = C_{2j3l} = \begin{bmatrix} C_{56} & C_{46} & C_{36} \\ C_{25} & C_{24} & C_{23} \\ C_{45} & C_{44} & C_{34} \end{bmatrix}$$

$$C_{jl}^{zx} = C_{3j1l} = \begin{bmatrix} C_{15} & C_{56} & C_{55} \\ C_{14} & C_{46} & C_{45} \\ C_{13} & C_{36} & C_{35} \end{bmatrix} = C_{lj}^{xz}$$

$$C_{jl}^{zy} = C_{3j2l} = \begin{bmatrix} C_{56} & C_{25} & C_{45} \\ C_{46} & C_{24} & C_{44} \\ C_{36} & C_{23} & C_{34} \end{bmatrix} = C_{lj}^{yz}$$

$$C_{jl}^{zz} = C_{3j3l} = \begin{bmatrix} C_{55} & C_{45} & C_{35} \\ C_{45} & C_{44} & C_{34} \\ C_{35} & C_{34} & C_{33} \end{bmatrix}$$

$$e_{il}^{x} = e_{i1l} = \begin{bmatrix} e_{11} & e_{16} & e_{15} \\ e_{21} & e_{26} & e_{25} \\ e_{31} & e_{36} & e_{35} \end{bmatrix}$$

$$e_{il}^{y} = e_{i2l} = \begin{bmatrix} e_{16} & e_{12} & e_{14} \\ e_{26} & e_{22} & e_{24} \\ e_{36} & e_{32} & e_{34} \end{bmatrix}$$

$$e_{il}^{z} = e_{i3l} = \begin{bmatrix} e_{15} & e_{14} & e_{13} \\ e_{25} & e_{24} & e_{23} \\ e_{35} & e_{34} & e_{33} \end{bmatrix}$$

$$\lambda_{j}^{x} = \lambda_{1j} = \begin{Bmatrix} \lambda_1 \\ \lambda_6 \\ \lambda_5 \end{Bmatrix}$$

$$\lambda_{j}^{y} = \lambda_{2j} = \begin{Bmatrix} \lambda_6 \\ \lambda_2 \\ \lambda_4 \end{Bmatrix}$$

$$\lambda_j^z = \lambda_{3j} = \left\{ \begin{array}{c} \lambda_5 \\ \lambda_4 \\ \lambda_3 \end{array} \right\}$$

$$\mu_j^x = \mu_{1j} = \left\{ \begin{array}{c} \mu_1 \\ \mu_6 \\ \mu_5 \end{array} \right\}$$

$$\mu_j^y = \mu_{2j} = \left\{ \begin{array}{c} \mu_6 \\ \mu_2 \\ \mu_4 \end{array} \right\}$$

$$\mu_j^z = \mu_{3j} = \left\{ \begin{array}{c} \mu_5 \\ \mu_4 \\ \mu_3 \end{array} \right\}$$

$$\kappa_{ip}^{Mx} = \kappa_{ij1l}^{M} = \left[\begin{array}{cccccc} \kappa_{11}^{Mx} & \kappa_{12}^{Mx} & \kappa_{13}^{Mx} & \kappa_{14}^{Mx} & \kappa_{15}^{Mx} & \kappa_{16}^{Mx} \\ \kappa_{21}^{Mx} & \kappa_{22}^{Mx} & \kappa_{23}^{Mx} & \kappa_{24}^{Mx} & \kappa_{25}^{Mx} & \kappa_{26}^{Mx} \\ \kappa_{31}^{Mx} & \kappa_{32}^{Mx} & \kappa_{33}^{Mx} & \kappa_{34}^{Mx} & \kappa_{35}^{Mx} & \kappa_{36}^{Mx} \end{array} \right]$$

$$\kappa_{ip}^{My} = \kappa_{ij1l}^{M} = \left[\begin{array}{cccccc} \kappa_{11}^{My} & \kappa_{12}^{My} & \kappa_{13}^{My} & \kappa_{14}^{My} & \kappa_{15}^{My} & \kappa_{16}^{My} \\ \kappa_{21}^{My} & \kappa_{22}^{My} & \kappa_{23}^{My} & \kappa_{24}^{My} & \kappa_{25}^{My} & \kappa_{26}^{My} \\ \kappa_{31}^{My} & \kappa_{32}^{My} & \kappa_{33}^{My} & \kappa_{34}^{My} & \kappa_{35}^{My} & \kappa_{36}^{My} \end{array} \right]$$

$$\kappa_{ip}^{Mz} = \kappa_{ij1l}^{M} = \left[\begin{array}{cccccc} \kappa_{11}^{Mz} & \kappa_{12}^{Mz} & \kappa_{13}^{Mz} & \kappa_{14}^{Mz} & \kappa_{15}^{Mz} & \kappa_{16}^{Mz} \\ \kappa_{21}^{Mz} & \kappa_{22}^{Mz} & \kappa_{23}^{Mz} & \kappa_{24}^{Mz} & \kappa_{25}^{Mz} & \kappa_{26}^{Mz} \\ \kappa_{31}^{Mz} & \kappa_{32}^{Mz} & \kappa_{33}^{Mz} & \kappa_{34}^{Mz} & \kappa_{35}^{Mz} & \kappa_{36}^{Mz} \end{array} \right]$$

$$\kappa_{ip}^{E} = \kappa_{ijl}^{E} = \left[\begin{array}{cccccc} \kappa_{11}^{E} & \kappa_{12}^{E} & \kappa_{13}^{E} & \kappa_{14}^{E} & \kappa_{15}^{E} & \kappa_{16}^{E} \\ \kappa_{21}^{E} & \kappa_{22}^{E} & \kappa_{23}^{E} & \kappa_{24}^{E} & \kappa_{25}^{E} & \kappa_{26}^{E} \\ \kappa_{31}^{E} & \kappa_{32}^{E} & \kappa_{33}^{E} & \kappa_{34}^{E} & \kappa_{35}^{E} & \kappa_{36}^{E} \end{array} \right]$$

$$\kappa_{ij}^{T} = \left[\begin{array}{ccc} \kappa_{11}^{T} & \kappa_{12}^{T} & \kappa_{13}^{T} \\ \kappa_{21}^{T} & \kappa_{22}^{T} & \kappa_{23}^{T} \\ \kappa_{31}^{T} & \kappa_{32}^{T} & \kappa_{33}^{T} \end{array} \right]$$

$$\kappa_{ij}^{H} = \left[\begin{array}{ccc} \kappa_{11}^{H} & \kappa_{12}^{H} & \kappa_{13}^{H} \\ \kappa_{21}^{H} & \kappa_{22}^{H} & \kappa_{23}^{H} \\ \kappa_{31}^{H} & \kappa_{32}^{H} & \kappa_{33}^{H} \end{array} \right]$$

$$\zeta_{ip}^{Mx} = \zeta_{ij1l}^{M} = \left[\begin{array}{cccccc} \zeta_{11}^{Mx} & \zeta_{12}^{Mx} & \zeta_{13}^{Mx} & \zeta_{14}^{Mx} & \zeta_{15}^{Mx} & \zeta_{16}^{Mx} \\ \zeta_{21}^{Mx} & \zeta_{22}^{Mx} & \zeta_{23}^{Mx} & \zeta_{24}^{Mx} & \zeta_{25}^{Mx} & \zeta_{26}^{Mx} \\ \zeta_{31}^{Mx} & \zeta_{32}^{Mx} & \zeta_{33}^{Mx} & \zeta_{34}^{Mx} & \zeta_{35}^{Mx} & \zeta_{36}^{Mx} \end{array} \right]$$

$$\zeta_{ip}^{My} = \zeta_{ij1l}^{M} = \left[\begin{array}{cccccc} \zeta_{11}^{My} & \zeta_{12}^{My} & \zeta_{13}^{My} & \zeta_{14}^{My} & \zeta_{15}^{My} & \zeta_{16}^{My} \\ \zeta_{21}^{My} & \zeta_{22}^{My} & \zeta_{23}^{My} & \zeta_{24}^{My} & \zeta_{25}^{My} & \zeta_{26}^{My} \\ \zeta_{31}^{My} & \zeta_{32}^{My} & \zeta_{33}^{My} & \zeta_{34}^{My} & \zeta_{35}^{My} & \zeta_{36}^{My} \end{array} \right]$$

$$\zeta_{ip}^{Mz} = \zeta_{ij1l}^{M} = \left[\begin{array}{cccccc} \zeta_{11}^{Mz} & \zeta_{12}^{Mz} & \zeta_{13}^{Mz} & \zeta_{14}^{Mz} & \zeta_{15}^{Mz} & \zeta_{16}^{Mz} \\ \zeta_{21}^{Mz} & \zeta_{22}^{Mz} & \zeta_{23}^{Mz} & \zeta_{24}^{Mz} & \zeta_{25}^{Mz} & \zeta_{26}^{Mz} \\ \zeta_{31}^{Mz} & \zeta_{32}^{Mz} & \zeta_{33}^{Mz} & \zeta_{34}^{Mz} & \zeta_{35}^{Mz} & \zeta_{36}^{Mz} \end{array} \right]$$

$$\zeta_{ip}^E = \zeta_{ijl}^E = \begin{bmatrix} \zeta_{11}^E & \zeta_{12}^E & \zeta_{13}^E & \zeta_{14}^E & \zeta_{15}^E & \zeta_{16}^E \\ \zeta_{21}^E & \zeta_{22}^E & \zeta_{23}^E & \zeta_{24}^E & \zeta_{25}^E & \zeta_{26}^E \\ \zeta_{31}^E & \zeta_{32}^E & \zeta_{33}^E & \zeta_{34}^E & \zeta_{35}^E & \zeta_{36}^E \end{bmatrix}$$

$$\zeta_{ij}^T = \begin{bmatrix} \zeta_{11}^T & \zeta_{12}^T & \zeta_{13}^T \\ \zeta_{21}^T & \zeta_{22}^T & \zeta_{23}^T \\ \zeta_{31}^T & \zeta_{32}^T & \zeta_{33}^T \end{bmatrix}$$

$$\zeta_{ij}^H = \begin{bmatrix} \zeta_{11}^H & \zeta_{12}^H & \zeta_{13}^H \\ \zeta_{21}^H & \zeta_{22}^H & \zeta_{23}^H \\ \zeta_{31}^H & \zeta_{32}^H & \zeta_{33}^H \end{bmatrix}$$

Also, since δu, δv, δw, $\delta\phi$, $\delta\theta$, and $\delta\gamma$ are arbitrary and independent, we can rewrite the final weak statement in component form as

$$\int_\Omega \delta u \rho \ddot{u} d\Omega + \int_\Omega \{\nabla\delta u\}^T([C^{xx}]\{\nabla u\} + [C^{xy}]\{\nabla v\} + [C^{xz}]\{\nabla w\} + [e^x]^T\{\nabla\phi\} - \{\lambda^x\}\theta - \{\mu^x\}\gamma)d\Omega = \oint_\Gamma \delta u t_x d\Gamma \tag{3.37}$$

$$\int_\Omega \delta v \rho \ddot{v} d\Omega + \int_\Omega \{\nabla\delta v\}^T([C^{yx}]\{\nabla u\} + [C^{yy}]\{\nabla v\} + [C^{yz}]\{\nabla w\} + [e^y]^T\{\nabla\phi\} - \{\lambda^y\}\theta - \{\mu^y\}\gamma)d\Omega = \oint_\Gamma \delta v t_y d\Gamma \tag{3.38}$$

$$\int_\Omega \delta w \rho \ddot{w} d\Omega + \int_\Omega \{\nabla\delta w\}^T([C^{zx}]\{\nabla u\} + [C^{zy}]\{\nabla v\} + [C^{zz}]\{\nabla w\} + [e^z]^T\{\nabla\phi\} - \{\lambda^z\}\theta - \{\mu^z\}\gamma)d\Omega = \oint_\Gamma \delta w t_z d\Gamma \tag{3.39}$$

$$\int_\Omega \{\nabla\delta\phi\}^T([e^x]\{\nabla u\} + [e^y]\{\nabla v\} + [e^z]\{\nabla w\} - [\epsilon]\{\nabla\phi\} + \{r\}\theta + \{\chi\}\gamma)d\Omega = \oint_\Gamma \delta\phi D_n d\Gamma \tag{3.40}$$

$$\int_\Omega \delta\theta T_0(-\{\lambda^x\}^T\{\nabla\dot{u}\} - \{\lambda^y\}^T\{\nabla\dot{v}\} - \{\lambda^z\}^T\{\nabla\dot{w}\} + \{r\}^T\{\nabla\dot{\phi}\} - \frac{\rho c_v}{T_0}\dot{\theta} + d_t\dot{\gamma})d\Omega + \int_\Omega \{\nabla\delta\theta\}^T([\kappa^{Mx}]\{\nabla\nabla u\} + [\kappa^{My}]\{\nabla\nabla v\} + [\kappa^{Mz}]\{\nabla\nabla w\} + [\kappa^E]\{\nabla\nabla\phi\} - [\kappa^T]\{\nabla\theta\} - [\kappa^H]\{\nabla\gamma\})d\Omega = \oint_\Gamma \delta\theta p_n d\Gamma \tag{3.41}$$

$$\int_\Omega (-\delta\gamma\dot{\gamma})d\Omega + \int_\Omega \{\nabla\delta\gamma\}^T([\zeta^{Mx}]\{\nabla\nabla u\} + [\zeta^{My}]\{\nabla\nabla v\} + [\zeta^{Mz}]\{\nabla\nabla w\} + [\zeta^E]\{\nabla\nabla\phi\} - [\zeta^T]\{\nabla\theta\} - [\zeta^H]\{\nabla\gamma\})d\Omega = \oint_\Gamma \delta\gamma q_n d\Gamma \tag{3.42}$$

Now, we can seek an approximate solution to the system of partial differential equations of the hygrothermopiezoelectric medium. Any solution that satifies these

final weak form equations is an approximate solution. In the next section, an analytical model which is the most general form of these solutions is demonstrated first. Then, the more specific solution (or model) suitable for laminated plate problems will be developed further in the next chapter.

3.5.2 Analytical Model

The weak form equations (3.37) to (3.42) can yield approximate solutions to the actual problems. In fact, there can be an infinite number of such solutions depending on the approximation functions (or shape functions) used. Here we seek the solution to the weak form in the most general form namely an analytical model for a homogeneous medium in three dimensions. Essential (or primary) variables to be sought are displacement components (u, v, and w), electric potential (ϕ), temperature (θ), and moisture concentration (γ). We note that once these essential variables are solved, all the non-essential (or secondary) variables can be obtained from the constitutive relations (3.5) to (3.11).

For an analytical model, the approximations of variables u, v, w, ϕ, θ, and γ, and the weight functions δu, δv, δw, $\delta\phi$, $\delta\theta$, and $\delta\gamma$ can be assumed in the following forms [55]:

$$\begin{aligned} a(x,y,z,t) &= N_0^a(x,y,z,t) + \sum_{j=1}^{n_a} N_j^a(x,y,z)a_j(t) \\ &= N_0^a(x,y,z,t) + \lfloor N^a(x,y,z)\rfloor\{a(t)\} \end{aligned} \tag{3.43}$$

$$\delta a = \lfloor N^a(x,y,z)\rfloor^T \tag{3.44}$$

where

$$\lfloor N^a(x,y,z)\rfloor = \lfloor N_1^a(x,y,z)\cdots N_j^a(x,y,z)\cdots N_{n_a}^a(x,y,z)\rfloor$$

$$\{a(t)\} = \left\{ \begin{array}{c} a_1(t) \\ \vdots \\ a_j(t) \\ \vdots \\ a_{n_a}(t) \end{array} \right\}$$

In the above equations, a represents the variables u, v, w, ϕ, θ, and γ, N_0^a is the approximation function with the lowest order possible which satisfies the exact form of the essential boundary condition (i.e., $N_0^a = \hat{a}$ on Γ_1^a), and N_j^a is the j-th term of approximation function which satifies the homogeneous form of the essential boundary condition (i.e., $N_j^a = 0$ on Γ_1^a.) The number of terms of approximation for variable a is denoted by n_a. Then, their derivatives are

$$\{\nabla a\} = \{\nabla N_0^a\} + [\nabla N^a]\{a\} \tag{3.45}$$

$$\{\nabla\nabla a\} = \{\nabla\nabla N_0^a\} + [\nabla\nabla N^a]\{a\} \tag{3.46}$$

$$\dot{a} = \dot{N}_0^a + \lfloor N^a \rfloor \{\dot{a}\} \tag{3.47}$$

$$\ddot{a} = \ddot{N}_0^a + \lfloor N^a \rfloor \{\ddot{a}\} \tag{3.48}$$

$$\{\nabla \dot{a}\} = \{\nabla \dot{N}_0^a\} + [\nabla N^a]\{\dot{a}\} \tag{3.49}$$

$$\{\nabla \delta a\}^T = [\nabla N^a]^T \tag{3.50}$$

where

$$\begin{aligned}
[\nabla N^a] &= \{\nabla \lfloor N^a \rfloor\} = \lfloor \{\nabla N^a\} \rfloor \\
&= \lfloor \{\nabla N_1^a\} \cdots \{\nabla N_j^a\} \cdots \{\nabla N_{n_a}^a\} \rfloor \\
&= \left[\begin{array}{ccccc} N_{1,x}^a & \cdots & N_{j,x}^a & \cdots & N_{n_a,x}^a \\ N_{1,y}^a & \cdots & N_{j,y}^a & \cdots & N_{n_a,y}^a \\ N_{1,z}^a & \cdots & N_{j,z}^a & \cdots & N_{n_a,z}^a \end{array} \right] \\
[\nabla\nabla N^a] &= \{\nabla\nabla \lfloor N^a \rfloor\} = \lfloor \{\nabla\nabla N^a\} \rfloor \\
&= \lfloor \{\nabla\nabla N_1^a\} \cdots \{\nabla\nabla N_j^a\} \cdots \{\nabla\nabla N_{n_a}^a\} \rfloor
\end{aligned}$$

$$= \begin{bmatrix} N^a_{1,xx} & \cdots & N^a_{j,xx} & \cdots & N^a_{n_a,xx} \\ N^a_{1,yy} & \cdots & N^a_{j,yy} & \cdots & N^a_{n_a,yy} \\ N^a_{1,zz} & \cdots & N^a_{j,zz} & \cdots & N^a_{n_a,zz} \\ 2N^a_{1,yz} & \cdots & 2N^a_{j,yz} & \cdots & 2N^a_{n_a,yz} \\ 2N^a_{1,xz} & \cdots & 2N^a_{j,xz} & \cdots & 2N^a_{n_a,xz} \\ 2N^a_{1,xy} & \cdots & 2N^a_{j,xy} & \cdots & 2N^a_{n_a,xy} \end{bmatrix}$$

After we substitute these functions for the variables u, v, w, ϕ, θ, and γ into the weak form equations, we obtain

$$\begin{aligned}
&\int_\Omega \lfloor N^u \rfloor^T \rho(\ddot{N}^u_0 + \lfloor N^u \rfloor \{\ddot{u}\}) d\Omega \\
&+ \int_\Omega [\nabla N^u]^T ([C^{xx}](\{\nabla N^u_0\} + [\nabla N^u]\{u\}) \\
&\qquad +[C^{xy}](\{\nabla N^v_0\} + [\nabla N^v]\{v\}) \\
&\qquad +[C^{xz}](\{\nabla N^w_0\} + [\nabla N^w]\{w\}) \\
&\qquad +[e^x]^T(\{\nabla N^\phi_0\} + [\nabla N^\phi]\{\phi\}) \\
&\qquad -\{\lambda^x\}(N^\theta_0 + \lfloor N^\theta \rfloor \{\theta\}) \\
&\qquad -\{\mu^x\}(N^\gamma_0 + \lfloor N^\gamma \rfloor \{\gamma\})) d\Omega \\
&= \oint_\Gamma \lfloor N^u \rfloor^T t_x d\Gamma \qquad (3.51) \\
&\int_\Omega \lfloor N^v \rfloor^T \rho(\ddot{N}^v_0 + \lfloor N^v \rfloor \{\ddot{v}\}) d\Omega \\
&+ \int_\Omega [\nabla N^v]^T ([C^{yx}](\{\nabla N^u_0\} + [\nabla N^u]\{u\}) \\
&\qquad +[C^{yy}](\{\nabla N^v_0\} + [\nabla N^v]\{v\}) \\
&\qquad +[C^{yz}](\{\nabla N^w_0\} + [\nabla N^w]\{w\}) \\
&\qquad +[e^y]^T(\{\nabla N^\phi_0\} + [\nabla N^\phi]\{\phi\}) \\
&\qquad -\{\lambda^y\}(N^\theta_0 + \lfloor N^\theta \rfloor \{\theta\}) \\
&\qquad -\{\mu^y\}(N^\gamma_0 + \lfloor N^\gamma \rfloor \{\gamma\})) d\Omega \\
&= \oint_\Gamma \lfloor N^v \rfloor^T t_y d\Gamma \qquad (3.52) \\
&\int_\Omega \lfloor N^w \rfloor^T \rho(\ddot{N}^w_0 + \lfloor N^w \rfloor \{\ddot{w}\}) d\Omega \\
&+ \int_\Omega [\nabla N^w]^T ([C^{zx}](\{\nabla N^u_0\} + [\nabla N^u]\{u\})
\end{aligned}$$

$$
\begin{aligned}
&+[C^{zy}](\{\nabla N_0^v\}+[\nabla N^v]\{v\})\\
&+[C^{zz}](\{\nabla N_0^w\}+[\nabla N^w]\{w\})\\
&+[e^z]^T(\{\nabla N_0^\phi\}+[\nabla N^\phi]\{\phi\})\\
&-\{\lambda^z\}(N_0^\theta+\lfloor N^\theta\rfloor\{\theta\})\\
&-\{\mu^z\}(N_0^\gamma+\lfloor N^\gamma\rfloor\{\gamma\}))d\Omega\\
=&\oint_\Gamma \lfloor N^w\rfloor^T t_z d\Gamma \qquad (3.53)\\
\int_\Omega &[\nabla N^\phi]^T([e^x](\{\nabla N_0^u\}+[\nabla N^u]\{u\})\\
&+[e^y](\{\nabla N_0^v\}+[\nabla N^v]\{v\})\\
&+[e^z](\{\nabla N_0^w\}+[\nabla N^w]\{w\})\\
&-[\epsilon](\{\nabla N_0^\phi\}+[\nabla N^\phi]\{\phi\})\\
&+\{r\}(N_0^\theta+\lfloor N^\theta\rfloor\{\theta\})\\
&+\{\chi\}(N_0^\gamma+\lfloor N^\gamma\rfloor\{\gamma\}))d\Omega\\
=&\oint_\Gamma \lfloor N^\phi\rfloor^T D_n d\Gamma \qquad (3.54)\\
\int_\Omega &\lfloor N^\theta\rfloor^T T_0(-\{\lambda^x\}^T(\{\nabla \dot{N}_0^u\}+[\nabla N^u]\{\dot{u}\})\\
&-\{\lambda^y\}^T(\{\nabla \dot{N}_0^v\}+[\nabla N^v]\{\dot{v}\})\\
&-\{\lambda^z\}^T(\{\nabla \dot{N}_0^w\}+[\nabla N^w]\{\dot{w}\})\\
&+\{r\}^T(\{\nabla \dot{N}_0^\phi\}+[\nabla N^\phi]\{\dot{\phi}\})\\
&-\frac{\rho c_v}{T_0}(\dot{N}_0^\theta+\lfloor N^\theta\rfloor\{\dot{\theta}\})\\
&+d_t(\dot{N}_0^\gamma+\lfloor N^\gamma\rfloor\{\dot{\gamma}\}))d\Omega\\
+\int_\Omega &[\nabla N^\theta]^T([\kappa^{Mx}](\{\nabla\nabla N_0^u\}+[\nabla\nabla N^u]\{u\})\\
&+[\kappa^{My}](\{\nabla\nabla N_0^v\}+[\nabla\nabla N^v]\{v\})\\
&+[\kappa^{Mz}](\{\nabla\nabla N_0^w\}+[\nabla\nabla N^w]\{w\})\\
&+[\kappa^E](\{\nabla\nabla N_0^\phi\}+[\nabla\nabla N^\phi]\{\phi\})
\end{aligned}
$$

$$
\begin{aligned}
&-[\kappa^T](\{\nabla N_0^\theta\}+[\nabla N^\theta]\{\theta\}) \\
&-[\kappa^H](\{\nabla N_0^\gamma\}+[\nabla N^\gamma]\{\gamma\}))d\Omega \\
&= \oint_\Gamma \lfloor N^\theta \rfloor^T p_n d\Gamma \qquad (3.55) \\
&\int_\Omega(-\lfloor N^\gamma \rfloor^T(\dot{N}_0^\gamma+\lfloor N^\gamma \rfloor\{\dot{\gamma}\}))d\Omega \\
&+\int_\Omega[\nabla N^\gamma]^T([\zeta^{Mx}](\{\nabla\nabla N_0^u\}+[\nabla\nabla N^u]\{u\}) \\
&\qquad +[\zeta^{My}](\{\nabla\nabla N_0^v\}+[\nabla\nabla N^v]\{v\}) \\
&\qquad +[\zeta^{Mz}](\{\nabla\nabla N_0^w\}+[\nabla\nabla N^w]\{w\}) \\
&\qquad +[\zeta^{E}](\{\nabla\nabla N_0^\phi\}+[\nabla\nabla N^\phi]\{\phi\}) \\
&\qquad -[\zeta^{T}](\{\nabla N_0^\theta\}+[\nabla N^\theta]\{\theta\}) \\
&\qquad -[\zeta^{H}](\{\nabla N_0^\gamma\}+[\nabla N^\gamma]\{\gamma\}))d\Omega \\
&= \oint_\Gamma \lfloor N^\gamma \rfloor^T q_n d\Gamma \qquad (3.56)
\end{aligned}
$$

These equations may be written in a matrix form as

$$
\begin{bmatrix}
[M^{uu}] & [0] & [0] & [0] & [0] & [0] \\
[0] & [M^{vv}] & [0] & [0] & [0] & [0] \\
[0] & [0] & [M^{ww}] & [0] & [0] & [0] \\
[0] & [0] & [0] & [0] & [0] & [0] \\
[0] & [0] & [0] & [0] & [0] & [0] \\
[0] & [0] & [0] & [0] & [0] & [0]
\end{bmatrix}
\begin{Bmatrix}
\{\ddot{u}\} \\ \{\ddot{v}\} \\ \{\ddot{w}\} \\ \{\ddot{\phi}\} \\ \{\ddot{\theta}\} \\ \{\ddot{\gamma}\}
\end{Bmatrix}
$$

$$
+\begin{bmatrix}
[0] & [0] & [0] & [0] & [0] & [0] \\
[0] & [0] & [0] & [0] & [0] & [0] \\
[0] & [0] & [0] & [0] & [0] & [0] \\
[0] & [0] & [0] & [0] & [0] & [0] \\
\left[C^{\theta u}\right] & \left[C^{\theta v}\right] & \left[C^{\theta w}\right] & \left[C^{\theta\phi}\right] & \left[C^{\theta\theta}\right] & \left[C^{\theta\gamma}\right] \\
[0] & [0] & [0] & [0] & [0] & [C^{\gamma\gamma}]
\end{bmatrix}
\begin{Bmatrix}
\{\dot{u}\} \\ \{\dot{v}\} \\ \{\dot{w}\} \\ \{\dot{\phi}\} \\ \{\dot{\theta}\} \\ \{\dot{\gamma}\}
\end{Bmatrix}
$$

$$
+\begin{bmatrix}
[K^{uu}] & [K^{uv}] & [K^{uw}] & \left[K^{u\phi}\right] & \left[K^{u\theta}\right] & [K^{u\gamma}] \\
[K^{vu}] & [K^{vv}] & [K^{vw}] & \left[K^{v\phi}\right] & \left[K^{v\theta}\right] & [K^{v\gamma}] \\
[K^{wu}] & [K^{wv}] & [K^{ww}] & \left[K^{w\phi}\right] & \left[K^{w\theta}\right] & [K^{w\gamma}] \\
\left[K^{\phi u}\right] & \left[K^{\phi v}\right] & \left[K^{\phi w}\right] & \left[K^{\phi\phi}\right] & \left[K^{\phi\theta}\right] & \left[K^{\phi\gamma}\right] \\
\left[K^{\theta u}\right] & \left[K^{\theta v}\right] & \left[K^{\theta w}\right] & \left[K^{\theta\phi}\right] & \left[K^{\theta\theta}\right] & \left[K^{\theta\gamma}\right] \\
[K^{\gamma u}] & [K^{\gamma v}] & [K^{\gamma w}] & \left[K^{\gamma\phi}\right] & \left[K^{\gamma\theta}\right] & [K^{\gamma\gamma}]
\end{bmatrix}
\begin{Bmatrix}
\{u\} \\ \{v\} \\ \{w\} \\ \{\phi\} \\ \{\theta\} \\ \{\gamma\}
\end{Bmatrix}
$$

$$= \left\{ \begin{array}{c} \{F^u\} \\ \{F^v\} \\ \{F^w\} \\ \{F^\phi\} \\ \{F^\theta\} \\ \{F^\gamma\} \end{array} \right\} \tag{3.57}$$

where

$$[K^{uu}] = \int_\Omega [\nabla N^u]^T [C^{xx}] [\nabla N^u] d\Omega$$
$$[K^{uv}] = \int_\Omega [\nabla N^u]^T [C^{xy}] [\nabla N^v] d\Omega$$
$$[K^{uw}] = \int_\Omega [\nabla N^u]^T [C^{xz}] [\nabla N^w] d\Omega$$
$$[K^{u\phi}] = \int_\Omega [\nabla N^u]^T [e^x]^T [\nabla N^\phi] d\Omega$$
$$[K^{u\theta}] = -\int_\Omega [\nabla N^u]^T \{\lambda^x\} \lfloor N^\theta \rfloor d\Omega$$
$$[K^{u\gamma}] = -\int_\Omega [\nabla N^u]^T \{\mu^x\} \lfloor N^\gamma \rfloor d\Omega$$
$$[K^{vu}] = \int_\Omega [\nabla N^v]^T [C^{yx}] [\nabla N^u] d\Omega = [K^{uv}]^T$$
$$[K^{vv}] = \int_\Omega [\nabla N^v]^T [C^{yy}] [\nabla N^v] d\Omega$$
$$[K^{vw}] = \int_\Omega [\nabla N^v]^T [C^{yz}] [\nabla N^w] d\Omega$$
$$[K^{v\phi}] = \int_\Omega [\nabla N^v]^T [e^y]^T [\nabla N^\phi] d\Omega$$
$$[K^{v\theta}] = -\int_\Omega [\nabla N^v]^T \{\lambda^y\} \lfloor N^\theta \rfloor d\Omega$$
$$[K^{v\gamma}] = -\int_\Omega [\nabla N^v]^T \{\mu^y\} \lfloor N^\gamma \rfloor d\Omega$$
$$[K^{wu}] = \int_\Omega [\nabla N^w]^T [C^{zx}] [\nabla N^u] d\Omega = [K^{uw}]^T$$
$$[K^{wv}] = \int_\Omega [\nabla N^w]^T [C^{zy}] [\nabla N^v] d\Omega = [K^{vw}]^T$$
$$[K^{ww}] = \int_\Omega [\nabla N^w]^T [C^{zz}] [\nabla N^w] d\Omega$$
$$[K^{w\phi}] = \int_\Omega [\nabla N^w]^T [e^z]^T [\nabla N^\phi] d\Omega$$
$$[K^{w\theta}] = -\int_\Omega [\nabla N^w]^T \{\lambda^z\} \lfloor N^\theta \rfloor d\Omega$$
$$[K^{w\gamma}] = -\int_\Omega [\nabla N^w]^T \{\mu^z\} \lfloor N^\gamma \rfloor d\Omega$$

$$[K^{\phi u}] = \int_\Omega [\nabla N^\phi]^T [e^x] [\nabla N^u] d\Omega = [K^{u\phi]}]^T$$

$$[K^{\phi v}] = \int_\Omega [\nabla N^\phi]^T [e^y] [\nabla N^v] d\Omega = [K^{v\phi}]^T$$

$$[K^{\phi w}] = \int_\Omega [\nabla N^\phi]^T [e^z] [\nabla N^w] d\Omega = [K^{w\phi}]^T$$

$$[K^{\phi\phi}] = -\int_\Omega [\nabla N^\phi]^T [\epsilon] [\nabla N^\phi] d\Omega$$

$$[K^{\phi\theta}] = \int_\Omega [\nabla N^\phi]^T \{r\} \lfloor N^\theta \rfloor d\Omega$$

$$[K^{\phi\gamma}] = \int_\Omega [\nabla N^\phi]^T \{\chi\} \lfloor N^\gamma \rfloor d\Omega$$

$$[K^{\theta u}] = \int_\Omega [\nabla N^\theta]^T [\kappa^{Mx}] [\nabla\nabla N^u] d\Omega$$

$$[K^{\theta v}] = \int_\Omega [\nabla N^\theta]^T [\kappa^{My}] [\nabla\nabla N^v] d\Omega$$

$$[K^{\theta w}] = \int_\Omega [\nabla N^\theta]^T [\kappa^{Mz}] [\nabla\nabla N^w] d\Omega$$

$$[K^{\theta\phi}] = \int_\Omega [\nabla N^\theta]^T [\kappa^E] [\nabla\nabla N^\phi] d\Omega$$

$$[K^{\theta\theta}] = -\int_\Omega [\nabla N^\theta]^T [\kappa^T] [\nabla N^\theta] d\Omega$$

$$[K^{\theta\gamma}] = -\int_\Omega [\nabla N^\theta]^T [\kappa^H] [\nabla N^\gamma] d\Omega$$

$$[K^{\gamma u}] = \int_\Omega [\nabla N^\gamma]^T [\zeta^{Mx}] [\nabla\nabla N^u] d\Omega$$

$$[K^{\gamma v}] = \int_\Omega [\nabla N^\gamma]^T [\zeta^{My}] [\nabla\nabla N^v] d\Omega$$

$$[K^{\gamma w}] = \int_\Omega [\nabla N^\gamma]^T [\zeta^{Mz}] [\nabla\nabla N^w] d\Omega$$

$$[K^{\gamma\phi}] = \int_\Omega [\nabla N^\gamma]^T [\zeta^E] [\nabla\nabla N^\phi] d\Omega$$

$$[K^{\gamma\theta}] = -\int_\Omega [\nabla N^\gamma]^T [\zeta^T] [\nabla N^\theta] d\Omega$$

$$[K^{\gamma\gamma}] = -\int_\Omega [\nabla N^\gamma]^T [\zeta^H] [\nabla N^\gamma] d\Omega$$

$$[M^{uu}] = \int_\Omega \rho \lfloor N^u \rfloor^T \lfloor N^u \rfloor d\Omega$$

$$[M^{vv}] = \int_\Omega \rho \lfloor N^v \rfloor^T \lfloor N^v \rfloor d\Omega$$

$$[M^{ww}] = \int_\Omega \rho \lfloor N^w \rfloor^T \lfloor N^w \rfloor d\Omega$$

$$[C^{\theta u}] = -\int_\Omega T_0 \lfloor N^\theta \rfloor^T \{\lambda^x\}^T [\nabla N^u] d\Omega = T_0 [K^{u\theta}]^T$$

$$[C^{\theta v}] = -\int_\Omega T_0 \lfloor N^\theta \rfloor^T \{\lambda^y\}^T [\nabla N^v] d\Omega = T_0 [K^{v\theta}]^T$$

$$[C^{\theta w}] = -\int_\Omega T_0 \lfloor N^\theta \rfloor^T \{\lambda^z\}^T [\nabla N^w] d\Omega = T_0 [K^{w\theta}]^T$$
$$[C^{\theta\phi}] = \int_\Omega T_0 \lfloor N^\theta \rfloor^T \{r\}^T [\nabla N^\phi] d\Omega = T_0 [K^{\phi\theta}]^T$$
$$[C^{\theta\theta}] = -\int_\Omega \rho c_v \lfloor N^\theta \rfloor^T \lfloor N^\theta \rfloor d\Omega$$
$$[C^{\theta\gamma}] = \int_\Omega T_0 d_t \lfloor N^\theta \rfloor^T \lfloor N^\gamma \rfloor d\Omega$$
$$[C^{\gamma\gamma}] = -\int_\Omega \lfloor N^\gamma \rfloor^T \lfloor N^\gamma \rfloor d\Omega$$

Also, the elements of the force vector $\{F\}$ are computed from the specified essential and natural boundary conditions (3.12) to (3.19). The natural boundary conditions are the specified surface traction components ($\hat{t}_x$, $\hat{t}_y$, and $\hat{t}_z$), normal electric displacement ($\hat{D}_n$), normal heat flux ($\hat{p}_n$), and normal moisture flux ($\hat{q}_n$). We let $\{F_0^u\}$, $\{F_0^v\}$, $\{F_0^w\}$, $\{F_0^\phi\}$, $\{F_0^\theta\}$, and $\{F_0^\gamma\}$ represent the effects of the specified essential boundary conditions to the force vector of the variables u, v, w, ϕ, θ, and γ, respectively. Then, we can write

$$\{F^u\} = \oint_\Gamma \lfloor N^u \rfloor^T t_x d\Gamma - \{F_0^u\} = \int_{\Gamma_2^u} \lfloor N^u \rfloor^T \hat{t}_x d\Gamma - \{F_0^u\}$$
$$\{F^v\} = \oint_\Gamma \lfloor N^v \rfloor^T t_y d\Gamma - \{F_0^v\} = \int_{\Gamma_2^v} \lfloor N^v \rfloor^T \hat{t}_y d\Gamma - \{F_0^v\}$$
$$\{F^w\} = \oint_\Gamma \lfloor N^w \rfloor^T t_z d\Gamma - \{F_0^w\} = \int_{\Gamma_2^w} \lfloor N^w \rfloor^T \hat{t}_z d\Gamma - \{F_0^w\}$$
$$\{F^\phi\} = \oint_\Gamma \lfloor N^\phi \rfloor^T D_n d\Gamma - \{F_0^\phi\} = \int_{\Gamma_2^\phi} \lfloor N^\phi \rfloor^T \hat{D}_n d\Gamma - \{F_0^\phi\}$$
$$\{F^\theta\} = \oint_\Gamma \lfloor N^\theta \rfloor^T p_n d\Gamma - \{F_0^\theta\} = \int_{\Gamma_2^\theta} \lfloor N^\theta \rfloor^T \hat{p}_n d\Gamma - \{F_0^\theta\}$$
$$\{F^\gamma\} = \oint_\Gamma \lfloor N^\gamma \rfloor^T q_n d\Gamma - \{F_0^\gamma\} = \int_{\Gamma_2^\gamma} \lfloor N^\gamma \rfloor^T \hat{q}_n d\Gamma - \{F_0^\gamma\}$$

where

$$\begin{aligned}\{F_0^u\} = &\int_\Omega \rho \lfloor N^u \rfloor^T \ddot{N}_0^u d\Omega \\ &+ \int_\Omega [\nabla N^u]^T ([C^{xx}]\{\nabla N_0^u\} + [C^{xy}]\{\nabla N_0^v\} + [C^{xz}]\{\nabla N_0^w\} \\ &\qquad + [e^x]^T \{\nabla N_0^\phi\} - \{\lambda^x\} N_0^\theta - \{\mu^x\} N_0^\gamma) d\Omega\end{aligned}$$
$$\{F_0^v\} = \int_\Omega \rho \lfloor N^v \rfloor^T \ddot{N}_0^v d\Omega$$

$$+\int_\Omega [\nabla N^v]^T([C^{yx}]\{\nabla N_0^u\}+[C^{yy}]\{\nabla N_0^v\}+[C^{yz}]\{\nabla N_0^w\}$$
$$+[e^y]^T\{\nabla N_0^\phi\}-\{\lambda^y\}N_0^\theta-\{\mu^y\}N_0^\gamma)d\Omega$$

$$\{F_0^w\}=\int_\Omega \rho\lfloor N^w\rfloor^T\ddot{N}_0^w d\Omega$$
$$+\int_\Omega [\nabla N^w]^T([C^{zx}]\{\nabla N_0^u\}+[C^{zy}]\{\nabla N_0^v\}+[C^{zz}]\{\nabla N_0^w\}$$
$$+[e^z]^T\{\nabla N_0^\phi\}-\{\lambda^z\}N_0^\theta-\{\mu^z\}N_0^\gamma)d\Omega$$

$$\{F_0^\phi\}=\int_\Omega [\nabla N^\phi]^T([e^x]\{\nabla N_0^u\}+[e^y]\{\nabla N_0^v\}+[e^z]\{\nabla N_0^w\}$$
$$-[\epsilon]\{\nabla N_0^\phi\}+\{r\}N_0^\theta+\{\chi\}N_0^\gamma)d\Omega$$

$$\{F_0^\theta\}=\int_\Omega T_0\lfloor N^\theta\rfloor^T(-\{\lambda^x\}^T\{\nabla\dot{N}_0^u\}-\{\lambda^y\}^T\{\nabla\dot{N}_0^v\}-\{\lambda^z\}^T\{\nabla\dot{N}_0^w\}$$
$$+\{r\}^T\{\nabla\dot{N}_0^\phi\}-\frac{\rho c_v}{T_0}\dot{N}_0^\theta+d_t\dot{N}_0^\gamma)d\Omega$$
$$+\int_\Omega [\nabla N^\theta]^T([\kappa^{Mx}]\{\nabla\nabla N_0^u\}+[\kappa^{My}]\{\nabla\nabla N_0^v\}+[\kappa^{Mz}]\{\nabla\nabla N_0^w\}$$
$$+[\kappa^E]\{\nabla\nabla N_0^\phi\}-[\kappa^T]\{\nabla N_0^\theta\}-[\kappa^H]\{\nabla N_0^\gamma\})d\Omega$$

$$\{F_0^\gamma\}=\int_\Omega(-\lfloor N^\gamma\rfloor^T\dot{N}_0^\gamma)d\Omega$$
$$+\int_\Omega [\nabla N^\gamma]^T([\zeta^{Mx}]\{\nabla\nabla N_0^u\}+[\zeta^{My}]\{\nabla\nabla N_0^v\}+[\zeta^{Mz}]\{\nabla\nabla N_0^w\}$$
$$+[\zeta^E]\{\nabla\nabla N_0^\phi\}-[\zeta^T]\{\nabla N_0^\theta\}-[\zeta^H]\{\nabla N_0^\gamma\})d\Omega$$

The equation (3.57) is written in a standard matrix form for transient problems. For a steady-state problem, the first two terms are zero, and we solve a linear system equation $[K]\{X\}=\{F\}$ for the unknown vectors $\{u\}$, $\{v\}$, $\{w\}$, $\{\phi\}$, $\{\theta\}$, and $\{\gamma\}$. For a transient problem, the system of ordinary differential equations cannot be uncoupled (i.e., the coefficient matrices $[K]$ and $[C]$ are not diagonalizable) because of the non-symmetric forms of the coefficient matrices. Therefore, in this research, we choose to employ a direct step-by-step integration method (the Newmark-beta method) [2, 14, 31] to solve the transient problem subject to the specified initial conditions (3.20) to (3.24).

The analytical model just shown is developed for a homogeneous anisotropic hy-

grothermopiezoelectric medium in three-dimensions. The model which is applicable to solve our problems of multilayered laminated plates is needed to be developed slightly further. In this research, a discrete-layer model is developed and implemented to solve problems of adaptive composite plates. In the discrete-layer model, the structural behavior in 3-D space is approximated by products of in-plane shape functions and through-thickness shape functions. The shape functions of all unknowns in the direction through the thickness of the plate are assumed piecewise linear and separated from the ones in the perpendicular plane. The in-plane variables are approximated by different types of shape functions, and they are shown in details in the following chapter.

CHAPTER 4

NUMERICAL MODEL AND EXAMPLES

In problems of multilayered composite plates, the laminated structures are composed of layers of different material properties, either different materials or different alignments of the same material. Unlike the homogeneous plate structures, the response of the laminate in the direction through the thickness is not completely continuous, for example, strains. This is due to the continuous stresses but different (or discontinuous) material properties in this direction. As a result, the transverse shear strains and the transverse normal strains cannot be continuous at the interfaces of these layers of different properties. These through-thickness effects cannot be described by any of those equivalent-single-layer theories (e.g., classical lamination theory, first- and higher-order shear deformation theories) which are analysis methods in two dimensions. Therefore, to overcome these limitations, a discrete-layer model in three dimensions is developed here in this research. This model is capable of representing the discontinuity behavior in the through-thickness direction, and a more accurate result to the laminated plate problem can be obtained.

In this chapter, we first derive the discrete-layer model for solving the laminated plate problems under the effects of elastic, electric, temperature, and moisture fields simultaneously. Then, the model is applied to solve several example problems of laminated composite plates subject to various types of excitations in both steady-state and transient cases.

4.1 Discrete-Layer Model

In the previous chapter, an analytical model has been developed for a homogeneous anisotropic hygrothermopiezoelectric medium. Now, to be able to apply it to problems of laminated plates, we modify the previous model by imposing the layerwise theory [51, 56, 57], yielding a discrete-layer model. This new model is capable of representing the variation in the direction through the thickness of a multilayered composite plate. By applying the method of separation of variables, the approximation functions (or shape functions) in three dimensions are separated to be products of 1-D functions in the through-thickness direction z and 2-D functions in x-y plane.

The approximate solutions for the displacement components (u, v, and w), electric potential (ϕ), temperature change (θ), and moisture change (γ) are sought in the following form:

$$a(x,y,z,t) = \sum_{k=1}^{m_a} \sum_{l=1}^{n_a} N_{kl}^a(x,y,z) a_{kl}(t) = \lfloor N^a(x,y,z) \rfloor \{a(t)\} \tag{4.1}$$

and the weight functions are used as

$$\delta a = \lfloor N^a(x,y,z) \rfloor^T \tag{4.2}$$

where

$$\lfloor N^a(x,y,z) \rfloor = \lfloor N_{11}^a(x,y,z) \cdots N_{kl}^a(x,y,z) \cdots N_{m_a n_a}^a(x,y,z) \rfloor \tag{4.3}$$

$$\{a(t)\} = \left\{ \begin{array}{c} a_{11}(t) \\ \vdots \\ a_{kl}(t) \\ \vdots \\ a_{m_a n_a}(t) \end{array} \right\} \tag{4.4}$$

It is noted that a and δa represent the variables u, v, w, ϕ, θ, and γ and the associated weight functions. Their derivatives then become

$$\{\nabla a\} = [\nabla N^a]\{a\} \tag{4.5}$$

$$\{\nabla\nabla a\} = [\nabla\nabla N^a]\{a\} \tag{4.6}$$

$$\dot{a} = \lfloor N^a \rfloor \{\dot{a}\} \tag{4.7}$$

$$\ddot{a} = \lfloor N^a \rfloor \{\ddot{a}\} \tag{4.8}$$

$$\{\nabla\dot{a}\} = [\nabla N^a]\{\dot{a}\} \tag{4.9}$$

$$\{\nabla\delta a\}^T = [\nabla N^a]^T \tag{4.10}$$

where

$$\begin{aligned}
[\nabla N^a] &= \lfloor \{\nabla N^a_{11}\} \cdots \{\nabla N^a_{kl}\} \cdots \{\nabla N^a_{m_a n_a}\} \rfloor \\
&= \begin{bmatrix} N^a_{11,x} & \cdots & N^a_{kl,x} & \cdots & N^a_{m_a n_a,x} \\ N^a_{11,y} & \cdots & N^a_{kl,y} & \cdots & N^a_{m_a n_a,y} \\ N^a_{11,z} & \cdots & N^a_{kl,z} & \cdots & N^a_{m_a n_a,z} \end{bmatrix}
\end{aligned} \tag{4.11}$$

$$\begin{aligned}
[\nabla\nabla N^a] &= \lfloor \{\nabla\nabla N^a_{11}\} \cdots \{\nabla\nabla N^a_{kl}\} \cdots \{\nabla\nabla N^a_{m_a n_a}\} \rfloor \\
&= \begin{bmatrix} N^a_{11,xx} & \cdots & N^a_{kl,xx} & \cdots & N^a_{m_a n_a,xx} \\ N^a_{11,yy} & \cdots & N^a_{kl,yy} & \cdots & N^a_{m_a n_a,yy} \\ N^a_{11,zz} & \cdots & N^a_{kl,zz} & \cdots & N^a_{m_a n_a,zz} \\ 2N^a_{11,yz} & \cdots & 2N^a_{kl,yz} & \cdots & 2N^a_{m_a n_a,yz} \\ 2N^a_{11,xz} & \cdots & 2N^a_{kl,xz} & \cdots & 2N^a_{m_a n_a,xz} \\ 2N^a_{11,xy} & \cdots & 2N^a_{kl,xy} & \cdots & 2N^a_{m_a n_a,xy} \end{bmatrix}
\end{aligned} \tag{4.12}$$

In the discrete-layer model, the approximation function $N^a_{kl}(x,y,z)$ in 3-D space is separated to be a product of a 2-D function in the x-y plane and a 1-D function in the z-direction as

$$N^a_{kl}(x,y,z) = \Psi^a_k(x,y)\Xi^a_l(z) \tag{4.13}$$

where $\Psi^a_k(x,y)$ is the k-th term of the approximation function in the x-y plane, and $\Xi^a_l(z)$ is the l-th term of the approximation function in the z-direction. Then their derivatives are

$$\{\nabla N^a_{kl}\} = \begin{Bmatrix} N^a_{kl,x} \\ N^a_{kl,y} \\ N^a_{kl,z} \end{Bmatrix} = \begin{Bmatrix} \Psi^a_{k,x}\Xi^a_l \\ \Psi^a_{k,y}\Xi^a_l \\ \Psi^a_k\Xi^a_{l,z} \end{Bmatrix} \tag{4.14}$$

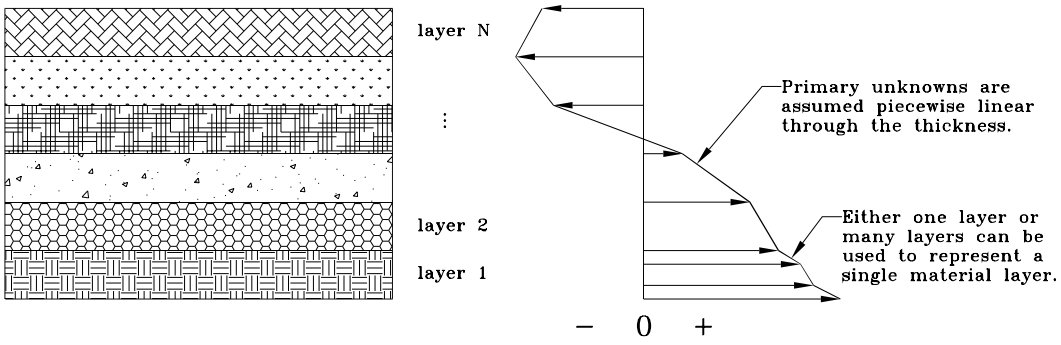

Figure 4.1: Discrete-layer model in the through-thickness direction.

$$\{\nabla\nabla N^a_{kl}\} = \left\{ \begin{array}{c} N^a_{kl,xx} \\ N^a_{kl,yy} \\ N^a_{kl,zz} \\ 2N^a_{kl,yz} \\ 2N^a_{kl,xz} \\ 2N^a_{kl,xy} \end{array} \right\} = \left\{ \begin{array}{c} \Psi^a_{k,xx}\Xi^a_l \\ \Psi^a_{k,yy}\Xi^a_l \\ \Psi^a_k\Xi^a_{l,zz} \\ 2\Psi^a_{k,y}\Xi^a_{l,z} \\ 2\Psi^a_{k,x}\Xi^a_{l,z} \\ 2\Psi^a_{k,xy}\Xi^a_l \end{array} \right\} \tag{4.15}$$

In the through-thickness direction (z-direction), since only C^0-continuity is required, the approximation functions are assumed as layerwise Lagrange interpolation functions (see Figure 4.1). The same functions are used for all variables u, v, w, ϕ, θ, and γ, that is, $\Xi^u_j(z) = \Xi^v_j(z) = \Xi^w_j(z) = \Xi^\phi_j(z) = \Xi^\theta_j(z) = \Xi^\gamma_j(z) = \Xi_j(z)$. Employing the linear interpolation functions, a laminated plate of N layers constitutes a number of planes $n = N + 1$. In each layer, there are two non-zero shape functions, and the ones for j-th layer are

$$\Xi_j(z) = \frac{z_{j+1} - z}{h_j} \tag{4.16}$$

$$\Xi_{j+1}(z) = \frac{z - z_j}{h_j} \tag{4.17}$$

where $j = 1, ..., N$, N is the total number of layers, and $h_j = z_{j+1} - z_j$.

For the domains in the x-y plane of the laminated plate structure, the approximation functions are employed as two approaches: the use of analytical functions (e.g., trigonometric or polynomial functions) and the use of the finite element functions. These two approaches each have some advantages over the other. The use of

analytical functions can provide a far more accurate solution than the finite element functions. The problem is that this approach can be applied only to the laminated plates with simple geometry and boundary conditions, for example, a rectangular plate with simple supports. Unfortunately, many actual plate structures we have to deal with do not have those simple characteristics, and the analytical function approach is therefore not applicable. Hence, the second approach, using the finite element functions, which has no limitation on the types of geometry and boundary conditions, is needed to solve such structures.

In the analytical function approach, the domains of investigation are $0 \leq x \leq L_x$, $0 \leq y \leq L_y$, $0 \leq z \leq h$, and $t \geq 0$. Here a limitation is made so that the essential boundary conditions, if any, in the x-y plane are allowed only in homogeneous forms. The approximation functions in the x-y plane $\Psi_k^a(x, y)$ must satisfy the homogeneous form of the in-plane essential boundary conditions. These functions can be used as trigonometric or polynomial functions. They are selected differently for each particular problem depending on the prescribed in-plane boundary conditions. These procedures are shown in details for each of the numerical examples in the next section.

For the finite element function approach, the variables in the in-plane domains (x- and y-directions) are approximated by 2-D finite element functions. With the use of such functions, the problems of laminated plates with any type of geometry (i.e., irregular shape or with a cutout) and boundary conditions can now be modeled. In this method, the domains in the x-y plane are discretized into meshes of nodes and elements. Here, identically for all variables u, v, w, ϕ, θ, and γ, the in-plane shape function $\Psi_k(x, y)$ is used as an 8-noded serendipity quadrilateral element. For more details of these elements and their shape functions, see Reddy [58]. Accuracy of the

finite element method depends strongly on the domain discretization process. That is, better accuracy can be obtained by refining the finite element meshes.

After substituting these approximation functions (or shape functions) into the final weak form equations (3.37) to (3.42), the discrete-layer model yields a matrix equation in the same general form as those for the analytical model, equation (3.57). Furthermore, the matrices $[K]$, $[M]$, and $[C]$, and the vector $\{F\}$ share the same general forms with those of the analytical model except that the vectors $\{F_0^u\}$, $\{F_0^v\}$, $\{F_0^w\}$, $\{F_0^\phi\}$, $\{F_0^\theta\}$, and $\{F_0^\gamma\}$ are all zeroes for the discrete-layer model. Imposing the boundary conditions and initial conditions allows us to solve for the primary unknowns $\{u\}$, $\{v\}$, $\{w\}$, $\{\phi\}$, $\{\theta\}$, and $\{\gamma\}$. The transient problems are solved by a direct step-by-step integration using the Newmark beta method [2, 14, 31].

Once the essential variables are obtained, the non-essential variables can be computed from the constitutive relations. Normally, the weak form equations (3.37) to (3.42) yield the solutions which satisfy only the essential boundary conditions. The natural boundary conditions are relaxed and hence are satisfied only in an average sense, not pointwise on the solid boundary. Moreover, in the discrete-layer model, the essential variables are C^0-continuous through the thickness. As a result, the non-essential variables, which are products of the derivatives of the essential variables, are not continuous; the continuity is violated at the layer interfaces. Therefore, the values for these non-essential variables are computed only at mid-height of each layer.

4.2 Numerical Results Using In-Plane Analytical Functions

We demonstrate three numerical problems using the discrete-layer model with in-plane analytical functions. The first two problems compare the results of the discrete-layer model with available exact solutions. The steady-state problem of a simply-supported laminated piezoelectric plate with applied load and applied electric po-

tential is investigated first. Next, the transient problem of coupled diffusion of heat and moisture fields in an infinite plate is examined. The last example problem illustrates the behavior of a simply-supported graphite-epoxy/PZT-4 laminated plate under specified steady-state and transient conditions of surface traction, electric potential, temperature, and moisture.

4.2.1 Example 1: Simply-Supported Laminated Piezoelectric Plate

This problem is intended to verify the discrete-layer model developed in this study by comparing the results with the exact solutions by Heyliger [28]. Two-layered laminated composite plates with rectangular geometry $L_x = 2L_y$ and simply-supported boundary conditions are considered. The laminates are composed of piezoelectric materials, PVDF at the bottom and PZT-4 on the top with same thickness of 0.0025 m for both layers. Aspect ratios of $L_x/h = 4$ and 10 are examined. The essential variables of interest here are displacement components (u, v and w) and electric potential (ϕ). Each geometry is subjected to two types of steady-state excitation: applied transverse load of $\hat{t}_z = \sin(\pi x/L_x)\sin(\pi y/L_y)$ on top surface with electric potential held at zero on top and bottom surfaces, and applied electric potential of $\hat{\phi} = \sin(\pi x/L_x)\sin(\pi y/L_y)$ on the top surface with the electric potential held at zero on the bottom surface. The material properties of PVDF are as follows: elastic constants (in GPa) $C_{11} = 238.0$, $C_{22} = 23.6$, $C_{33} = 10.6$, $C_{12} = 3.98$, $C_{13} = 2.19$, $C_{23} = 1.92$, $C_{44} = 2.15$, $C_{55} = 4.4$, $C_{66} = 6.43$; piezoelectric constants (in C/m^2) $e_{15} = e_{24} = -0.01$, $e_{31} = -0.13$, $e_{32} = -0.14$, $e_{33} = -0.28$; and relative permittivities $\epsilon_{11}/\epsilon_0 = 12.5$, $\epsilon_{22}/\epsilon_0 = \epsilon_{33}/\epsilon_0 = 11.98$. PZT-4 has the following properties: elastic constants (in GPa) $C_{11} = C_{22} = 139.0$, $C_{33} = 115.0$, $C_{12} = 77.8$, $C_{13} = C_{23} = 74.3$, $C_{44} = C_{55} = 25.6$, $C_{66} = 30.6$; piezoelectric constants (in C/m^2) $e_{15} = e_{24} = 12.72$,

$e_{31} = e_{32} = -5.20$, $e_{33} = 15.08$; and relative permittivities $\epsilon_{11}/\epsilon_0 = \epsilon_{22}/\epsilon_0 = 1475$, $\epsilon_{33}/\epsilon_0 = 1300$, where the permittivity of free space is $\epsilon_0 = 8.85 \times 10^{-12}$ F/m.

The essential boundary conditions of the simply-supported laminates are given as follows:

$$u(x,0,z) = u(x,L_y,z) = 0 \tag{4.18}$$

$$v(0,y,z) = v(L_x,y,z) = 0 \tag{4.19}$$

$$w(0,y,z) = w(L_x,y,z) = w(x,0,z) = w(x,L_y,z) = 0 \tag{4.20}$$

$$\phi(0,y,z) = \phi(L_x,y,z) = \phi(x,0,z) = \phi(x,L_y,z) = 0 \tag{4.21}$$

Because of the nature of all the loadings applied, one-term in-plane approximations can be used. The shape functions for the discrete-layer model satisfying the above essential boundary conditions are taken as

$$\Psi^u(x,y) = \cos(\frac{\pi x}{L_x})\sin(\frac{\pi y}{L_y}) \tag{4.22}$$

$$\Psi^v(x,y) = \sin(\frac{\pi x}{L_x})\cos(\frac{\pi y}{L_y}) \tag{4.23}$$

$$\Psi^w(x,y) = \sin(\frac{\pi x}{L_x})\sin(\frac{\pi y}{L_y}) \tag{4.24}$$

$$\Psi^\phi(x,y) = \sin(\frac{\pi x}{L_x})\sin(\frac{\pi y}{L_y}) \tag{4.25}$$

First, a convergence study of the discrete-layer model is examined for the case of applied load on the laminate with $L_x/h = 4$. The through-thickness domain z is discretized into various numbers of sublayers of equal thickness. Results for the cases of 2, 4, 8, 16, 32, and 64 sublayers are shown in Table 4.1. Maximum values for both essential variables (u, v, w, and ϕ) and nonessential variables (σ_x, σ_y, σ_z, σ_{xy}, σ_{yz}, σ_{xz}, and D_z) are given at the top, bottom, and mid-plane levels. Since the discrete-layer model has C^0-continuity (i.e., only the essential variables are enforced, whereas the nonessential variables are relaxed) in the through-thickness direction, the

Number of sub-layers	2	4	8	16	32	64
At top surface:						
u ($\times 10^{-14}$)	-5.0585	-5.8069	-6.1322	-6.2269	-6.2516	-6.2578
v ($\times 10^{-14}$)	-7.3863	-8.8216	-9.4128	-9.5846	-9.6293	-9.6406
w ($\times 10^{-13}$)	2.9327	3.1508	3.2501	3.2796	3.2873	3.2893
σ_x	1.4073	3.0015	3.1373	3.1975	3.2155	3.2207
σ_y	0.9527	4.1115	4.3222	4.4289	4.4621	4.4719
σ_{xy}	-0.2536	-0.9488	-1.0149	-1.0499	-1.0611	-1.0643
D_z ($\times 10^{-10}$)	2.3092	2.6158	2.4872	2.3885	2.3543	2.3446
At bottom surface:						
u ($\times 10^{-14}$)	1.7753	2.9844	3.3912	3.5101	3.5411	3.5490
v ($\times 10^{-14}$)	5.4989	8.2796	9.1717	9.4252	9.4908	9.5074
w ($\times 10^{-13}$)	2.4204	2.6945	2.8053	2.8378	2.8463	2.8485
σ_x	-1.4628	-0.8280	-1.2474	-1.3763	-1.4180	-1.4299
σ_y	-0.9666	-0.4511	-0.6413	-0.6951	-0.7113	-0.7158
σ_{xy}	0.2259	0.1007	0.1479	0.1618	0.1661	0.1674
D_z ($\times 10^{-13}$)	-791.29	-2.7778	-1.9758	-1.8601	-1.8600	-1.8652
At mid-plane:						
ϕ ($\times 10^{-5}$)	1.7393	1.2688	1.1484	1.1175	1.1096	1.1077
σ_z	0.3611	0.2921	0.2514	0.2376	0.2337	0.2327
σ_{xz}	0.3186	0.3965	0.3900	0.3763	0.3671	0.3619
σ_{yz}	0.4773	0.5652	0.5135	0.4634	0.4325	0.4156

Table 4.1: Convergence study of the discrete-layer model by varying the number of sub-layers used in analyzing a laminated plate.

results for nonessential variables are discontinuous, and they do not satisfy the natural boundary conditions at the sublayer interfaces, nor at the top and bottom surfaces. Therefore, these values are first computed at the mid-height of each sublayer. Then, the values elsewhere through the thickness are calculated by linear interpolation and extrapolation. From Table 4.1, doubling the number of sublayers from 32 to 64 results in less than 0.3% and 0.9% changes in all the essential and nonessential variables, respectively, except for 1.4% in σ_{xz} and 3.9% for σ_{yz}. Thus, the discretization of 64 subayers is used for the bulk of the examples.

For this simply-supported laminate problem, using the discretization of 64 sublayers yields 260 unknowns in the discrete-layer model. Results from the discrete-layer

	$L_x/h = 4$		$L_x/h = 10$	
	Exact	DLM	Exact	DLM
At top surface:				
u ($\times 10^{-14}$)	-6.2574	-6.2578	-87.000	-87.036
v ($\times 10^{-14}$)	-9.6408	-9.6406	-111.86	-111.91
w ($\times 10^{-13}$)	3.2885	3.2893	66.004	66.021
σ_x	3.2246	3.2207	13.142	13.124
σ_y	4.4761	4.4719	18.397	18.385
σ_{xy}	-1.0649	-1.0643	-5.4961	-5.4982
D_z ($\times 10^{-10}$)	2.3409	2.3446	2.0111	2.0100
At bottom surface:				
u ($\times 10^{-14}$)	3.5524	3.5490	70.679	70.687
v ($\times 10^{-14}$)	9.5134	9.5074	200.57	200.60
w ($\times 10^{-13}$)	2.8503	2.8485	65.167	65.178
σ_x	-1.4347	-1.4299	-11.463	-11.460
σ_y	-0.71755	-0.71583	-6.0339	-6.0329
σ_{xy}	0.16785	0.16737	1.3814	1.3812
D_z ($\times 10^{-13}$)	-1.7048	-1.8652	82.096	81.268
At mid-plane:				
ϕ ($\times 10^{-5}$)	1.1147	1.1077	11.675	11.696
σ_z	0.23228	0.23268	0.35705	0.35733
σ_{xz}	0.35629	0.36192	1.1491	1.1573
σ_{yz}	0.39776	0.41562	1.3367	1.3601

Table 4.2: Comparison of exact and discrete-layer model results for the case of applied load on the laminated piezoelectric plates.

model and the exact solutions are compared in Table 4.2 and 4.3. Table 4.2 shows the results for the applied load case, and Table 4.3 for the applied potential case. Maximum values of displacement, in-plane stresses, and normal electric displacement are given at the top and bottom surfaces, with the electric potential and transverse stresses at mid-plane. In the discrete-layer model, stresses and electric displacement are computed at the mid-level of each sublayer. The values at top, bottom, and mid-plane are then obtained from linear interpolation or extrapolation of the two adjacent levels. The results from the discrete-layer model are in excellent agreement with the exact solutions. The agreements of the primary unknowns are within 0.63% for the

	$L_x/h = 4$		$L_x/h = 10$	
	Exact	DLM	Exact	DLM
At top surface:				
u ($\times 10^{-11}$)	-6.7845	-6.7978	-3.5347	-3.5426
v ($\times 10^{-11}$)	-13.885	-13.908	-7.6708	-7.6851
w ($\times 10^{-10}$)	-2.3409	-2.3422	-2.0111	-2.0083
σ_x	-1941.7	-1953.2	-364.25	-366.30
σ_y	74.713	66.822	89.578	88.489
σ_{xy}	-1319.6	-1321.7	-283.40	-283.97
D_z ($\times 10^{-7}$)	-46.248	-46.254	-9.5036	-9.5042
At bottom surface:				
u ($\times 10^{-11}$)	-1.8380	-1.8352	-1.6402	-1.6382
v ($\times 10^{-11}$)	-4.5792	-4.5729	-4.2402	-4.2343
w ($\times 10^{-10}$)	-1.6239	-1.6222	-2.0599	-2.0578
σ_x	721.50	718.75	237.96	237.61
σ_y	325.25	324.24	95.501	95.385
σ_{xy}	-83.379	-83.094	-30.384	-30.335
D_z ($\times 10^{-8}$)	-2.6329	-2.6344	-4.1175	-4.1195
At mid-plane:				
ϕ	0.65943	0.65977	0.92243	0.92253
σ_z	-66.387	-66.248	-3.7377	-3.7312
σ_{xz}	-40.090	-39.006	-6.9023	-6.7799
σ_{yz}	-45.704	-42.134	-4.5247	-4.0824

Table 4.3: Comparison of exact and discrete-layer model results for the case of applied potential on the laminated piezoelectric plates.

applied load case and 0.22% for the applied potential case.

4.2.2 Example 2: Coupled Heat and Moisture Diffusions of an Infinite Plate

This example problem demonstrates the coupled diffusion of heat and moisture in an infinite plate subject to changes in temperature and moisture on the top and bottom surfaces. Only temperature (θ) and moisture concentration (γ) are essential variables to be considered. A single layer of graphite-epoxy composite, 0.001 m thick, is considered. Two types of excitation are investigated: a sudden change of a unit moisture concentration and a sudden change of a unit temperature on the top and

bottom surfaces (i.e., $\hat{\gamma} = 1.0$ kg/m^3, $z = 0$ and h, $t > 0$ for the case of change in moisture, and $\hat{\theta} = 1.0$ K, $z = 0$ and h, $t > 0$ for the case of change in temperature). Material properties of graphite-epoxy are assumed as follows [71]: $\rho = 1600$ kg/m^3; $c_v = 1000$ Nm/kgK; $\kappa_{11}^T = \kappa_{22}^T = \kappa_{33}^T = 4.090 \times 10^{-7}$ N/sK; $\kappa_{11}^H = \kappa_{22}^H = \kappa_{33}^H = 8.396 \times 10^{-8}$ m^4/s^3; $\zeta_{11}^T = \zeta_{22}^T = \zeta_{33}^T = 3.118 \times 10^{-14}$ kg/mKs; and $\zeta_{11}^H = \zeta_{22}^H = \zeta_{33}^H = 2.556 \times 10^{-14}$ m^2/s.

Since there is no in-plane variation for this problem, one-term approximation is applicable. In-plane shape functions $\Psi^\theta(x, y) = \Psi^\gamma(x, y) = 1$ are used in the discrete-layer model. The through-thickness domain z is divided into 64 sublayers of equal thickness, and the direct step-by-step integration (the constant acceleration method) is computed at a time interval of 20,000 s. Results from the discrete-layer model are then plotted and compared with the exact solutions given by [71] in Figures 4.2 and 4.3. The variations of temperature and moisture concentration are plotted through the thickness at various times, and the plots of transient temperature and moisture are the values at mid-plane level. The discrete-layer model solutions agree very well with the exact solutions, and they almost coincide with each other on the time plots.

4.2.3 Example 3: Simply-Supported Laminated Graphite-Epoxy/PZT-4 Plate

Now, a laminated plate composed of a layer of graphite-epoxy composite at the bottom and a layer of PZT-4 on the top with simply-supported boundary conditions is considered. Both layers have the same thickness of 0.0025 m with $L_x = 0.05$ m and $L_y = 0.025$ m. All the essential variables (u, v, w, ϕ, θ, and γ) are studied in this problem. Four types of excitation are investigated. The first two excitations are applied steady-state loading $\hat{t}_z = \sin(\pi x/L_x)\sin(\pi y/L_y)$ on the top surface with the top and bottom surfaces of PZT-4 held at zero potential, and applied steady-state

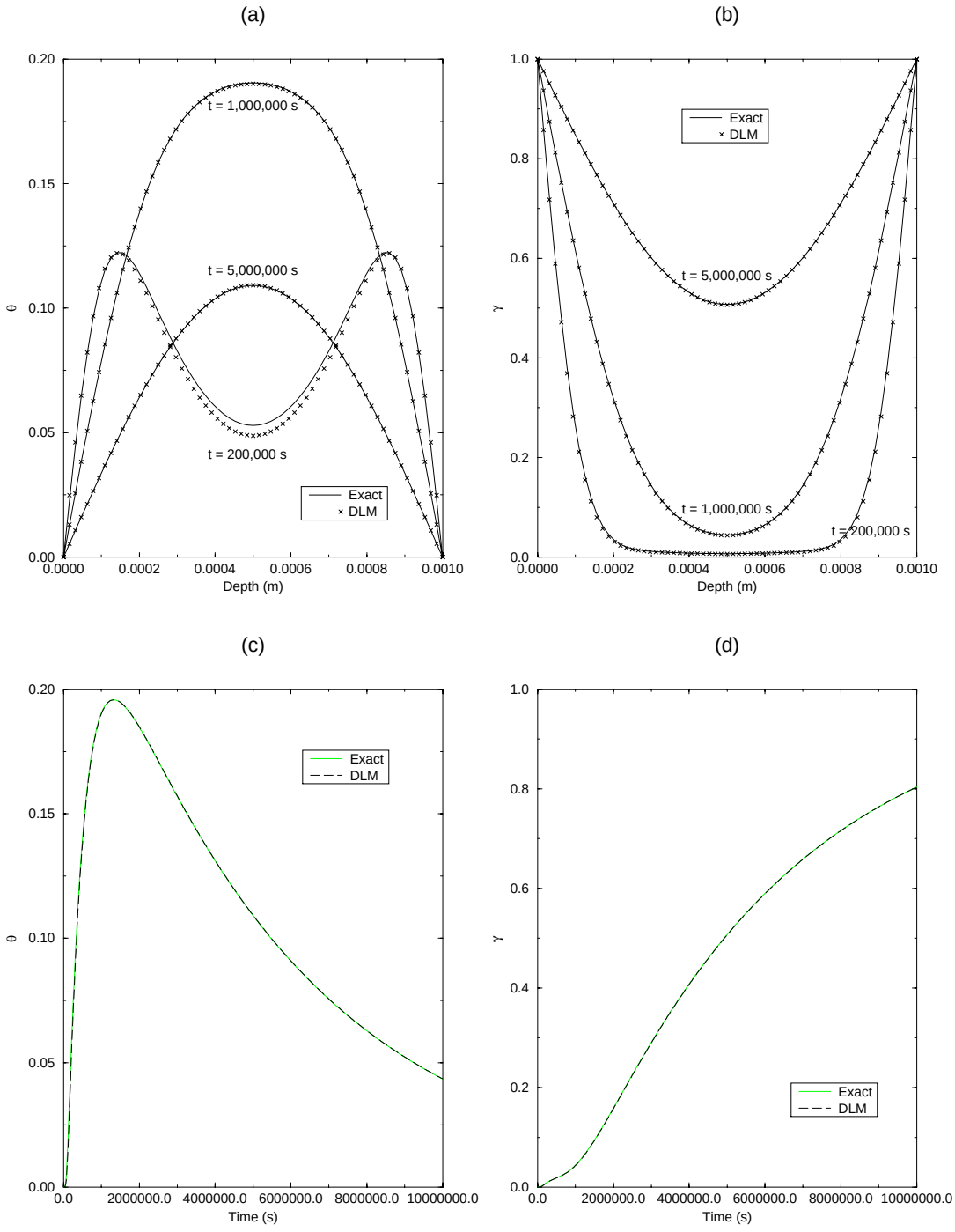

Figure 4.2: Infinite plate subject to change in moisture: (a) through-thickness temperature, (b) through-thickness moisture, (c) transient mid-plane temperature, and (d) transient mid-plane moisture.

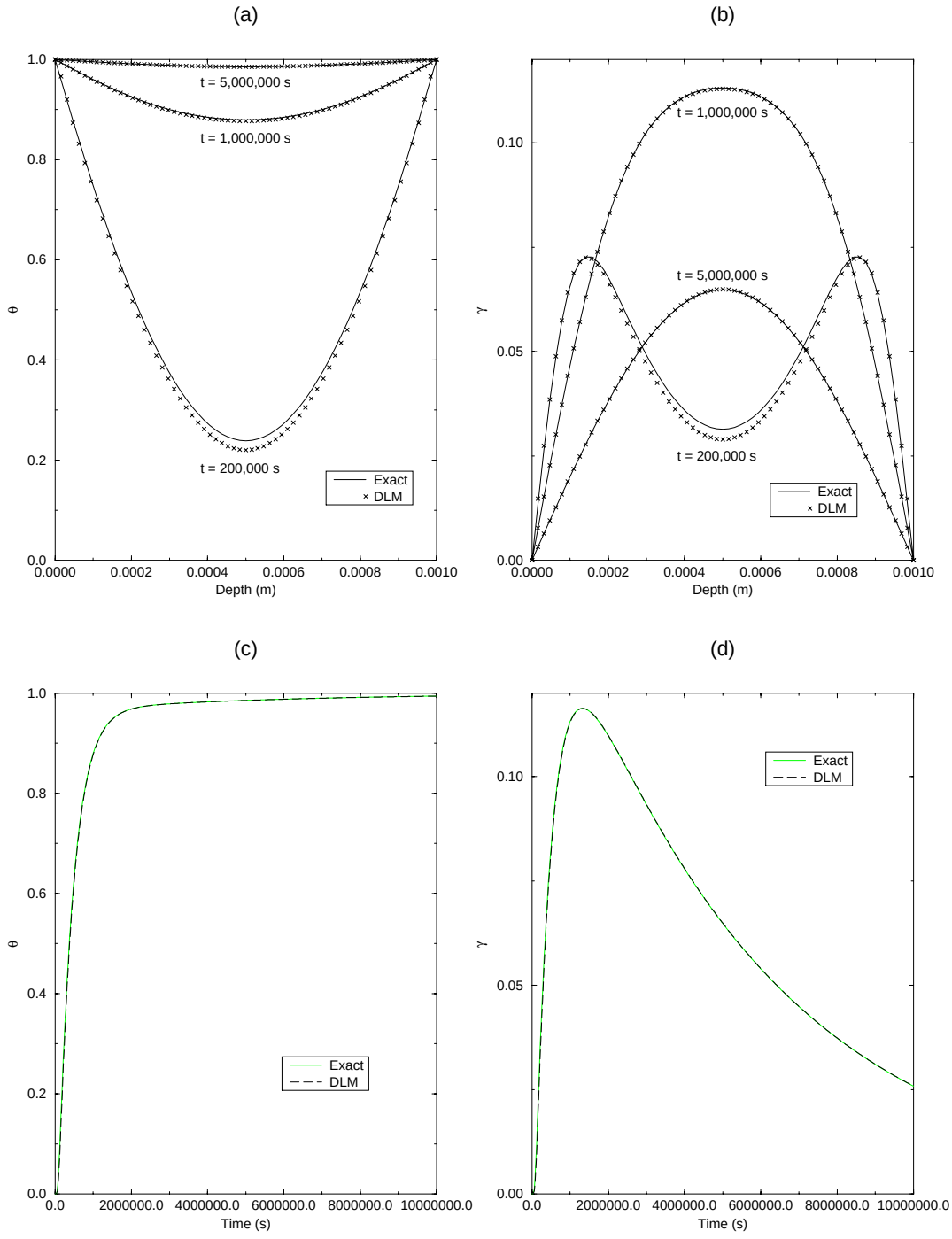

Figure 4.3: Infinite plate subject to change in temperature: (a) through-thickness temperature, (b) through-thickness moisture, (c) transient mid-plane temperature, and (d) transient mid-plane moisture.

voltage $\hat{\phi} = \sin(\pi x/L_x)\sin(\pi y/L_y)$ on the top surface with the bottom surface of PZT-4 held at zero potential. For these two cases, the changes in temperature and moisture on the top and bottom surfaces of the laminate are held at zero. In the last two cases, the transient behavior of the laminate is examined subject to a sudden change in temperature $\hat{\theta} = \sin(\pi x/L_x)\sin(\pi y/L_y)$, and a sudden change in moisture $\hat{\gamma} = \sin(\pi x/L_x)\sin(\pi y/L_y)$ on the top and bottom surfaces of the laminate with the top and bottom surfaces of PZT-4 held at zero potential.

The properties of PZT-4 in addition to the ones in Example 1 are assumed as follows: $\rho = 7600$ kg/m^3; $c_v = 420$ Nm/kgK; $\lambda_1 = \lambda_2 = 5.822 \times 10^5$ (all in N/m^{2}K), $\lambda_3 = 5.272 \times 10^5$; $r_1 = r_2 = r_3 = -2.5 \times 10^{-4}$ C/m^{2}K; $\kappa_{11}^T = \kappa_{22}^T = \kappa_{33}^T = 1.8$ N/sK; $\zeta_{11}^H = \zeta_{22}^H = \zeta_{33}^H = 2.5 \times 10^{-13}$ m^2/s. Material properties of the graphite-epoxy in addition to the ones in Example 2 are used as follows [32]: $C_{11} = 158.0$ (all in GPa), $C_{22} = C_{33} = 15.51$, $C_{44} = 3.20$, $C_{55} = C_{66} = 4.40$, $C_{12} = C_{13} = 5.64$, $C_{23} = 7.21$; $\epsilon_{11}/\epsilon_0 = 3.5$, $\epsilon_{22}/\epsilon_0 = \epsilon_{33}/\epsilon_0 = 3.0$; $\lambda_1 = 2.713 \times 10^5$ (all in N/m^{2}K), $\lambda_2 = \lambda_3 = 5.52 \times 10^5$; $\mu_1 = 7.687 \times 10^7$ (all in m^2/s^2), $\mu_2 = \mu_3 = 1.092 \times 10^8$. The reference temperature of the laminate is $T_0 = 200$ K.

Essential boundary conditions are used the same as those in Example 1 along with the following conditions:

$$\theta(0, y, z) = \theta(L_x, y, z) = \theta(x, 0, z) = \theta(x, L_y, z) = 0 \tag{4.26}$$

$$\gamma(0, y, z) = \gamma(L_x, y, z) = \gamma(x, 0, z) = \gamma(x, L_y, z) = 0 \tag{4.27}$$

The same in-plane approximations as in Example 1 are also employed here for the discrete-layer model with additional approximation functions as follows:

$$\Psi^\theta(x, y) = \sin(\frac{\pi x}{L_x})\sin(\frac{\pi y}{L_y}) \tag{4.28}$$

$$\Psi^\gamma(x, y) = \sin(\frac{\pi x}{L_x})\sin(\frac{\pi y}{L_y}) \tag{4.29}$$

Each of the two layers of the laminate is discretized into 32 sublayers of equal thickness in the discrete-layer model. Direct step-by-step integrations (the constant acceleration method) are performed at a time interval of 200,000 and 2,000,000 s for the transient analyses subject to the changes in temperature and moisture, respectively. Steady-state results by the discrete-layer model of the applied load and applied voltage on the laminate are shown in Figure 4.4. Normalized vaules of vertical displacement (w^*), electric potential (ϕ^*), stresses (σ_x^*, σ_y^*, and σ_z^*), and electric diplacement (D_z^*) at the center point ($x = 0.025$ m, $y = 0.0125$ m) of the laminate are plotted through the thickness. (Stresses and electric displacement are computed at the mid-level of each layer.) These normalized values are computed from the original values divided by their maximum values, for instance, $w^* = w/w_{max}$. The maximum values for these variables are $w_{max} = 8.1076 \times 10^{-12}$, $\phi_{max} = 1.3288 \times 10^{-4}$, $\sigma_{x,max} = 14.359$, $\sigma_{y,max} = 20.258$, $\sigma_{z,max} = 0.99932$, and $D_{z,max} = 6.8013 \times 10^{-10}$ for the applied load case, with $w_{max} = 6.8842 \times 10^{-10}$, $\phi_{max} = 1.0$, $\sigma_{x,max} = 4376.2$, $\sigma_{y,max} = 2543.8$, $\sigma_{z,max} = 19.446$, and $D_{z,max} = 6.6171 \times 10^{-6}$ for the applied voltage case.

The discrete-layer model results for the transient analyses subject to the sudden changes in temperature and moisture are shown in Figure 4.5 and 4.6, respectively. All these values are also computed at the center point of the laminate. The time plots of vertical displacement (w) are the values at the mid-plane level. The electric potential (ϕ), temperature (θ), and moisture (γ) are plotted through the thickness at various times.

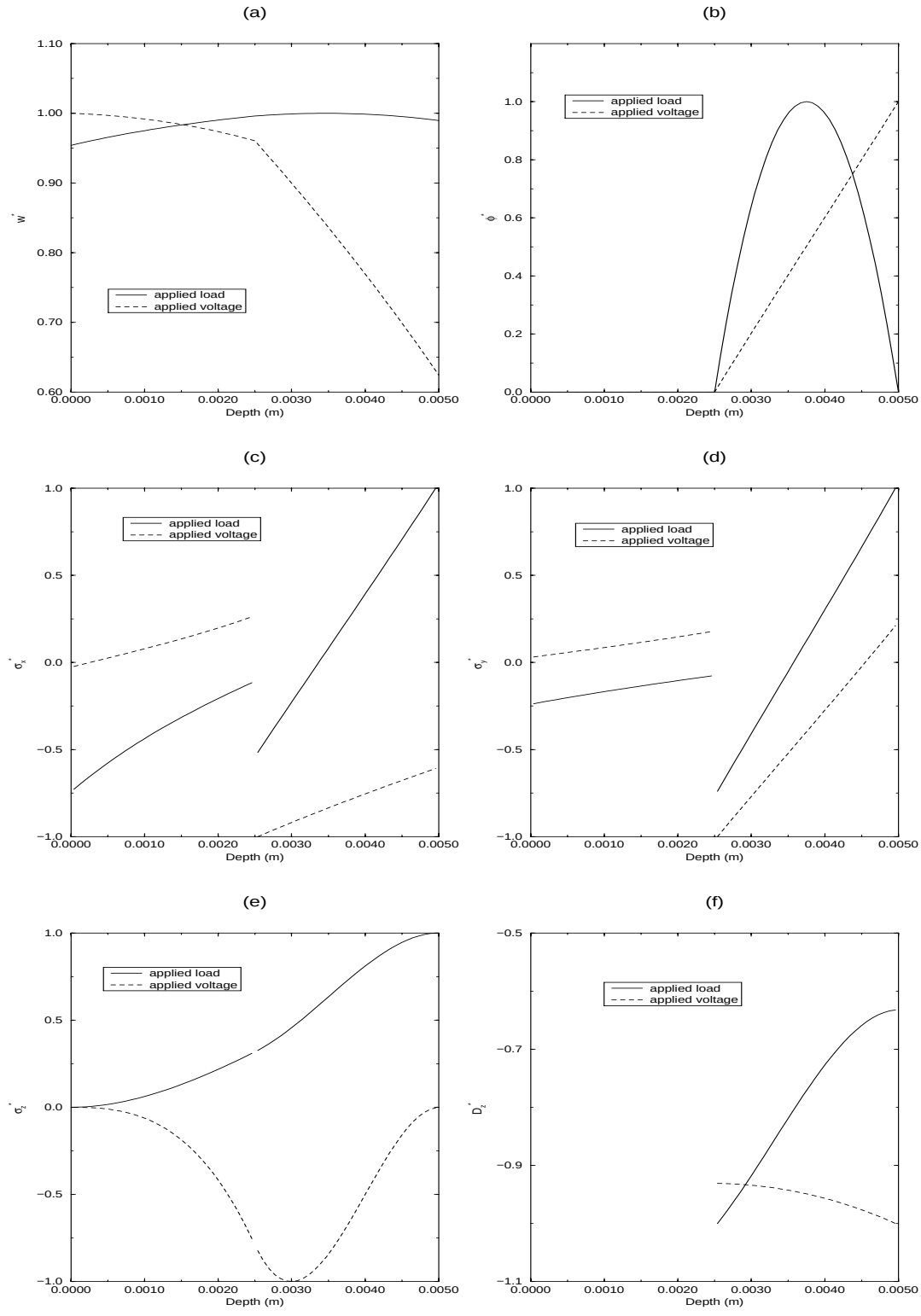

Figure 4.4: Graphite-epoxy/PZT-4 laminate subject to applied steady-state load and voltage: (a) normalized displacement w^*, (b) normalized electric potential ϕ^*, (c) normalized stress σ_x^*, (d) normalized stress σ_y^*, (e) normalized stress σ_z^*, and (f) normalized electric displacement D^*.

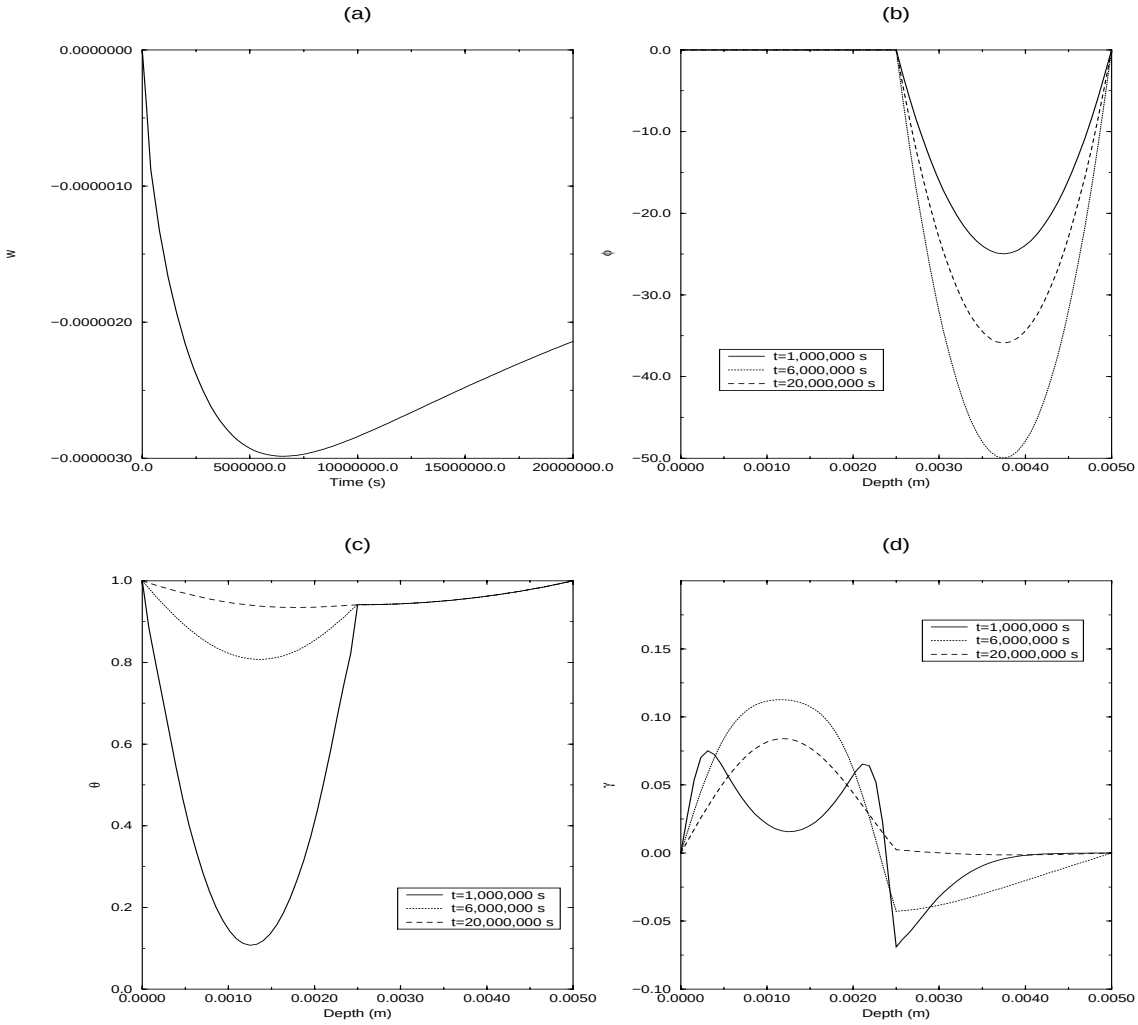

Figure 4.5: Graphite-epoxy/PZT-4 laminate subject to sudden change in temperature: (a) displacement w, (b) electric potential ϕ, (c) temperature θ, and (d) moisture γ.

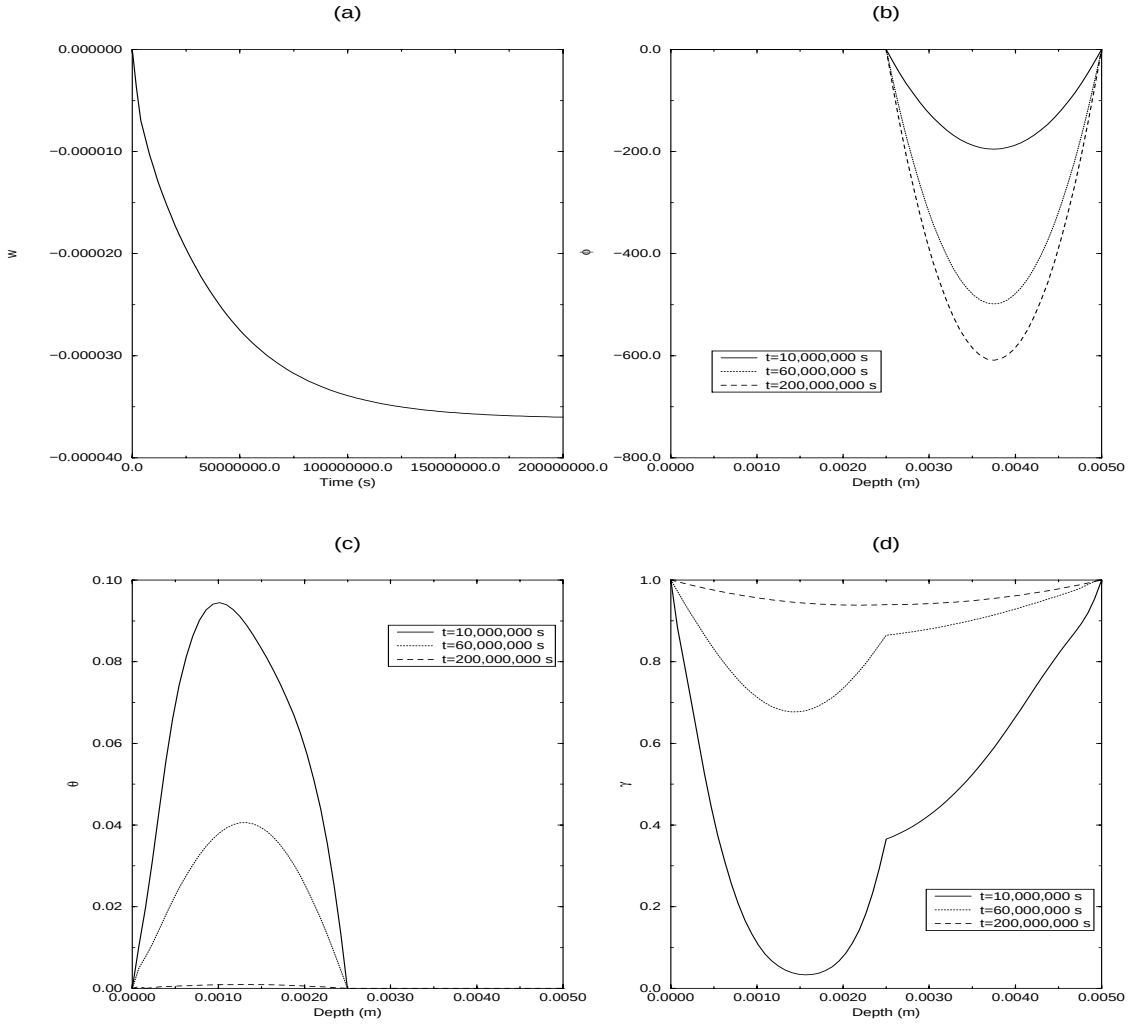

Figure 4.6: Graphite-epoxy/PZT-4 laminate subject to sudden change in moisture: (a) displacement w, (b) electric potential ϕ, (c) temperature θ, and (d) moisture γ.

4.3 Numerical Results Using In-Plane Finite Element Functions

Similar to many structural materials, one major concern in using wood as structural elements is that wood material has a tendency to expand or contract in a changing environment, particularly changes in temperature and moisture. Thus, the wood drying (or soaking) problem has received a considerable amount of attention from structural engineers. However, the discrete-layer model developed in this research yields an improvement over some earlier studies in that the differing material properties for each layer are all taken into account. In addition, this model allows for the application of an electric field to further change the shape of the wood composite.

In this section, problems of an adaptive wood composite plate, composed of layers of wood and piezoelectric material and subject to the changes in temperature and moisture, are simulated. Both steady-state and transient behaviors of the laminate are analyzed using the discrete-layer model with in-plane finite element functions in Examples 4 and 5, respectively. The response of interest is the out-of-plane deflection (or warping) of the plate. Throughout this section, we choose to represent the wood material with the walnut species [4, 13, 18, 26, 70, 83], and piezoelectric material with PZT-4. These materials are assumed to have the properties shown in Table 4.4. Also, the piezoelectric effect is examined in order to evaluate the potential use of the piezoelectric material as a distributed actuator in the composite. Voltage is applied to the piezoelectric layer and the resulting deflection is analyzed. We can then visualize the capacity of the piezoelectric layer to actuate the composite or counterbalance the warping caused by the temperature and moisture changes. In our analyses, the piezoelectric effect of the wood material is ignored since its effect is three orders of magnitude smaller than that of the piezoelectric material (PZT-4) used in these

Properties	Wood	PZT-4
Mass density: (kg/m^3)		
ρ	660.8	7600.0
Specific heat coefficient: (Nm/kgK)		
c_v	1360.0	420.0
Elastic constants: (GPa)		
C_{11}	12.22	139.0
C_{22}	0.6699	139.0
C_{33}	1.273	115.0
C_{44}	0.2432	25.6
C_{55}	0.9846	25.6
C_{66}	0.7182	30.6
C_{12}	0.4682	77.8
C_{13}	0.6872	74.3
C_{23}	0.0905	74.3
Piezoelectric constants: (C/m^2)		
e_{15}	0	12.72
e_{24}	0	12.72
e_{31}	0	-5.20
e_{32}	0	-5.20
e_{33}	0	15.08
Relative permittivities:		
ϵ_{11}/ϵ_0	3.50	1475
ϵ_{22}/ϵ_0	2.33	1475
ϵ_{33}/ϵ_0	2.33	1300
Thermal expansion coefficients: (10^{-6}/K)		
α_1	3.5	2.0
α_2	40.0	2.0
α_3	30.0	2.0
Moisture expansion coefficients: (m^3/kg)		
β_1	0	0
β_2	0.00016	0
β_3	0.00011	0
Pyroelectric coefficients: (C/m^{2}K)		
r_1	0	-0.00025
r_2	0	-0.00025
r_3	0	-0.00025
Thermal conductivity coefficients: (N/sK)		
κ_{11}^T	0.383	1.8
κ_{22}^T	0.158	1.8
κ_{33}^T	0.158	1.8
Moisture diffusivity coefficients: (10^{-12} m^2/s)		
ζ_{11}^H	1731.0	0.25
ζ_{22}^H	512.0	0.25
ζ_{33}^H	525.0	0.25

Note: The permittivity of free space is $\epsilon_0 = 8.85 \times 10^{-12}$ F/m.

Table 4.4: Material properties for wood and PZT-4.

examples.

4.3.1 Example 4: Adaptive Wood Composite Under Steady-State Excitations

A 50-mm by 50-mm composite laminate with a layer of wood 6 mm thick on the bottom and a layer of PZT-4 0.5 mm thick on the top is examined under three types of steady-state excitations: applied moisture, temperature, and voltage. The boundary conditions of the laminate, for the mechanical variables used in all these cases, are treated as traction-free boundary conditions. Effects of environmental conditions on the deflection of the laminate are simulated in the first and second cases. A unit value of moisture and temperature change is assumed as a representation. In the first case, a simulated change in moisture concentration of 1.0 kg/m^3 is applied at the top and bottom surfaces of the laminate while the temperature at these surfaces is kept constant. In the second case, a simulated change in temperature of 1.0 K is applied at the top and bottom surfaces of the laminate while the moisture concentration at these surfaces is kept constant. Also, the top and bottom faces of the PZT-4 layer are grounded at zero potential. To investigate the capability of piezoelectric actuation on the laminate, we apply an electric field to the PZT-4 layer in the third case. The voltage of -200.0 V is applied on the top surface while the bottom face of PZT-4 is grounded at zero voltage. The top and bottom surfaces of the laminate are kept at constant temperature and moisture concentration.

The discrete-layer models of the laminate are discretized as six sublayers, three for each material, in the through-thickness direction. Using the advantage of structural symmetry, a quarter of the domain in x-y plane is modeled. Results of the three cases of steady-state excitation are shown in Figure 4.7. Deflected shapes of the laminate subject to the applied moisture, temperature and voltage are plotted in

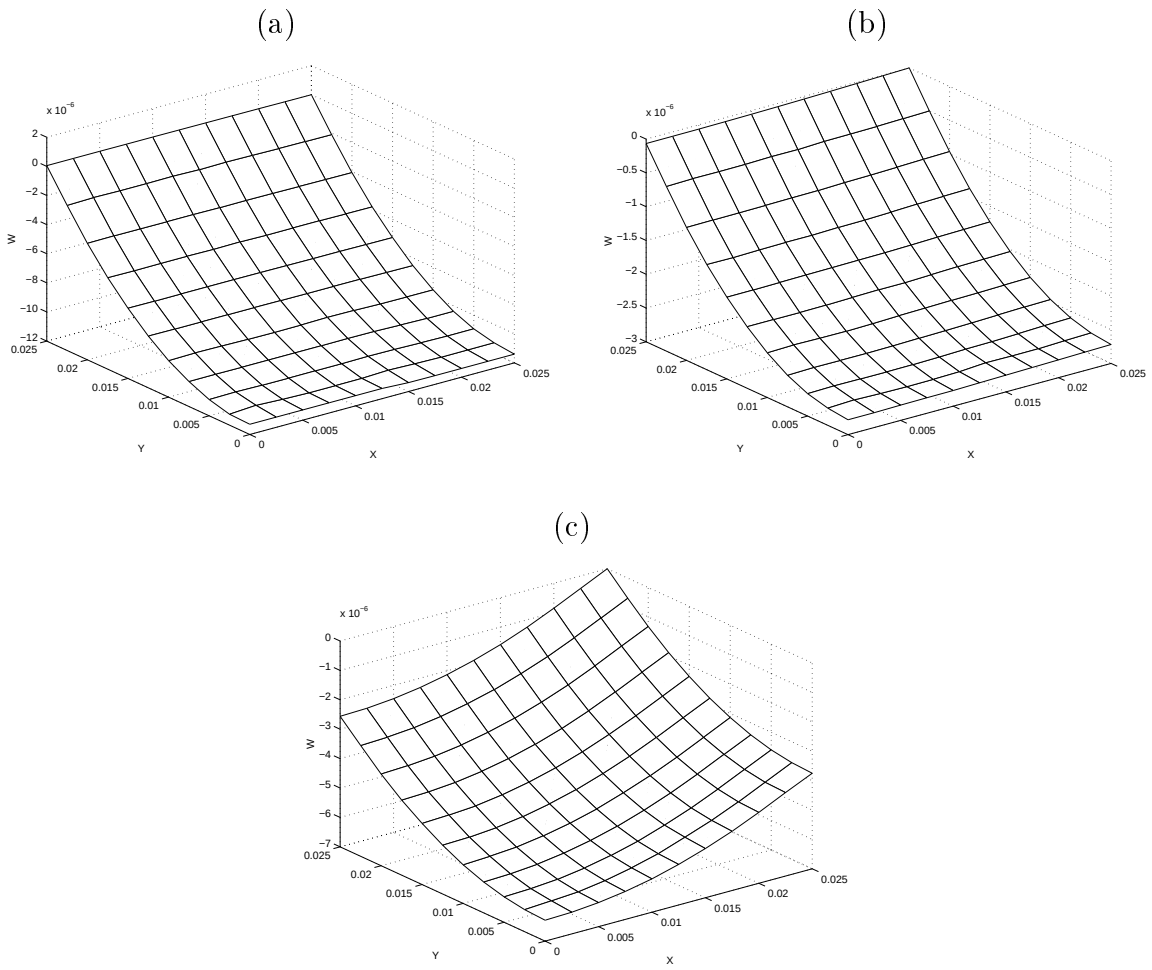

Figure 4.7: Deflected shapes of adaptive wood composite plate subject to (a) applied moisture, (b) applied temperature, and (c) applied voltage.

three dimensions. Deflections on only a quarter of the domain are shown where planes $x = 0$ and $y = 0$ are the planes of symmetry. When subjecting to the changes in moisture (Figure 4.7(a)) and temperature (Figure 4.7(b)), the composite plate under traction-free boundary conditions behaves similarly to one-way slab structures. This is due to the very high degree of anisotropy in x-y plane for wood material, but low degree for PZT-4. However, for a different type of (mechanical) boundary condition (e.g., simple support in both x- and y-directions), the laminate will no longer have only one-way behavior. In Figure 4.7(c), the deflected shape of the composite as a response to the applied voltage on the piezoelectric layer is plotted. This is to show how much actuation can be obtained and to see the potential use of the PZT-4 material as an actuator in the wood structures. The composite under the applied voltage exhibits a two-way deflection with the stiffness in the x-direction higher than that in the y-direction.

To examine the convergence of the numerical models, the in-plane domain is divided into several different grids: 2×2, 3×3, and 4×4. Results from these different discretizations in the x-y plane are shown in Table 4.5, where the values of the deflection at plate center on the bottom surface ($x = 0$, $y = 0$, $z = 0$) are given. The maximum differences occur when the composite is subjected to the applied voltage. These differences are 0.40% between the 2×2 and 3×3 grids, and 0.22% between 3×3 and 4×4 grids.

Cases	2×2	3×3	4×4
Applied moisture ($\times 10^{-5}$ m)	-1.1325	-1.1315	-1.1309
Applied temperature ($\times 10^{-6}$ m)	-2.7815	-2.7791	-2.7775
Applied voltage ($\times 10^{-6}$ m)	-6.3283	-6.3030	-6.2891

Table 4.5: Convergence study of adaptive wood composite plate where the maximum values of the deflection are given for the different in-plane discretizations: 2×2, 3×3, and 4×4 elements.

4.3.2 Example 5: Adaptive Wood Composite Under Transient Excitations

The same laminated structure as in Example 4 is again considered under traction-free boundary conditions and with all the initial conditions set equal to zero. The composite plate is next examined with two types of transient excitations. First, a change of moisture concentration at the top and bottom surfaces of the laminate is applied as a bilinear change, first being increased linearly from zero value at time $t = 0$ to 1.0 kg/m^3 at time $t = 20,000$ s, then kept constant with time at 1.0 kg/m^3. Temperature at the top and bottom surfaces is kept constant for this case. For the second case, an applied temperature change at the top and bottom surfaces is increased linearly from zero value at time $t = 0$ to the value of 1.0 K at time $t = 20$ s, then kept constant afterward. The moisture concentration at the top and bottom surfaces is kept constant. In both cases, the reference temperature T_0 is assumed as 300.0 K, and the top and bottom surfaces of the PZT-4 layer are fixed at zero voltage at all times.

For these transient cases, only one type of discretization of the domain is used for the discrete-layer models. Again, with the use of symmetry, the model consists of a quarter of the in-plane domain with four finite elements (two in x-direction by two in y-direction) and twelve sublayers (six for each material) in the through-thickness z-direction. Transient responses of the laminate to the applied excitations are then calculated using direct step-by-step integration (the constant acceleration method) at each time interval of 1,000 s and 1 s for the cases of applied moisture and applied temperature, respectively. Figure 4.8 shows the transient responses of the wood laminate at the center point of the plate ($x = 0$, $y = 0$). Deflections at the bottom level ($z = 0$) subject to the applied moisture (Figure 4.8(a)) and the

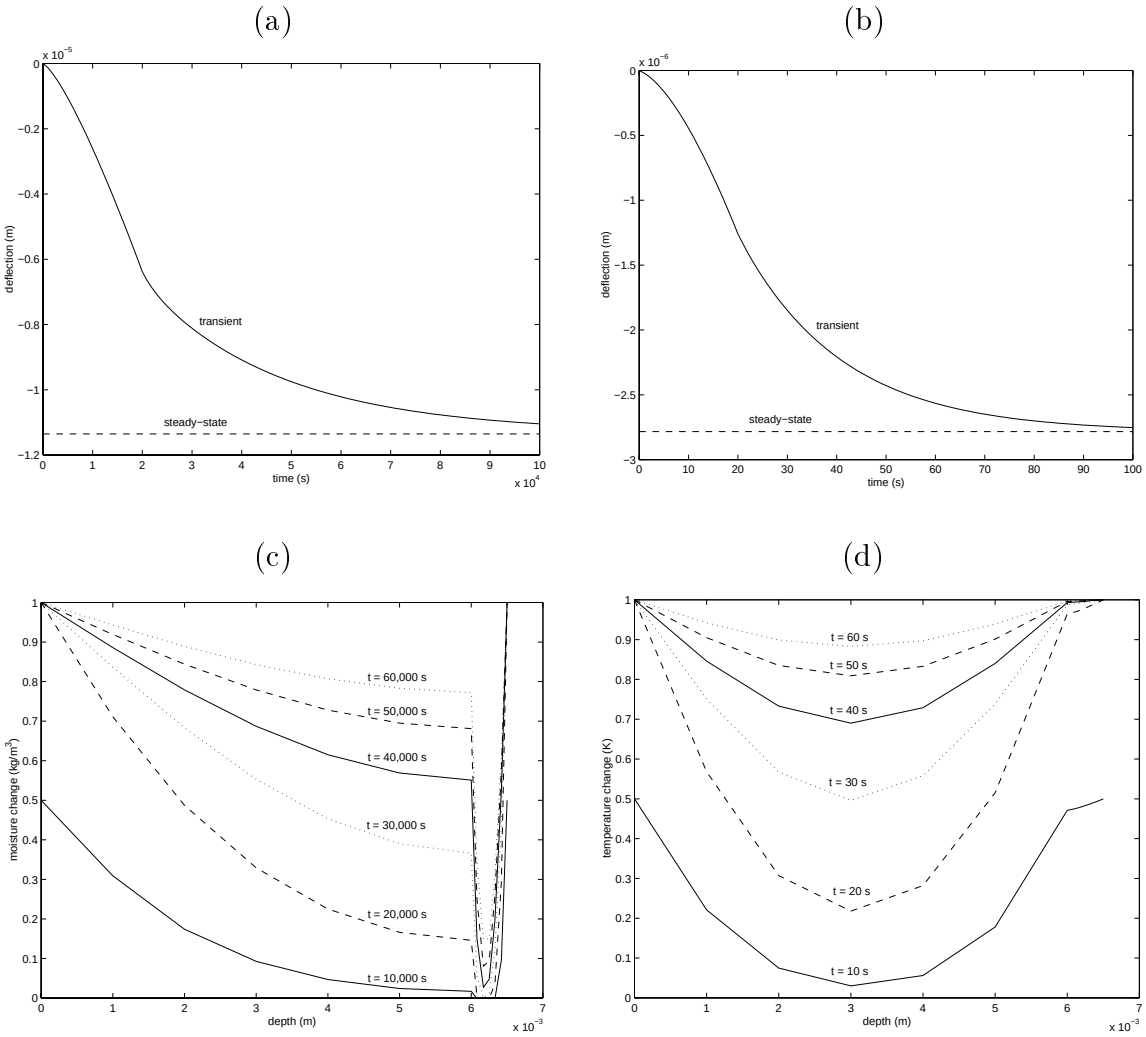

Figure 4.8: Transient responses at center of adaptive wood composite plate: (a) transient deflection due to applied moisture, (b) transient deflection due to applied temperature, (c) through-thickness moisture change due to applied moisture, and (d) through-thickness temperature change due to applied temperature.

applied temperature (Figure 4.8(b)) are plotted with time. As the time increases, these transient results converge to the steady-state results. In these graphs, the curvature is changed at the point when the excitation reaches the maximum applied value ($t = 20,000$ s for applied moisture, and $t = 20$ s for applied temperature). The discontinuity of the slope of the applied moisture and temperature is the cause of this. Figure 4.8(c) shows the moisture variation through the thickness of the laminate at various times for the applied moisture case, and similarly Figure 4.8(d) for the temperature variation for the applied temperature case. Wood material has a greater value of moisture diffusivity, but a smaller value of thermal diffusivity than PZT-4. Hence the through-thickness plots of moisture and temperature changes show jumps at the interface between the two materials.

CHAPTER 5

EXPERIMENTS

5.1 Test Procedures

In order to verify our mathematical models and to generate some ideas on how much actuation can be obtained in adaptive wood composite structures, a series of experiments were completed. Our samples of adaptive wood composites were represented by laminated composite plates consisted of wood and piezoelectric layers. The wood layers selected were poplar and pine species, and the piezoelectric material used was PZT-5A as manufactured by Morgan Matroc, Inc. The wood and PZT-5A layers were bonded together with an epoxy adhesive. We assume that the laminae are perfectly bonded together, and that the adhesive forms a very thin layer. In the test procedures, DC voltages were applied to the PZT-5A layer to activate the composites, and then the deformation of the composites were measured by strain gages attached on the top and bottom surfaces. These composites were subjected to traction free boundary conditions. The environmental conditons of temperature and moisture were kept constant at all times. We then compared our results to the mathematical models developed in earlier chapters.

5.1.1 Physical Models

Two samples of composite plates were constructed: pine/PZT-5A and poplar/PZT-5A. Figure 5.1 shows the layout of the composite samples. Each sample is composed

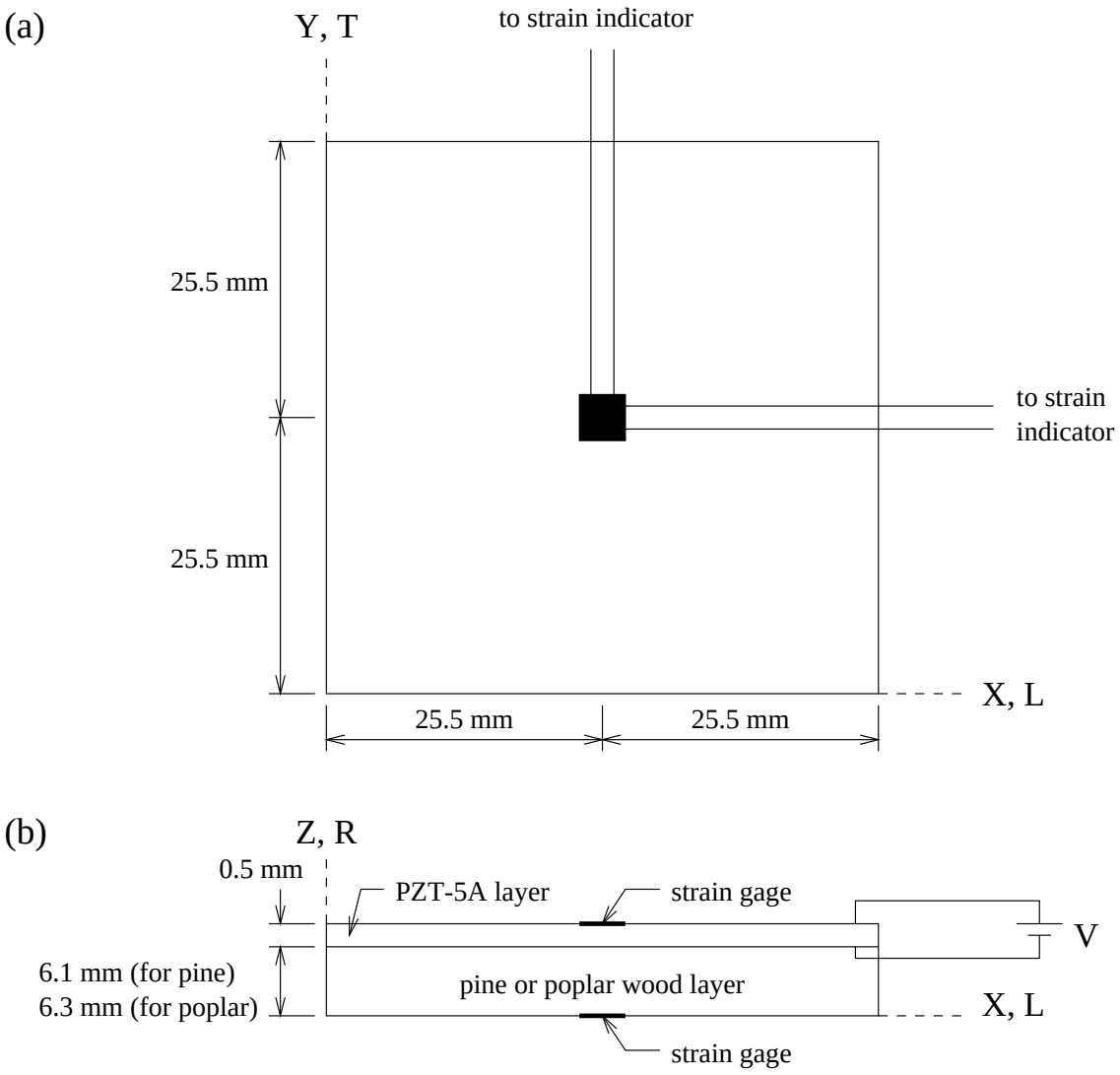

Figure 5.1: Layout of experimental samples: (a) top view and (b) front view.

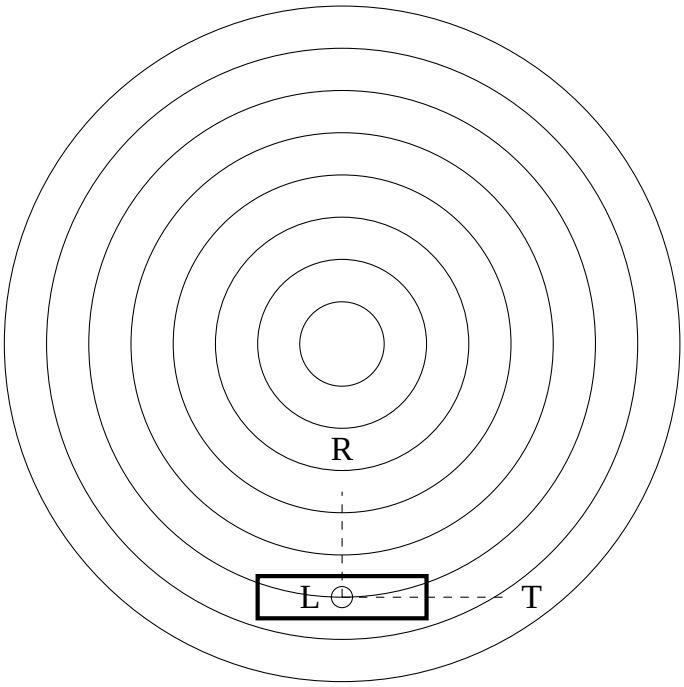

Figure 5.2: Grain orientations of the selected wood pieces.

of a layer of wood at the bottom and a layer of PZT-5A on the top. These layers are bonded together with an epoxy adhesive (Hardman) as manufactured by Harcros Chemicals, Inc. The dimensions in the x-y plane of all samples are 51 mm by 51 mm. The thickness of the PZT-5A layer is 0.5 mm and the wood layer is 6.1 mm for pine and 6.3 mm for poplar. The alignments of the wood materials (both pine and poplar) were chosen to be such that the longitudinal, tangential, and radial directions coincided with the x-, y-, and z-directions, respectively (see Figure 5.2). The 90-degree rosette strain gages (Type CEA-06-032WT-120 by Measurements Group, Inc.) were installed on the top surface (PZT-5A side) and bottom surface (wood side) of the composites at the center point. These strain gages have the active gage length equal to 0.032 in (0.8128 mm). Figure 5.3 shows the prepared samples of the adaptive wood composites.

To prevent the environmental effects from temperature and moisture change, the composite samples were kept at constant temperature and moisture by enclosing each

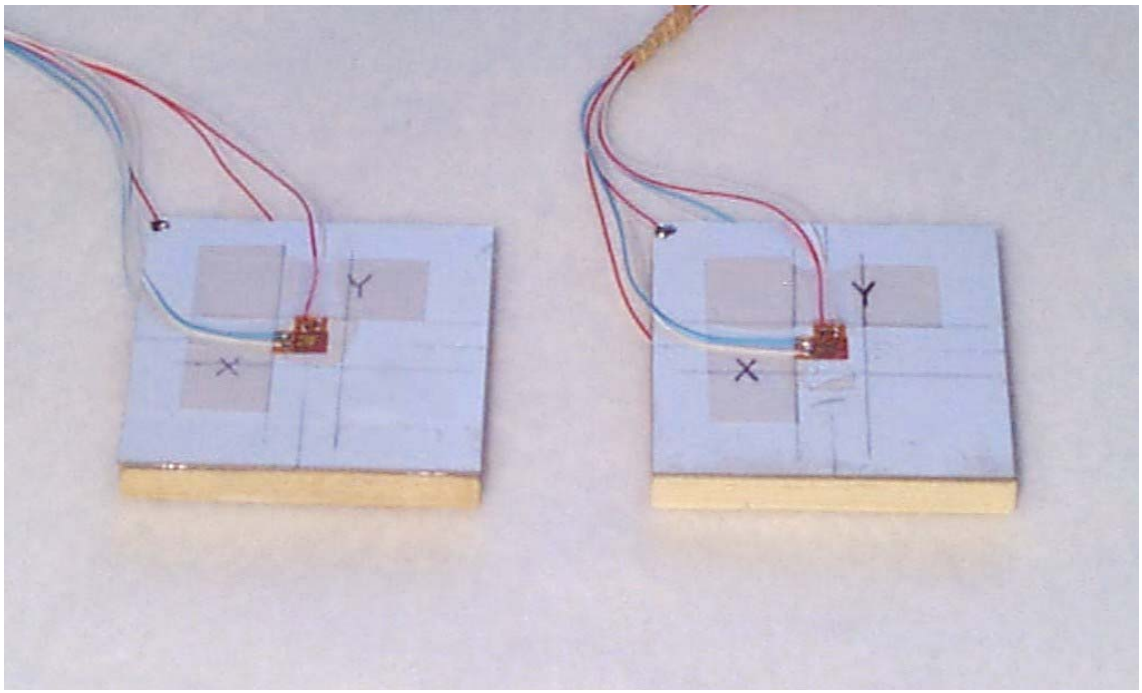

Figure 5.3: Adaptive wood composite samples.

sample within 8 layers of bubble wrap (see Figure 5.4). The experimental set-up is shown in Figure 5.5. We monitored the strain in each strain gage one direction at a time. The electrodes on both sides of the PZT-5A layer were connected to the DC power supply, and the strain gage leads were attached to the strain indicator (Model P-3500 by Measurements Group, Inc.). Voltages of 0, 50, 100, 150, and 200 V were applied to the PZT-5A layer, and the strains were read by the strain indicator. (The upper operating limit of the PZT-5A material is somewhere between 250 V and 500 V.) The measurements were repeated twice for the strain in each direction, and the average values were computed.

5.1.2 Numerical Models

The pine/PZT-5A and poplar/PZT-5A composites which were experimentally subject to applied voltages as described in the Physical Models Section were also analyzed numerically using the discrete-layer model developed in the earlier chapter. The

Figure 5.4: The adaptive wood composite sample covered by 8 layers of bubble wrap.

domain in the through-thickness z-direction is discretized as 16 sublayers (8 sublayers of equal thicknesses for each material) with the approximation functions used as Lagrange linear interpolation functions. Using the finite element method in the x-y plane, 9 (8-noded serendipity quadrilateral) elements of equal dimensions (3×3 meshes) are employed. Material properties for the PZT-5A layer are assumed the same as those given by Berlincourt et al. [3], and for pine and poplar woods given by Bodig and Jayne [4]. These values are given in Table 5.1. The PZT-5A material has the symmetric properties of a hexagonal crystal, whereas the woods are orthotropic materials. All the material properties are assumed within the linear range, and all the residual effects are ignored in these analyses. In the analyses by the discrete-layer model, after the primary unknowns of displacements and electric potential are solved, the results of the strains are computed at mid-level of each sublayer, and the values elsewhere are calculated by interpolation and extrapolation.

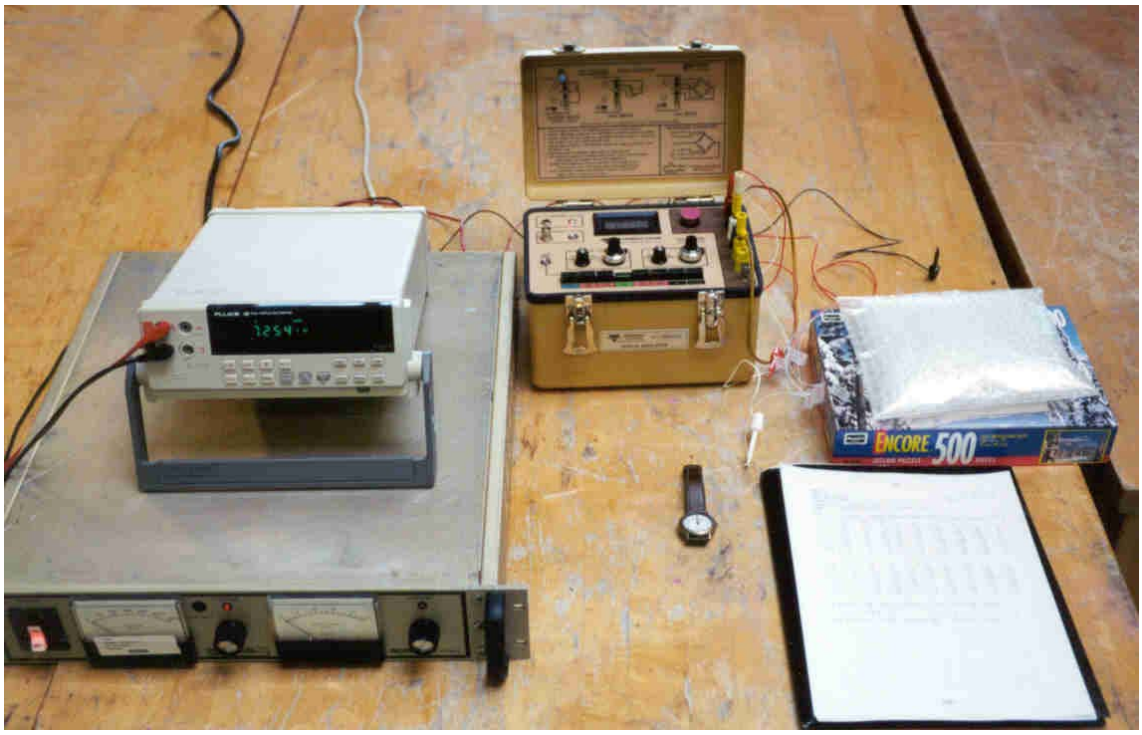

Figure 5.5: The experimental set-up.

5.2 Results and Discussion

Results of the strains in the pine/PZT-5A and poplar/PZT-5A composite plates as a response to the applied voltages to the PZT-5A layer are illustrated in Figure 5.6 to 5.11. The lateral strains (S_{xx} and S_{yy}) as measured in the experiments are plotted and compared with those predicted by the numerical analyses using the discrete-layer model. Figure 5.6 and 5.7 show the results of the strains in the x-direction (S_{xx}) and y-direction (S_{yy}), respectively, at the top and bottom surfaces of the pine/PZT-5A composite at various values of applied voltages. These lateral strains through the thickness of the pine/PZT-5A composite subject to the applied voltage of 200 V, as predicted by the discrete-layer model, are given in Figure 5.8. Also, similar to those for the pine/PZT-5A composite, the results of the lateral strains (S_{xx} and S_{yy}) for the poplar/PZT-5A composite are shown in Figure 5.9, 5.10, and 5.11.

Properties	PZT-5A	Pine	Poplar
Mass density: (kg/m^3)			
ρ	7700	476*	512**
Elastic constants: (GPa)			
C_{11}	120.0	9.185	12.04
C_{22}	120.0	0.4890	0.4452
C_{33}	111.0	0.8551	0.9945
C_{12}	75.2	0.1638	0.1647
C_{13}	75.1	0.2502	0.2965
C_{23}	75.1	0.2053	0.2410
C_{44}	21.1	0.0583	0.1548
C_{55}	21.1	0.6550	0.6709
C_{66}	22.6	0.6267	0.4826
Piezoelectric constants: (C/m^2)			
e_{31}	-5.35	0	0
e_{32}	-5.35	0	0
e_{33}	15.78	0	0
e_{24}	12.29	0	0
e_{15}	12.29	0	0
Relative permittivities:			
ϵ_{11}/ϵ_0	1730	3.50	3.50
ϵ_{22}/ϵ_0	1730	2.33	2.33
ϵ_{33}/ϵ_0	1700	2.33	2.33

Note: The permittivity of free space is $\epsilon_0 = 8.85 \times 10^{-12}$ F/m
* Moisture content = 7.8%
** Moisture content = 6.7%

Table 5.1: Material properties of PZT-5A, and pine and poplar woods.

It can be concluded from these graphs that the results for the pine/PZT-5A composite by the discrete-layer model agree to the experiments within 25.5% and 33.9% for the lateral strains in the x-direction (S_{xx}) and y-direction (S_{yy}), respectively. For the poplar/PZT-5A composite, these results agree within 25.3% in the x-direction and 34.1% in the y-direction. All the largest discrepancies occur on the top surface (PZT-5A face) of the composites when the applied voltage is 200 V. We note here that the piezoelectric effect which occurred in these experiments is not perfectly linear (with the applied voltage), as it can be observed from the experimental results in

Figure 5.6, 5.7, 5.9, and 5.10. That is, the behavior is somewhat beyond the linear range, and this can cause an inaccuracy in the mathematical models.

In these experimental demonstrations, the level of strain generated by applying electric field to the PZT-5A layer is in the order of 100 microstrain (on the PZT-5A surface). The values of strains in the x-direction (S_{xx}) are smaller than those in the y-direction (S_{yy}). This is clearly because of the higher value of modulus of elasticity in the x-direction (longitudinal direction) of the wood materials. (For PZT-5A material, the properties in the x- and y-directions are identical.) However, the poplar/PZT-5A composite exhibits a slightly higher stiffness in the x-direction than the pine/PZT-5A composite, but about the same value for the stiffness in the y-direction. Finally, the adaptive composite structures investigated here have a width to thickness ratio of approximately 8 and may be considered as thick plates. The deflections of the composites generated by the applied electric field to the piezoelectric layer are therefore small. However, for the similar composite plates with thinner layers, the induced strain gradients will be higher and, as a consequence, larger deflections can be obtained.

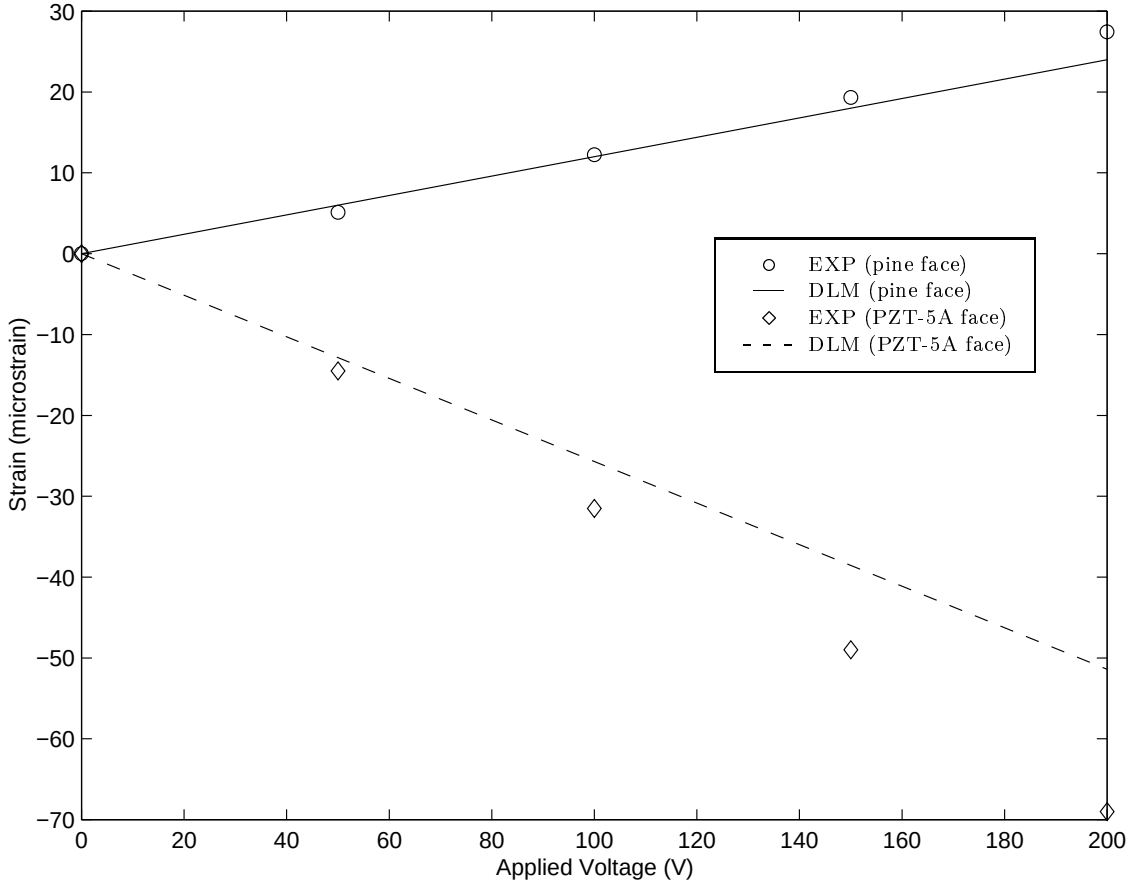

Figure 5.6: Strain in x-direction (S_{xx}) of pine/PZT-5A composite subject to applied voltage.

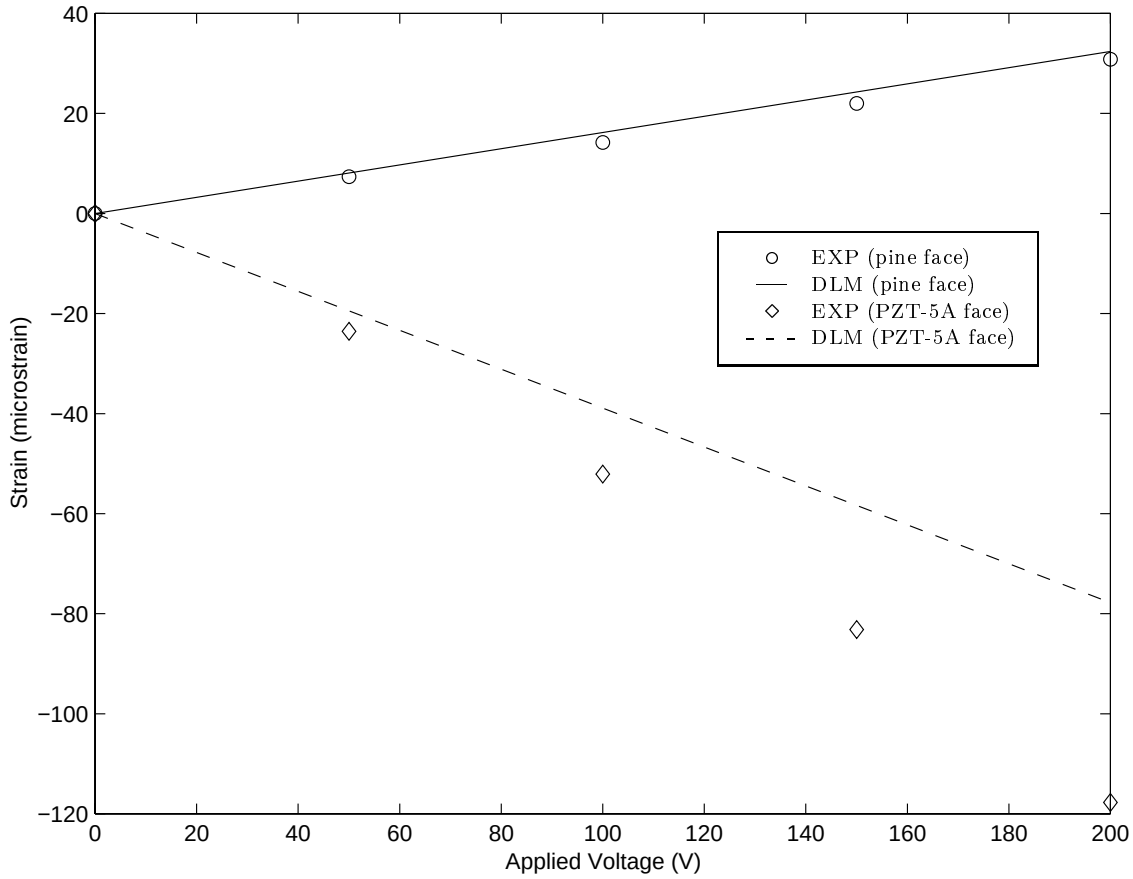

Figure 5.7: Strain in y-direction (S_{yy}) of pine/PZT-5A composite subject to applied voltage.

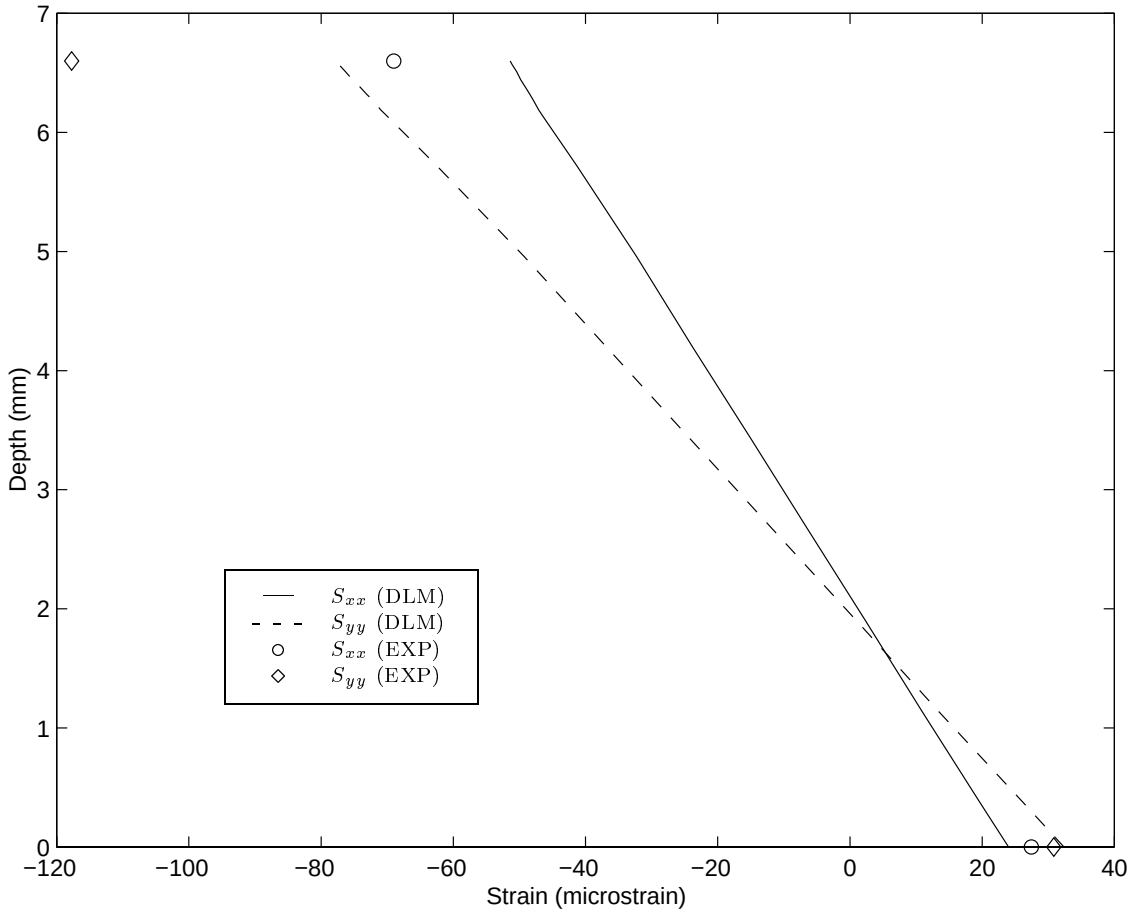

Figure 5.8: Through-thickness distribution of strains S_{xx} and S_{yy} of pine/PZT-5A composite under applied voltage of 200 V.

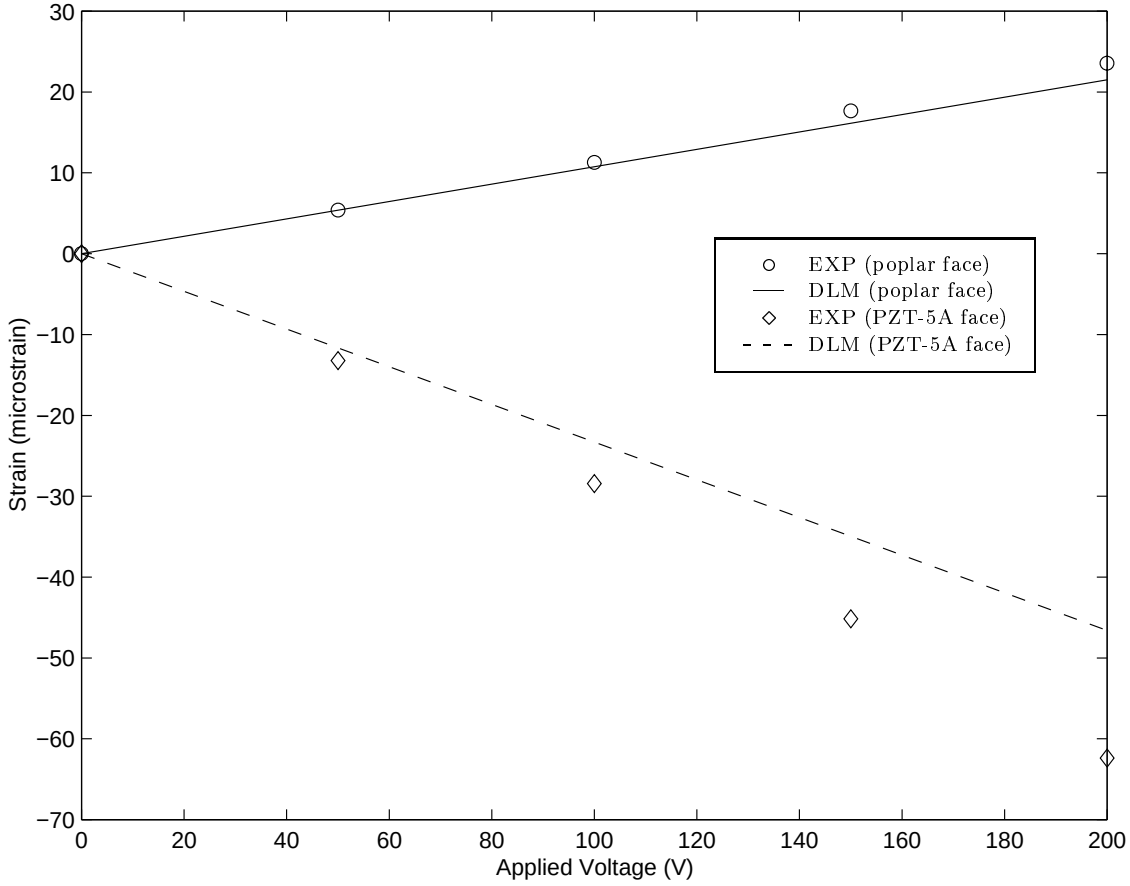

Figure 5.9: Strain in x-direction (S_{xx}) of poplar/PZT-5A composite subject to applied voltage.

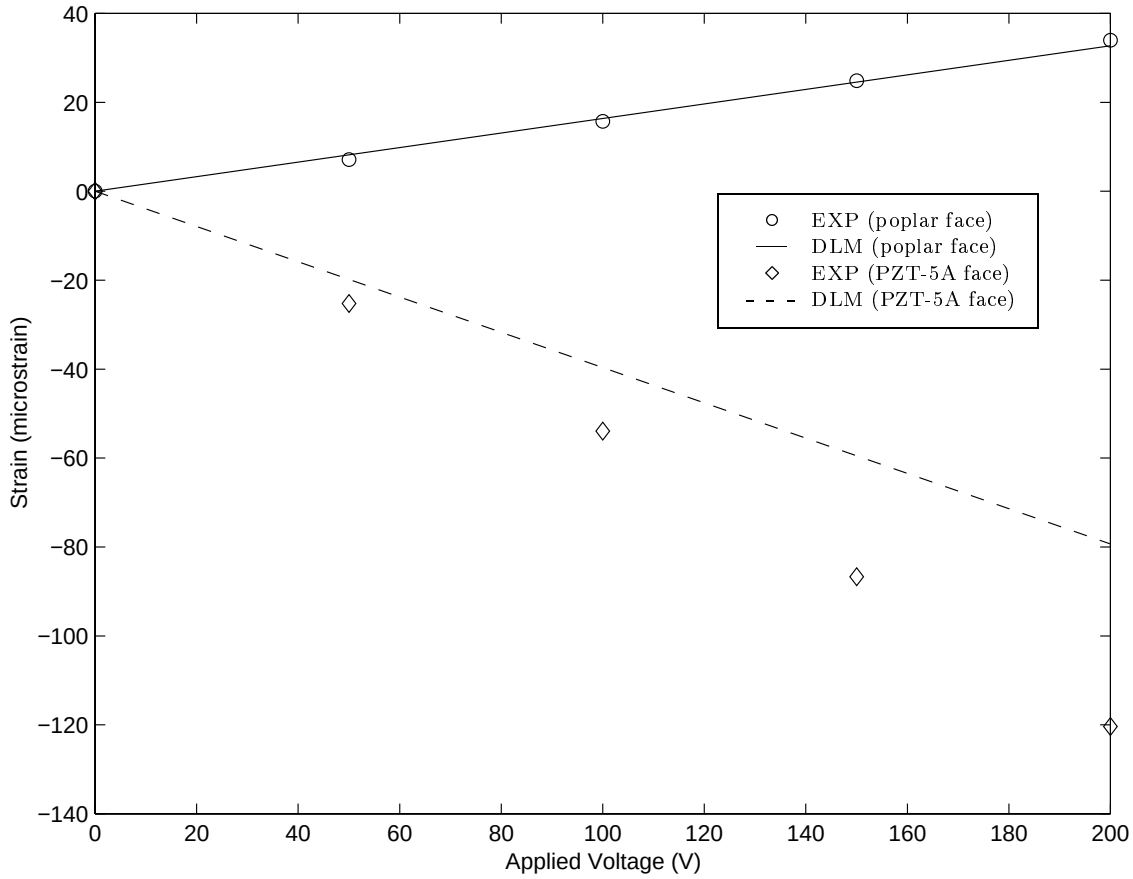

Figure 5.10: Strain in y-direction (S_{yy}) of poplar/PZT-5A composite subject to applied voltage.

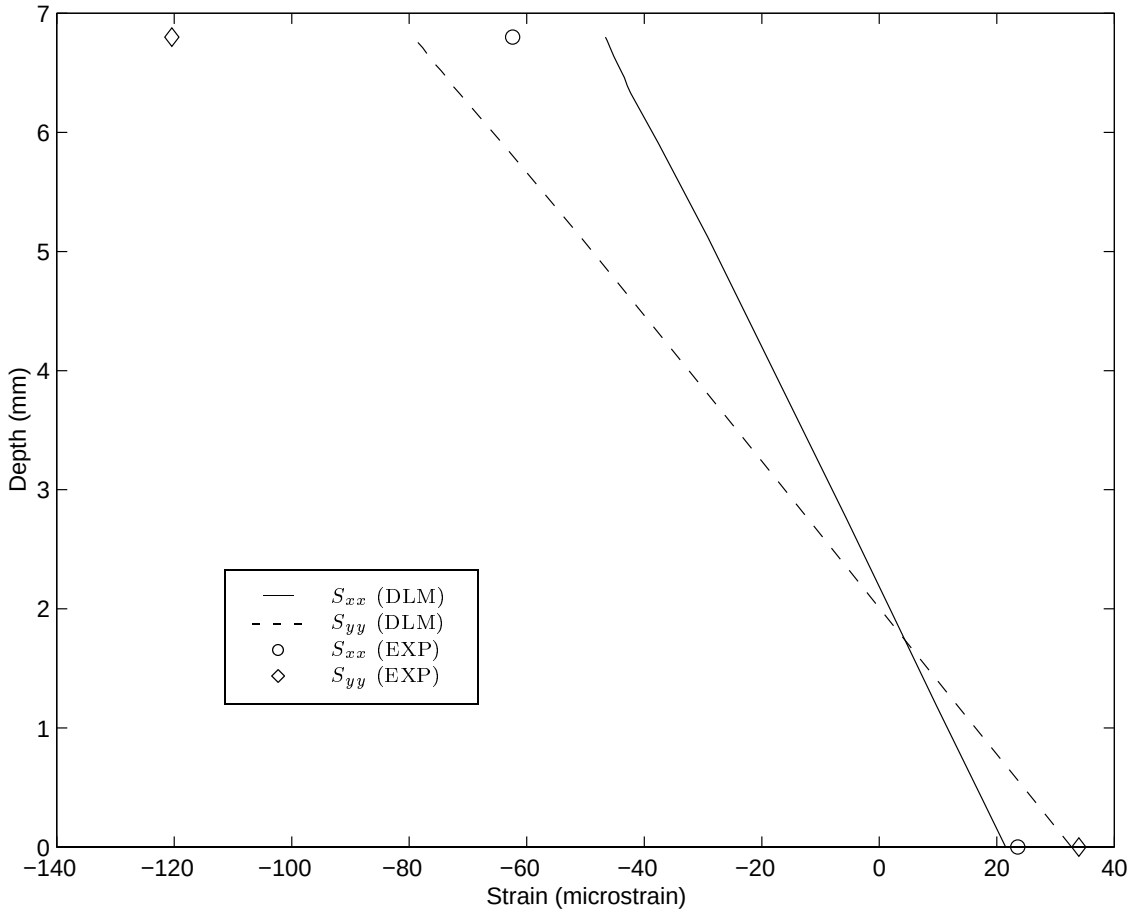

Figure 5.11: Through-thickness distribution of strains S_{xx} and S_{yy} of poplar/PZT-5A composite under applied voltage of 200 V.

CHAPTER 6

CONCLUSIONS

In this research, piezoelectric materials have been introduced to form adaptive wood composites configured as laminated plate structures. With the capability of being utilized as sensors and actuators, piezoelectric materials can be incorporated into structural elements to produce a system capable of self-monitoring and self-controlling. When adaptive wood composite structures are exposed to changes in enviromental conditions, temperature and moisture can cause significant effects such as warping. This is due to the differences in the material properties, not only in the different kinds of materials, but also in the different directions of an anisotropic material. However, these effects can be controlled or counter-acted by adjusting the electric field applied to the piezoelectric layer. Adaptive wood composites, composed of wood and piezoelectric materials, are structural components in which effects of elastic, electric, temperature, and moisture fields can have strong influences. The study of these four fields together on a solid is termed hygrothermopiezoelectricity.

Following the objectives as stated in Chapter 1, a mathematical model has been developed for analyzing the problems of laminated hygrothermopiezoelectric plates. The developed plate model was then employed to investigate the steady-state and transient behaviors of the adaptive wood composite laminates. Also, experiments have been conducted on adaptive wood composite samples in order to measure their adaptive actuation capability and to verify the theory. A summary and the major

conclusions of this study are described below.

The first objective of this work was to develop a mathematical model for a hygrothermopiezoelectric laminated plate. A discrete-layer model was developed for analyzing such a laminate under the coupled effects of mechanical, electrical, thermal, and moisture fields. By employing a layerwise plate theory, approximate solutions of the primary variables taken as displacements, electric potential, temperature, and moisture concentration were sought via the weak form of the governing equations. The discrete-layer model allowed for a break in slope of the primary unknowns, which is a critical feature of this approach. The solutions in three-dimensional space were approximated by one-dimensional approximation functions in the through-thickness direction and two-dimensional approximation functions in the plane of the plate.

In the through-thickness direction, only C^0-continuity was required and the one-dimensional approximation functions were employed as layerwise Lagrange linear interpolation functions. By the use of such approximation functions, variations through the thickness of the laminate were taken into account, and discontinuity behaviors between layers could also be represented.

The two-dimensional approximation functions in the plane of the plate were employed as two approaches: analytical functions (e.g., trigonometric or polynomial functions) and finite element funcions. The use of the analytical functions, when applicable, is far more accurate than that of the finite element functions. However, the approach of analytical functions is applicable only to limited problems of simple geometry and boundary conditions, for instance, simply-supported rectangular plates. Otherwise, the approach of finite element functions which can solve laminated plates with any type of geometry and boundary condition is needed. In fact, the discrete-layer model with the use of finite element functions in the plane of the plate is

equivalent to a conventional three-dimensional finite element model. Nevertheless, the discrete-layer model has advantages over the conventional finite element model in that the calculation for the global matrices can be simplified. The integration in the through-thickness domain z can be computed separately from the in-plane domains x and y. This helps reduce the cost of computer time for running the problems and allows our plate model a variable number of degrees of freedom.

For the sake of generality, the mathematical models developed in this study were capable of taking into account all the material constants possible for the behavior within the linear range (i.e., 21 elastic constants, 18 piezoelectric constants, 6 dielectric constants, 6 stress-temperature constants, 6 stress-moisture constants, 3 pyroelectric constants, and 3 electric-moisture constants). Also, for the transient problems, the equations formulated in a standard matrix form were solved by a direct step-by-step integration using the Newmark-beta method.

The numerical examples for various types of problems have demonstrated the accuracy of our mathematical model as well as demonstrated the basic behavior of the composite laminates under the coupled effects of the mechanical, electrical, thermal, and moisture fields. Results obtained by the discrete-layer model have been proved to be in excellent agreement with exact solutions.

- For the case of laminated piezoelectric plates, the accuracy of the primary unknowns was well within 1%.

- Plots of the results for the problem of coupled heat and moisture diffusion in an infinite plate have also shown excellent agreement.

- Finally, the example problem of the hygrothermopiezoelectric effects on a simply-supported laminated graphite-epoxy/PZT-4 plate demonstrated that not only the piezoelectric effects (when subjected to applied load and applied voltage),

but also the environmental effects (or the changes of temperature and moisture) can cause significant responses in the composites. The out-of-plane deflections caused by the applied unit load, voltage, temperature, and moisture were in the order of 8×10^{-12}, 7×10^{-10}, 3×10^{-6}, and 4×10^{-5} m, respectively.

The second objective was to apply the discrete-layer model to analyze representative problems of adaptive wood composites. Adaptive wood composites were selected to consist of a layer of a piezoelectric material (PZT-4) on the top and a layer of wood (walnut spices) at the bottom. The laminates were investigated subject to steady-state and transient excitations of the changes in environmental conditions under a traction-free boundary condition. Also, the actuation capability by the applied voltage on the PZT-4 layer was examined to see the potential use of this material as a distributed actuator in the wood composites. The response of interest was the out-of plane deflection (or warping) of the laminate.

These numerical examples have shown that PZT-4 is a possible candidate to be used as an actuator for the wood laminates. Deflections caused by the moisture and temperature changes can be controlled or counter-acted by adjusting the electric field applied to the piezoelectric layer.

- For the laminate studied here, an applied voltage of 200 V on the PZT-4 layer generated the out-of-plane displacement of the order 6×10^{-6} m.
- This level of actuation was enough to counter the deflection caused by moisture of the order 0.5 kg/m^3 or by temperature of the order 2 K.

The piezoelectric effect is instantaneous, and therefore the effect of applied voltage to the composite was only demonstrated for the steady-state case. Moreover, even though the effects of applied moisture, temperature, and electric field to the composite are separately shown in the examples, the combined results of these fields can be

easily computed as a linear combination using the method of superposition. These results therefore provide an indication of the level of response of adaptive wood composites, and the model provides a means of studying any laminated wood plate where the elastic, temperature, moisture, and electric fields influence the overall structural response.

The third objective was to construct the physical samples of adaptive wood composites and measure the levels of adaptive actuation. Experiments have been conducted for the adaptive wood composite plates (composed of a layer of wood and a layer of piezoelectric material). Wood materials were represented by pine and poplar species, while the piezoelectric material was chosen to be PZT-5A. Steady-state voltages between 0 and 200 V were applied to the piezoelectric layer in order to actuate the composites. Strains on the top and bottom surfaces of the laminates, as reponses to the excitation, were measured by strain gages. These experimental results were plotted and compared with the numerical results predicted by the discrete-layer model, and this can be concluded as follows:

- The levels of strains generated by applying electric field to the PZT-5A layer were in the order of 100 microstrain, a small but significant amount that allowed us to gage the response levels for these laminates.

- The results by the discrete-layer model were in a good agreement with the experimental results especially when the applied voltages were small. The discrete-layer model underpredicted the experiments, and the discrepancies became larger as the applied voltage increased. At the applied voltage of 200 V, the agreements of the strains were within 34%.

- Experimental wood composites were sensitive to temperature and required thermal insulation to prevent the effects from the change in environment and keep

the samples at constant temperature.

The experimental results have shown the degree of actuation provided by PZT-5A layer in the adaptive wood composites, and have also confirmed the validity of the discrete-layer model. The discrepency between the discrete-layer model prediction and the experimental result was due to the assumption made in the discrete-layer model and some uncertainties of the material properties used in the analysis. The assumption that all the material properties of the composites are within the linear range is not completely true. Some of these properties can be moderately to highly nonlinear. For example, the piezoelectric coefficients can vary with the applied voltage (or electric field). Also, the hygrothermal effects (from temperature and moisture) in solids are normally nonlinear. Hence, these mathematical models which based on the assumption of linear properties will yield good results only to problems concerning considerably small changes in those field variables.

Finally, some of the possibly-relevant material properties are not included in the example problems, for instance, χ_i, d_t, κ^M_{ijkl}, κ^E_{ijl}, ζ^M_{ijkl}, and ζ^E_{ijl}. This is primarily because of the lack of available data for these parameters and the desire to study the dominant effects of the fields in the examples shown. Also, it was not an objective of this work to determine all these properties for any specific material. Therefore, these other coupling effects were considered secondary in this work and are neglected in the examples. However, these effects in other materials may have a much stronger influence, and our mathematical models can incorporate these parameters if necessary.

BIBLIOGRAPHY

[1] G. A. Altay and M. C. Dokmeci, Fundamental Variational Equations of Discontinuous Thermopiezoelectric Fields, *International Journal of Engineering Science*, vol. 34, no. 7, pp. 769-782, 1996.

[2] K. J. Bathe, *Finite Element Procedures*, Prentice-Hall, Englewood Cliffs, New Jersey, 1996.

[3] D. A. Berlincourt, D. R. Curran, and H. Jaffe, Piezoelectric and Piezomagnetic Materials and Their Function in Transducers, *Physical Acoustics*, vol. I, part A, Methods and Devices (W. P. Mason, ed.), Academic Press, New York and London, pp. 169-270, 1964.

[4] J. Bodig and B. A. Jayne, *Mechanics of Wood and Wood Composites*, Van Norstrand Reinhold, New York, 1982.

[5] H. Bouadi and C. T. Sun, Hygrothermal Effects on the Stress Field of Laminated Composites, *Journal of Reinforced Plastics and Composites*, vol. 8, pp. 40-54, 1989.

[6] H. Bouadi and C. T. Sun, Hygrothermal Effects on Structural Stiffness and Structural Damping of Laminated Composites, *Journal of Materials Science*, vol. 25, pp. 499-505, 1990.

[7] D. E. Breyer, *Design of Wood Structures*, McGraw-Hill, New York, 1993.

[8] W. G. Cady, *Piezoelectricity*, rev. ed., vols I and II, Dover Publications, New York, 1964.

[9] W. J. Chang, Transient Hygrothermal Responses in a Solid Cylinder by Linear Theory of Coupled Heat and Moisture, *Applied Mathematical Modelling*, vol. 18, pp. 467-473, 1994.

[10] C. Q. Chen and Y. P. Shen, Piezothermoelasticity Analysis for a Circular Cylindrical Shell under the State of Axisymmetric Deformation, *International Journal of Engineering Science*, vol. 34, no. 14, pp. 1585-1600, 1996.

[11] T. C. Chen and B. H. Hwang, Transient Hygrothermal Stresses Induced in Two-Dimensional Problems by Nonlinear Theory of Coupled Heat and Moisture, *Journal of Applied Mechanics*, vol. 61, pp. 938-943, 1994.

[12] T. C. Chen, C. I. Weng, and W. J. Chang, Transient Hygrothermal Stresses Induced in General Plane Problems by Theory of Coupled Heat and Moisture, *Journal of Applied Mechanics*, vol. 59, pp. 510-516, 1992.

[13] E. T. Choong, T. F. Shupe, and Y. Chen, Effect of Steaming and Hot-Water Soaking on Extractive Distribution and Moisture Diffusivity in Southern Pine during Drying, *Wood and Fiber Science*, vol. 31, no. 2, pp. 143-150, 1999.

[14] R. W. Clough and J. Penzien, *Dynamics of Structures*, 2nd ed., McGraw-Hill, New York, NY, 1993.

[15] A. Cloutier and Y. Fortin, A Model of Moisture Movement in Wood Based on Water Potential and the Determination of the Effective Water Conductivity, *Wood Science and Technology*, vol. 27, pp. 95-114, 1993.

[16] A. Cloutier, Y. Fortin, and G. Dhatt, A Wood Drying Finite Element Model Based on the Water Potential Concept, *Drying Technology*, vol. 10, no. 5, pp. 1151-1181, 1992.

[17] P. Curie and J. Curie, *Comptes Rendus*, vol. 91, no. 294, 1880.

[18] H. E. Desch and J. M. Dinwoodie, *Timber: Structure, Properties, Conversion and Use*, 7th ed., Food Products Press, NY, 1996.

[19] L. E. Doxsee Jr., A Higher-Order Theory of Hygrothermal Behavior of Laminated Composite Shells, *International Journal of Solids and Structures*, vol. 25, no. 4, pp. 339-355, 1989.

[20] L. E. Doxsee Jr. and G. S. Springer, Hygrothermal Stresses and Strains in Axisymmetric Composite Shells, *Computers and Structures*, vol. 32, no. 2, pp. 395-407, 1989.

[21] H. Eslami and S. Maerz, Thermal Induced Vibration of a Symmetric Cross-Ply Plate with Hygrothermal Effects, *AIAA Journal*, vol. 33, no. 10, pp. 1986-1988, 1995.

[22] E. Fukada, Piezoelectricity as a Fundamental Property of Wood, *Wood Science and Technology*, vol. 2, pp. 299-307, 1968.

[23] Y. Q. Gui, E. W. Jones, F. W. Taylor, and C. A. Issa, An Application of Finite Element Analysis to Wood Drying, *Wood and Fiber Science*, vol. 26, no. 2, pp. 281-293, 1994.

[24] R. J. Hartranft and G. C. Sih, The Influence of the Soret and Dufour Effects on the Diffusion of Heat and Moisture in Solids, *International Journal of Engineering Science*, vol. 18, pp. 1375-1383, 1980.

[25] R. J. Hartranft, G. C. Sih, and T. S. Chen, *Interaction of Temperature and Moisture in Diffusion*, Lehigh University Institute of Fracture and Solid Mecanics Report IFSM-77-82, August, 1977.

[26] J. G. Haygreen and J. L. Bowyer, *Forest Products and Wood Science*, The Iowa State University Press, 1982.

[27] P. R. Heyliger, Static Behavior of Laminated Elastic/Piezoelectric Plates, *AIAA Journal*, vol. 32, pp. 2481-2484, 1994.

[28] P. R. Heyliger, Exact Solutions for Simply Supported Laminated Piezoelectric Plates, *Journal of Applied Mechanics*, vol. 64, pp. 299-306, 1997.

[29] P. R. Heyliger, G. Ramirez, and D. A. Saravanos, Coupled Discrete-Layer Finite Elements for Laminated Piezoelectric Plates, *Communications in Numerical Methods in Engineering*, vol. 10, pp. 971-981, 1994.

[30] P. R. Heyliger and D. A. Saravanos, Exact Free Vibration Analysis of Laminated Plates with Embedded Piezoelectric Layers, *Journal of the Acoustical Society of America*, vol. 98, pp. 1547-1557, 1995.

[31] K. H. Huebner, E. A. Thornton, and T. G. Byrom, *The Finite Element Method for Engineers*, 3rd ed., John Wiley & Sons, New York, NY, 1995.

[32] M. W. Hyer, *Stress Analysis of Fiber-Reinforced Composite Materials*, WCB/McGraw-Hill, Boston, Massachusetts, 1998.

[33] J. K. Irudayaraj, K. Haghighi, and R. L. Stroshine, Nonlinear Finite Element Analysis of Coupled Heat and Mass Transfer Problems with an Application to Timber Drying, *Drying Technology*, vol. 8, no. 4, pp. 731-749, 1990.

[34] R. M. Jones, *Mechanics of Composite Materials*, McGraw-Hill, New York, NY, 1975.

[35] K. D. Jonnalagadda, G. E. Blandford, and T. R. Tauchert, Piezothermoelastic Composite Plate Analysis Using First-Order Shear Deformation Theory, *Computers and Structures*, vol. 51, no. 1, pp. 79-89, 1994.

[36] S. Kapuria, G. P. Dube, P. C. Dumir, and S. Sengupta, Levy-Type Piezothermoelastic Solution for Hybrid Plate by Using First-Order Shear Deformation Theory, *Composites Part B*, vol. 28B, pp. 535-546, 1997.

[37] S. Kapuria, P. C. Dumir, and S. Sengupta, Exact Piezothermoelastic Axisymmetric Solution of a Finite Transversely Isotropic Cylindrical Shell, *Computers and Structures*, vol. 61, no. 6, pp. 1085-1099, 1996.

[38] S. Kapuria, P. C. Dumir, and S. Sengupta, Nonaxisymmetric Exact Piezothermoelastic Solution for Laminated Cylindrical Shell, *AIAA Journal*, vol. 35, no. 11, pp. 1792-1795, 1997.

[39] W. Knuffel and A. Pizzi, The Piezoelectric Effect in Structural Timber, *Holzforschung*, vol. 40, pp. 157-162, 1986.

[40] E. M. Lang, J. R. Loferski, and J. D. Dolan, Hygroscopic Deformation of Wood-Based Composite Panels, *Forest Products Journal*, vol. 45, no. 3, pp. 67-70, 1995.

[41] H. J. Lee and D. A. Saravanos, Coupled Layerwise Analysis of Thermopiezoelectric Composite Beams, *AIAA Journal*, vol. 34, no. 6, pp. 1231-1237, 1996.

[42] H. J. Lee and D. A. Saravanos, Generalized Finite Element Formulation for Smart Multilayered Thermal Piezoelectric Composite Plates, *International Journal of Solids and Structures*, vol. 34, no. 26, pp. 3355-3371, 1997.

[43] W. P. Mason, *Piezoelectric Crystals and Their Application to Ultrasonics*, D. Van Nostrand Co., New York, 1950.

[44] J. McMillen, Drying Stresses in Red Oak, *Forest Products Journal*, vol. 5, no. 1, pp. 71-76, 1955.

[45] R. D. Mindlin, On the Equations of Motion of Piezoelectric Crystals, *Problems of Continuum Mechanics*, edited by J. Radok, Society for Industrial and Applied Mathematics, Philadelphia, PA, pp. 282-290, 1961.

[46] R. D. Mindlin, Equations of High Frequency Vibrations of Thermopiezoelectric Crystal Plates, *International Journal of Solids and Structures*, vol. 10, no. 6, pp. 625-637, 1974.

[47] K. Morgan, H. R. Thomas, and R. W. Lewis, Numerical Modeling of Stress Reversal in Timber Drying, *Wood Sci.*, vol. 15, no. 2, pp. 139-149, 1982.

[48] E. Mougel, A. L. Beraldo, and Z. Zoulalian, Controlled Dimensional Variations of a Wood-Cement Composite, *Holzforschung*, vol. 49, pp. 471-479, 1995.

[49] W. Nowacki, *Dynamic Problems of Thermoelasticity*, Noordhoff International Publishing, Leyden, The Netherlands, 1975.

[50] N. J. Pagano, Exact Solutions for Rectangular Bidirectional Composites and Sandwich Plates, *Journal of Composite Materials*, vol. 4, pp. 20-34, 1970.

[51] K. E. Pauley and S. B. Dong, Analysis of Plane Waves in Laminated Piezoelectric Plates, *Wave Electronics*, vol. 1, pp. 265-285, 1976.

[52] O. A. Plumb, C. A. Brown, and B. A. Olmstead, Experimental Measurements of Heat and Mass Transfer During Convective Drying of Southern Pine, *Wood Science and Technology*, vol. 18, pp. 187-204, 1984.

[53] S. S. Rao and M. Sunar, Analysis of Distributed Thermopiezoelectric Sensors and Actuators in Advanced Intelligent Structures, *AIAA Journal*, vol. 31, no. 7, pp. 1280-1286, 1993.

[54] M. C. Ray, R. Bhattacharya, and B. Samata, Exact Solutions for Static Analysis of Intelligent Structures, *AIAA Journal*, vol. 31, pp. 1684-1691, 1993.

[55] J. N. Reddy, *Energy and Variational Methods in Applied Mechanics*, John Wiley & Sons, New York, NY, 1984.

[56] J. N. Reddy, A Generalization of Two-Dimensional Theories of Laminated Composite Plates, *Communications in Applied Numerical Methods*, vol. 3, pp. 173-180, 1987.

[57] J. N. Reddy, On the Generalization of Displacement-Based Laminate Theories, *Applied Mechanics Reviews*, vol. 42, no. 11, part 2, pp. S213-S222, 1989.

[58] J. N. Reddy, *An Introduction to the Finite Element Method*, 2nd ed., McGraw-Hill, New York, NY, 1993.

[59] J. N. Reddy, *Mechanics of Laminated Composite Plates: Theory and Analysis*, CRC Press, Boca Raton, FL, 1997.

[60] O. E. Rodgers, Effect on Plate Frequencies of Local Wood Removal from Violin Plates Supported at the Edges, *CAS Journal*, vol. 1, pp. 7-18, 1991.

[61] K. S. Sai Ram and P. K. Sinha, Hygrothermal Bending of Laminated Composite Plates with a Cutout, *Computers and Structures*, vol. 43, no. 6, pp. 1105-1115, 1992.

[62] K. S. Sai Ram and P. K. Sinha, Hygrothermal Effects on the Buckling of Laminated Composite Plates, *Composite Structures*, vol. 21, pp. 233-247, 1992.

[63] K. S. Sai Ram and P. K. Sinha, Hygrothermal Effects on the Free Vibration of Laminated Composite Plates, *Journal of Sound and Vibration*, vol. 158, no. 1, pp. 133-148, 1992.

[64] K. S. Sai Ram and P. K. Sinha, Vibration and Buckling of Laminated Plates with a Cutout in Hygrothermal Environment, *AIAA Journal*, vol. 30, no. 9, pp. 2353-2355, 1992.

[65] D. A. Saravanos, P. R. Heyliger, and D. A. Hopkins, Layerwise Mechanics and Finite Element for the Dynamic Analysis of Piezoelectric Composite Plates, *International Journal of Solids and Structures*, vol. 34, no. 3, pp. 359-378, 1997.

[66] R. Schumacher, Compliances of Wood for Violin Top Plates, *Journal of the Acoustical Society of America*, vol. 84, pp. 1223-1228, 1988.

[67] D. Sharp, Composite Structural Wood Products - Manufacturing and Application, *Journal of the Institute of Wood Science*, vol. 13, pp. 442-446, 1994.

[68] C. H. Shen and G. S. Springer, Moisture Absorption and Desorption of Composite Materials, *Journal of Composite Materials*, vol. 10, pp 2-20, 1976.

[69] C. D. Shirrell, Diffusion of Water Vapor in Graphite/Epoxy Composites, *Advanced Composite Materials – Environmental Effects*, edited by J. R. Vinson, American Society for Testing and Materials, STP 658, pp. 21-42, 1978.

[70] J. F. Siau, *Transport Processes in Wood*, Springer-Verlag, Berlin Heidelberg, Germany, 1984.

[71] G. C. Sih, J. G. Michopoulos, and S. C. Chou, *Hygrothermoelasticity*, Martinus Nijhoff, Dordrecht, The Netherlands, 1986.

[72] G. C. Sih, M. T. Shih, and S. C. Chou, Transient Hygrothermal Stresses in Composites: Coupling of Moisture and Heat with Temperature Varying Diffusivity, *International Journal of Engineering Science*, vol. 18, pp. 19-42, 1980.

[73] W. T. Simpson, Predicting Equilibrium Moisture Content of Wood by Mathematical Models, *Wood Fiber*, vol. 5, no. 1, pp. 41-49, 1973.

[74] C. Skaar, *Wood-Water Relations*, Springer-Verlag, New York, NY, 1988.

[75] I. S. Sokolnikoff, *Mathematical Theory of Elasticity*, 2nd ed., McGraw-Hill, New York, 1956.

[76] G. S. Springer, *Environmental Effects on Composite Materials*, vol. 2, Technomic Publishing Company, 1984.

[77] M. Sunar and S. S. Rao, Thermopiezoelectric Control Design and Actuator Placement, *AIAA Journal*, vol. 35, no. 3, pp. 534-539, 1997.

[78] Y. Y. Tang and K. Xu, Dynamic Analysis of a Piezothermoelastic Laminated Plate, *Journal of Thermal Stresses*, vol. 18, pp. 87-104, 1995.

[79] T. R. Tauchert, Piezothermoelastic Behavior of a Laminated Plate, *Journal of Thermal Stresses*, vol. 15, pp. 25-37, 1992.

[80] H. R. Thomas, R. W. Lewis, and K. Morgan, An Application of the Finite Element Method to the Drying of Timber, *Wood Fiber*, vol. 11, no. 4, pp. 237-243, 1980.

[81] H. F. Tiersten, *Linear Piezoelectric Plate Vibrations*, Plenum, New York, 1969.

[82] C. Tremblay, A. Cloutier, and B. Grandjean, Experimental Determination of the Ratio of Vapor Diffusion to the Total Water Movement in Wood during Drying, *Wood and Fiber Science*, vol. 31, no. 3, pp. 235-248, 1999.

[83] G. T. Tsoumis, *Science and Technology of Wood: Structure, Properties, Utilization*, Van Nostrand Reinhold, NY, 1991.

[84] H. S. Tzou and Y. Bao, A Theory on Anisotropic Piezothermoelastic Shell Laminates with Sensor/Actuator Applications, *Journal of Sound and Vibration*, vol. 184, no. 3, pp. 453-473, 1995.

[85] H. S. Tzou and Y. Bao, Nonlinear Piezothermoelasticity and Multi-Field Actuations, Part 1: Nonlinear Anisotropic Piezothermoelastic Shell Laminates, *Journal of Vibration and Acoustics*, vol. 119, pp. 374-381, 1997.

[86] H. S. Tzou and R. V. Howard, A Piezothermoelastic Thin Shell Theory Applied to Active Structures, *Journal of Vibration and Acoustics*, vol. 116, pp. 295-302, 1994.

[87] H. S. Tzou and R. Ye, Piezothermoelasticity and Precision Control of Piezoelectric Systems: Theory and Finite Element Analysis, *Journal of Vibration and Acoustics*, vol. 116, pp. 489-495, 1994.

[88] H. S. Tzou and Y. H. Zhou, Nonlinear Piezothermoelasticity and Multi-Field Actuations, Part 2: Control of Nonlinear Deflection, Buckling and Dynamics, *Journal of Vibration and Acoustics*, vol. 119, pp. 382-389, 1997.

[89] W. Voight, *Lehrbuch der Kristallphysik*, 2nd ed., B. G. Teubner, Leipzig, Germany, 1928.

[90] J. M. Whitney and J. E. Ashton, Effect of Environment on the Elastic Response of Layered Composite Plates, *AIAA Journal*, vol. 9, no. 9, pp. 1708-1713, 1971.

[91] D. Xu and O. Suchsland, A Modified Elastic Approach to the Theoretical Determination of the Hygroscopic Warping of Laminated Wood Panels, *Wood and Fiber Science*, vol. 28, no. 2, pp. 194-204, 1996.

[92] K. Xu, A. K. Noor, and Y. Y. Tang, Three-Dimensional Solutions for Coupled Thermoelectroelastic Response of Multilayered Plates, *Computer Methods in Applied Mechanics and Engineering*, vol. 126, pp. 355-371, 1995.